A STUDY OF A NEW MAGNETIC REFRIGERATING CYCLE

J. R. van GEUNS

A STUDY OF A NEW MAGNETIC REFRIGERATING CYCLE

PROEFSCHRIFT

TER VERKRIJGING VAN DE GRAAD VAN DOCTOR IN DE WISKUNDE EN NATUURWETENSCHAPPEN AAN DE RIJKSUNIVERSITEIT TE LEIDEN, OP GEZAG VAN DE RECTOR MAGNIFICUS DR. J. DANKMEIJER, HOOGLERAAR IN DE FACULTEIT DER GENEESKUNDE, TEN OVERSTAAN VAN EEN COMMISSIE UIT DE SENAAT TE VERDEDIGEN OP WOENSDAG 1 JUNI 1966 TE 15.00 UUR

DOOR

JOHANNES RUDOLPHUS van GEUNS

GEBOREN TE BATAVIA (THANS DJAKARTA), NED. INDIË (THANS INDONESIË) IN 1929

PROMOTOR: PROF. DR. H. B. G. CASIMIR

Aan mijn moeder

Aan mijn vrouw en kinderen

Teneinde te voldoen aan de wens van de Faculteit der Wis- en Natuurkunde volgt hier een overzicht van mijn studie.

Na het behalen van het eindexamen aan het Stedelijk Gymnasium te Zutphen in 1948, begon ik de studie in de Wis- en Natuurkunde aan de Rijksuniversiteit te Leiden.

In 1952 heb ik het candidaatsexamen D afgelegd. Mijn verdere opleiding vond plaats aan het Kamerlingh Onnes Laboratorium bij Prof. Dr. C. J. Gorter. Onder leiding van Dr. D. de Klerk heb ik medegewerkt aan de opbouw van een installatie voor het opwekken van grote magneetvelden.

In 1956 heb ik het doctoraal examen in de experimentele natuurkunde behaald, nadat ik de vereiste tentamens in de theoretische natuurkunde en de mechanica had afgelegd bij Dr. N. G. van Kampen en Dr. P. Mazur.

Van 1956 tot 1958 vervulde ik mijn militaire dienstplicht bij de Koninklijke Marine. Gedurende deze tijd was ik werkzaam op het Laboratorium voor Elektronische Ontwikkelingen voor de Krijgsmachten te Oegstgeest.

In 1958 trad ik in dienst van de N.V. Philips' Gloeilampenfabrieken. Sedertdien heb ik op het Natuurkundig Laboratorium deel uitgemaakt van de groep die zich bezig houdt met het onderzoek aan koudgaskoelmachines. Deze groep staat onder leiding van Dr. J. W. L. Köhler. Gedurende een aantal jaren heb ik gewerkt aan een kleine installatie, waarmede vloeibare zuurstof uit de lucht gewonnen kan worden. Sedert 1963 heb ik mij bezig gehouden met een theoretisch onderzoek naar de mogelijkheid een magnetische koelmachine voor een temperatuur van ongeveer 4 °K te vervaardigen. Hieruit is dit proefschrift voortgekomen.

Zeer erkentelijk ben ik de directie van het Natuurkundig Laboratorium voor het feit, dat zij mij in zo ruime mate de gelegenheid heeft gegeven de resultaten van dit onderzoek te bewerken voor mijn proefschrift.

Bijzonder dankbaar ben ik Dr. Köhler voor de grote en warme belangstelling, die hij voortdurend dit werk getoond heeft. Veel heb ik van hem mogen leren. De talrijke, prettige discussies, die wij samen hebben gevoerd, hebben in hoge mate bijgedragen tot het tot stand komen van dit proefschrift.

De medewerkers van de groep wil ik gaarne dank brengen voor de plezierige wijze, waarop zij mij steeds behulpzaam zijn geweest. Veel steun heb ik ondervonden van de heren W. A. H. J. Hermans en A. K. de Jonge, respectievelijk bij de metingen aan de paramagnetische stoffen en bij het opstellen van het programma voor de elektronische rekenmachine.

Dr. P. F. Bongers ben ik zeer erkentelijk voor het bereiden van de paramagnetische stoffen en Drs. R. P. van Stapele voor een aantal nuttige discussies.

Veel dank ben ik verschuldigd aan de heer A. Smith Hardy voor het corrigeren van de engelse tekst.

CONTENTS

1. INTRODUCTION

Temperatures attainable with liquid helium have long been used almost exclusively for the purpose of scientific research. This situation is now changing rapidly as a number of the new phenomena discovered at these low temperatures have recently led to technical applications of considerable importance, such as masers, superconducting computer elements and the use of superconductors for generating high magnetic fields. In all these applications the apparatus must be cooled to temperatures in the liquid-helium range. The conventional method of placing the apparatus in a well insulated container refilled periodically with liquid helium, is too elaborate and uneconomical. The amount of refrigeration required is often relatively great and large amounts of liquid helium must be supplied as it is only the small heat evaporation of helium that can provide the cooling at the required temperature. As a result the demand for compact, reliable and highly efficient refrigerators is growing fast.

Good refrigerators are available down to temperatures of approximately 10 °K. In all these refrigerators helium is compressed at room temperature and the refrigeration is obtained by expansion; in this expansion work is performed by the helium either on a piston or on a turbine. Recently, a two-stage gas refrigerating machine has been developed, using the Stirling principle, and generating temperatures down to 12 °K. In such a machine the compressor and the expander are combined into one unit.

At temperatures well below 10 °K none of these refrigerators operates properly for reasons that have been discussed extensively in literature. The only remaining refrigeration cycle for such low temperatures is the Joule-Thomson cycle, using helium as the working medium of course. However, this cycle must be used in combination with a precooler that supplies refrigeration at a temperature well below the inversion temperature of helium; in practice temperatures between 10 °K and 20 °K are used. Using an expander the precooling cycle can be built as an integrating part of the cycle.

The two-stage Stirling-refrigerating machine can also be used as precooler for a Joule-Thomson cycle. Its high efficiency makes such a choice very attractive. On the other hand the two cycles are now completely independent and therefore the question naturally arises whether other refrigerating cycles can be found for use in combination with the gas refrigerating machine. The aim must obviously be to find a cycle that surpasses the Joule-Thomson cycle in one of the following aspects: efficiency, reliability, ease of operation or temperature range, and is at least equivalent in other respects.

It therefore seemed attractive to consider the use of the magneto-caloric effects that have proved so successful in obtaining temperatures below 1 °K. However, the method of adiabatic demagnetization, being practically a discontinuous process, must be replaced by a continuous process. As a matter

of fact we have been able to design a new cycle that enables use to be made of the magneto-caloric effects in a continuously operating refrigerator working at much higher temperatures.

This new cycle is the magnetic analogue of the Stirling cycle used in gas refrigerating machines. The cycle is performed by a paramagnetic material and consists of

(a) magnetization at the precooling temperature,
(b) cooling in a regenerator to a lower temperature,
(c) demagnetization at the lower temperature,
(d) reheating in the regenerator to the precooling temperature.

In sec. 2.2 of this thesis we will discuss how this cycle can be realized. Here it is mentioned only that helium gas at a moderate pressure (e.g. 20 atmospheres) is pushed through the paramagnetic material to carry off the magnetization heat and to transport the refrigeration produced at another moment. Furthermore helium gas is used as a regenerator. The possibility to use this gas as a regenerator arises from its relatively high specific heat and the low specific heat of solids at low temperatures. This fact hampers the proper working of regenerators in gas refrigerating machines at very low temperatures. We have thus made a virtue of need by a useful application in the new cycle.

The decision to build such a new refrigerator would have far-reaching consequences since much effort and money must be spent on it. Moreover the development of a new refrigerator is not necessitated by the absence of other alternatives. It is therefore desirable to carry through a theoretical analysis prior to a possible experimental investigation, in order to make certain that the above-mentioned aims can be achieved.

In this thesis such an analysis is presented. It consists of three parts, dealing respectively with the theory of the new refrigerator, the complete calculations for such a refrigerator and an experimental investigation of some suitable paramagnetic materials. These subjects are discussed in three successive chapters of this thesis.

In chapter 2 we shall first discuss the principle of the new refrigerator and the idealized thermodynamic cycle. Subsequently a descriptive model will be introduced as the actual processes are too complex for a simple theory. Then the theory of the regenerator, which is the most complicated part of the refrigerator, will be discussed in a separate section. And finally the theory of the refrigerator will be completed on the basis of the descriptive model.

In a first analysis of an entirely new refrigerator it is hardly possible to cover all aspects in full detail. We are well aware of the fact that our theory is only a first approximation and that further refinements may be called for. However, an estimation of orders of magnitude as well as the experience gained with

similar calculations for a large variety of Stirling-type engines justifies the belief that we have certainly covered the essential features.

In chapter 3 the theory developed in the preceding chapter is applied to the complete calculation of the performance of a magnetic refrigerator. We have chosen for this example a refrigerator that is matched to the capacity of a model A 20 gas refrigerating machine to be used as precooler at 15 °K. These calculations were programmed for a C.D.C. 3600 computer, as a large number of numerical calculations are involved. The chapter ends with a discussion of the merits of the new cycle.

In chapter 4 susceptibility and entropy measurements on some paramagnetic materials are discussed. We had to do an experimental investigation of such materials ourselves as the paramagnetic salts used for adiabatic demagnetization below 2 °K are rather diluted. The output of a refrigerator using those materials will be very small. Moreover these materials are chemically not very stable. The most suitable working substance found in our investigation is $Dy_2Ti_2O_7$. It has therefore been used as working substance in the refrigerator discussed in chapter 3.

2. THEORY OF THE MAGNETIC REFRIGERATOR

2.1. Introduction

In 1926 Debeye [1]) and Giauque [2]) independently proposed the method of adiabatic demagnetization to obtain temperatures below 1 °K. The first experiments [3,4,5]) were performed in 1933 and since then this method has been used widely for the purpose. Although a number of experiments at much higher temperatures have been carried out with this method [6,7]), it has never been seriously considered for use in a refrigerator at temperatures above 1 °K. This is probably due to the fact that the method of adiabatic demagnetization itself is not very suited to a refrigerator performing full cycles in fast repetition. Daunt et al. [8]) have developed a magnetic refrigerator for 0·1 °K, performing an adiabatic demagnetization once every few minutes. The refrigerating capacity of this machine is consequently low. The new refrigerator that we shall discuss in this thesis can be operated at much higher speed, e.g. 150 cycles per minute. This obviously increases the capacity of such a refrigerator considerably. Moreover, the new cycle is suited to much higher temperatures by application of the principle of regeneration, as will be discussed later.

The principle of cooling by demagnetization has been discussed extensively in literature [9]). We shall briefly review the thermodynamic principles here.

The first law of thermodynamics applied to a magnetic material can be written:

$$\mathrm{d}q = \mathrm{d}u - H\,\mathrm{d}\sigma. \tag{2.1}$$

Here $\mathrm{d}q$ is the amount of heat delivered to the material, u its internal energy, H the magnetic field and σ the magnetization of the material. Both u and σ are used for one gramme of magnetic material *).

The existence of magneto-caloric effects (heating or cooling by a changing magnetic field) can be derived directly from the entropy of a magnetic material. Applying the first and the second law of thermodynamics, we can derive for the entropy:

$$s(H, T) = s(0, T) + \int_0^H \left(\frac{\delta\sigma}{\delta T}\right)_H \mathrm{d}H, \tag{2.2}$$

where $s(0, T) = \int_0^T (c_0/T)\,\mathrm{d}T$ is the entropy without magnetic field; c_0 is the specific heat without magnetic field.

---

*) Throughout this thesis we shall use non-capital characters for quantities related to one gramme of material.

If the magnetization of a material is temperature-dependent, its entropy in the magnetized state differs from that in the non-magnetized state. Thus only in this case can cooling effects be obtained. In general, use is made of paramagnetic materials the magnetization of which follows a Curie-Weiss law:

$$\sigma = cH/(T - \Theta). \tag{2.3}$$

Substitution of this equation in (2.2) gives

$$s(H, T) = s(0, T) - \tfrac{1}{2} c\alpha^2, \tag{2.4}$$

where $\alpha = H/(T - \Theta)$.

The entropy in a magnetic field is thus lower than without field. When the paramagnetic material is magnetized, heat must be removed to keep the temperature constant. Since no heat is supplied to the material during an adiabatic demagnetization, the temperature of the material will decrease when the magnetic field is removed again.

To use the magnetic cooling method for a continuously running refrigerator operating at higher temperatures, two problems must be solved. The first problem is the transfer of heat from and to the paramagnetic material in a short time. The second problem arises from the fact that the heat capacity of the material in zero field is relatively large at higher temperatures. Below 1 °K this heat capacity, which is mainly due to the lattice vibrations, is practically negligible. Then the cooling down of the lattice in each cycle consumes but a very small part of the refrigerating capacity. At higher temperatures the refrigerating capacity is reduced considerably by this effect and special precautions must be taken to remove the heat content of the lattice in some other way. The design of the new refrigerator contains the answers to both problems. In the next section we shall first discuss the principle of this machine.

2.2. Principle of the new magnetic refrigeration cycle

A schematic drawing of the new refrigerator is shown in fig. 2.1. It may operate, for example, between 15 °K and 4 °K. These temperatures have been chosen arbitrarily; there are in principle no reasons why the refrigerator should not operate at much lower temperatures. In general it is less suited for high operating temperatures (e.g. the warm side above 20 °K) for reasons that will be apparent from the further discussion.

The refrigerator consists of a cylinder C, in which five components are placed in juxtaposition. These components are a heat exchanger A_1 ("the freezer"), a stabilizer *) A_2, a container with finely divided paramagnetic material A_3,

*) We use the name stabilizer for a container filled with some finely divided material, e.g. in the shape of small spheres or gauzes. Its function is to prevent convection of the helium that fills the void space in this component.

a second stabilizer A_4 and a second heat exchanger A_5 ("the cooler"). This last heat exchanger is kept at constant temperature T_2 by means of some other refrigerator (the precooler). The cylinder is closed at each end by a piston; these pistons move exactly in phase, such that the volume between both pistons remains exactly the same. This volume, including the void spaces in the above-mentioned components, is filled with helium at a pressure above the critical pressure.

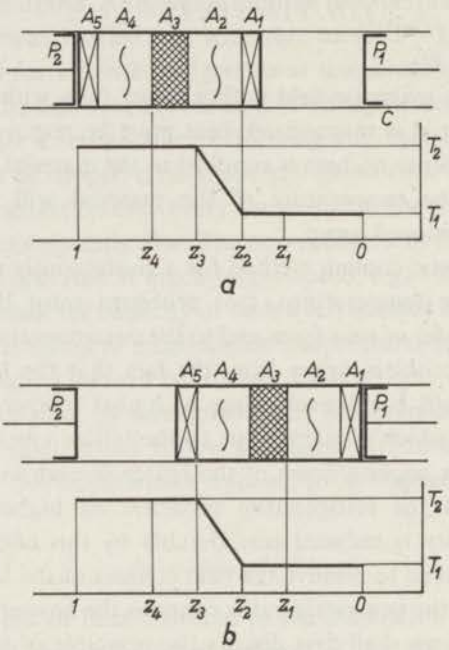

Fig. 2.1. Schematic drawing of the magnetic refrigerator; C cylinder, A_1 freezer, A_2 stabilizer, A_3 paramagnetic material, A_4 stabilizer, A_5 cooler, P_1 and P_2 pistons.

When the pistons are moved, the helium flows through the various components of the refrigerator. Suppose now that the temperature distribution in the helium is as shown in the curve below the schematic drawing in fig. 2.1*a*. The specific heat of helium gas is much higher than that of the solids used for the construction of the various components of the refrigerator. When the pistons are now moved to the right, the helium flows through and cools the components of the refrigerator. However, the temperature of the helium will hardly change owing to its high specific heat. As a first approximation we shall assume further that it does not change at all. Since the total gas volume is constant and no temperature fluctuations occur, the pressure of the helium thus remains constant too.

In the further discussion a coordinate system for the refrigerator must be

selected. The origin of such a coordinate system can, of course, be chosen somewhere in one of the stationary components of the refrigerator. However, it is more convenient to use a single coordinate fixed for the gas. We shall discuss this in more detail in sec. 2.7.2. Here we shall restrict ourselves to a very brief consideration. For that purpose let us consider a fictitious plane in the gas volume, perpendicular to the direction of the gas flow and moving such that the volume between this plane and the right-hand piston P_1 remains constant. It is obvious that the position of this plane can be described by a "coordinate" z, being the ratio of the latter volume to the total gas volume in the refrigerator. If we assume, merely as a simplification, that the cross-sectional area for the gas flow in all components is equal to the cross-sectional area of both pistons, z is a simple linear coordinate, as shown in fig. 2.1. The mass of the gas between any two coordinates z_a and z_b remains constant, since temperature and pressure fluctuations are neglected. We shall neglect any traverse movement of the helium gas.

The total gas volume is divided into five sections. The section between 0 and z_1 and the section between z_4 and 1, will be called the passive parts of the gas, since they have no active function in the process. The section between z_1 and z_2 is called the cold transport gas. It will carry the refrigeration from the paramagnetic material to the freezer. Analogously the section between z_3 and z_4 is called the warm transport gas, since it transports heat from the paramagnetic material to the cooler. Finally the part between z_2 and z_3 is the regenerative part of the gas volume or, in short, "the regenerator".

To explain the operation of the cycle we assume that it has been operating for some time. The temperature distribution of the gas along the axis of the cylinder is shown by the curves below figs 2.1*a* and 2.1*b* at two different moments. It will be noticed that this temperature distribution is the same at both moments, as was discussed before. From 0 to z_2 the gas has the temperature T_1, that is, equal to the temperature of the freezer. From z_2 to z_3 the temperature rises from T_1 to T_2 and, from z_3 to 1 the gas is equal in temperature to the cooler (T_2).

Let us first look at fig. 2.1*a*, where both pistons are at the end of their stroke in one direction. The volume between piston P_1 and freezer A_1 is maximum. The paramagnetic material is now completely at temperature T_2. At this moment a magnetic field is switched on, or somehow the whole system is brought into a magnetic field. Thus the paramagnetic material is magnetized and heat is developed in it. Since the heat transfer from the paramagnetic material to the helium gas is very good, most heat will flow to the helium. The specific heat of helium at a pressure for example of 20 atmospheres and at low temperatures is very high. Therefore the temperature of the helium changes but slightly. The magnetization of the paramagnetic material is thus carried out almost isothermally. When the pistons are thereupon moved to the left, the helium flows through

the components of the refrigerator. The regenerative part of the gas flows from the stabilizer A_2 through the paramagnetic material to the other stabilizer A_4. These components are thus cooled. The specific heat of the stabilizer material and that of the paramagnetic material is much lower, however, than that of the helium. Therefore the temperature distribution of the helium remains practically constant.

At the end of the stroke the point z_3 in the helium just reaches the entrance to the cooler A_5. This situation is shown in fig. 2.1*b*. However, for the sake of clarity we have kept the gas and the pistons at the same place as in fig. 2.1*a*, and have displaced the five components. In the situation as in fig. 2.1*b*, the paramagnetic material lies completely in the cold transport gas ($z_2 - z_1$) and the cooler contains the warm transport gas. The heat absorbed by the warm transport gas in the preceding phase of the cycle is now transferred to the cooler.

The regenerator has absorbed the heat discharged by the paramagnetic material and the stabilizers while they cooled. As will be seen later, this amount of heat is restored to these components during a later phase of the cycle.

In the situation shown in fig. 2.1*b*, the paramagnetic material has the temperature T_1. The magnetic field is then switched off. Due to the demagnetization the paramagnetic material can absorb heat from the cold transport gas. Demagnetization is practically isothermal for the same reason as at magnetization.

When the pistons are moved back to the right again, the cold transport gas (between z_2 and z_1) will bring the refrigeration produced to the freezer A_1. In this way the ultimate goal of the process, refrigeration at T_1 is attained. The cycle is finally completed when the pistons have returned to the position shown in fig. 2.1*a*.

The paramagnetic material and the stabilizers are reheated when they pass through the regenerator. During this part of the cycle the magnetic field is practically zero. The heat deposited by the above components in cooling must be absorbed by them again. However, this regeneration will only function properly if as much heat is deposited during cooling as these components can absorb again on reheating. The material of the stabilizers offers no problem in this respect, since its specific heat is not influenced by the magnetic field. However, we shall show that the paramagnetic material will only satisfy this condition if its magnetization is constant during cooling. The requirement that the paramagnetic material while cooling deposits in a small section of the regenerator as much heat as its absorbs on reheating, gives the equation

$$\int_{T_1}^{T_2} T\left\{\frac{\partial}{\partial T}[s(H,T)] + \frac{\partial}{\partial H}[s(H,T)]\frac{\mathrm{d}H}{\mathrm{d}T}\right\}\mathrm{d}T = \int_{T_1}^{T_2} T\frac{\mathrm{d}}{\mathrm{d}T}[s(0,T)]\,\mathrm{d}T. \qquad (2.5)$$

Here T_1 and T_2 are the temperatures at the beginning and the end of this section. Substitution of eq. (2.4) shows at once that $\alpha = H/(T - \Theta)$ must be

kept constant during cooling to satisfy this condition. According to eq. (2.3) the magnetization is then constant too.

In practice the magnetic field is often not exactly zero during the reheating, nor can a be made constant for every part of the paramagnetic material. Generally $H(/\bar{T} - \Theta)$ can only be made approximately constant. Here $\bar{T}$ is the mean temperature of the paramagnetic material. A discussion of the consequences of this is given in the theory of the regenerator (sec. 2.6).

In the cycle the helium gas has two kinds of functions. A part of it serves as regenerator and two other parts serve to transport heat from the paramagnetic material to the cooler and from the freezer to the paramagnetic material. It is obvious that the helium can perform these functions only if its specific heat per unit of volume is large. This restricts the use of this type of refrigerator to low temperatures, as remarked before.

Finally we shall call attention to the function of the stabilizers. They provide space for the regenerator when it is outside the paramagnetic material. From the preceding discussion of the cycle it is clear that the regenerator must pass completely through the paramagnetic material. It is obvious that the regenerator must not enter the freezer or the cooler. Thus spaces between the paramagnetic material and both heat exchangers are necessary. To prevent convection in those spaces that might disturb the temperature distribution of the regenerator, they are filled with a finely divided substance, e.g. metal or plastic gauzes. These spaces are therefore called the stabilizers.

2.3. The idealized cycle

The magnetic refrigerator cycle for idealized operation is shown in fig. 2.2 in a T-S diagram. The cycle consists of two isotherms and of two lines of constant magnetization. There is some analogy between this cycle and that of the Stirling cycle used in gas refrigerating machines and hot-gas engines. In those machines the gas performs a cycle for idealized operation that has also two isotherms. There is some confusion as to the other two lines. Most textbooks quote for the idealized Stirling cycle two isochores (lines of constant volume), but two isobars (lines of constant pressure) give a much better approximation of the actual cycle. In the magnetic equivalent the isobars are replaced by lines of constant magnetization.

As shown in the preceding section, the heat extracted from the paramagnetic material, when it is cooled along the line of constant magnetization σ_2, is equal to the amount absorbed by it on reheating along the line of magnetization $\sigma_1 = 0$. This heat is stored in the regenerator and the only input of heat from the outside occurs along the isotherm of T_1. Heat is discharged by the cycle to the outside only along the isotherm of T_2.

The entropy changes at both temperatures are equal, but in the opposite

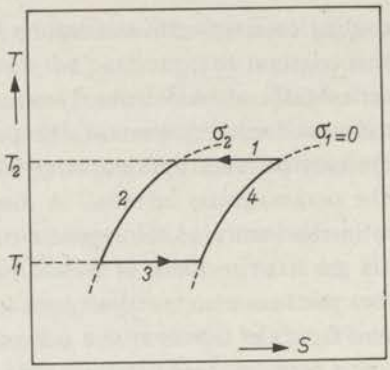

Fig. 2.2. The idealized cycle in a temperature versus entropy diagram. The cycle consists of two isotherms (1 and 3) and two lines of constant magnetization (2 and 4).

direction. This follows directly from eq. (2.4), which for both temperatures gives

$$\Delta s = \tfrac{1}{2}\, c\, (a_2)^2, \tag{2.6}$$

where $a_2 = \sigma_2/c$.

The refrigeration produced by one gramme of paramagnetic material in one cycle is

$$Q_1 = \tfrac{1}{2}\, c\, (a_2)^2\, T_1. \tag{2.7}$$

The heat developed at T_2 is

$$Q_2 = \tfrac{1}{2}\, c\, (a_2)^2\, T_2. \tag{2.8}$$

The work in the cycle is performed by means of the magnetic field, mechanically when the magnet or the paramagnetic material is moved away, or electrically, when the field is switched off. Obviously this work is

$$W = \tfrac{1}{2}\, c\, (a_2)^2\, (T_2 - T_1). \tag{2.9}$$

In sec. 2.5 we shall discuss this point in more detail for a displacement of the paramagnetic material.

The efficiency of the idealized cycle is

$$\eta = Q_1/W = T_1/(T_1 - T_2). \tag{2.10}$$

As could be expected, the efficiency of the idealized cycle of the magnetic refrigerator is equal to that of a Carnot cycle.

2.4. The stylized process

The actual processes that occur in the refrigerator are rather complicated. For an analysis of these processes it is necessary to introduce descriptive models.

In the theory of the Stirling thermal engines — hot-gas engine and gas refrigerating machine — such models have been called stylized processes. Since the analysis of the magnetic refrigerator resembles in some respects that of the Stirling thermal engines, we shall adopt the same name here.

For the analysis of the magnetic refrigerator we shall use the following stylization.

(1) The cycle of the magnetic refrigerator is split up into three stylized processes:
   (a) the cycle of the paramagnetic material,
   (b) the cycle of the warm transport gas,
   (c) the cycle of the cold transport gas.

(2) The above processes are analysed excluding the losses that arise from:
   (a) friction of the gas flow,
   (b) conduction of heat through parts that connect warm places with cold places,
   (c) heating by eddy currents,
   (d) heat influx through the insulation.

These losses are calculated separately and subtracted from the refrigerating capacity calculated with the aid of the three stylized processes.

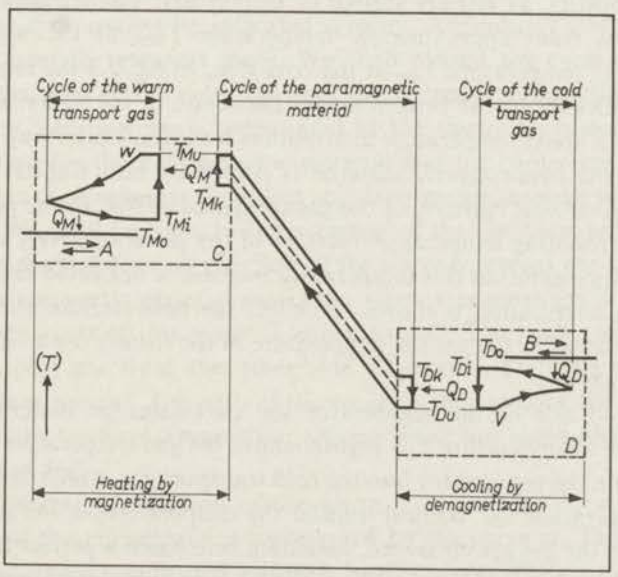

Fig. 2.3. A schematic representation of the magnetic refrigerating cycle.

A schematic representation of the magnetic refrigerator consisting of these three stylized processes is shown in fig. 2.3. It is represented in the coordinate system that was already used in sec. 2.2. This coordinate system is fixed for the

gas. In fig. 2.3 the helium gas is therefore stationary and the components of the refrigerator are moving with respect to the gas.

The cycle of the paramagnetic material is shown as the heavy solid line in the centre of the figure. This cycle is the real refrigerating cycle. Although some aspects of this cycle have already been covered by the discussion of the principle of the refrigerator in sec. 2.2 we shall discuss this cycle here in more detail.

The paramagnetic material moves from the warm transport gas, represented by square C, through the regenerator into the cold transport gas, represented by square D, and from there back again. When the paramagnetic material is in the warm transport gas the magnetic field is "switched on". The heat developed in the paramagnetic material by the magnetization is transferred for the greater part to the helium gas, since the heat transfer between the paramagnetic material and the gas is supposed to be very good and the heat capacity of the gas is much greater than that of the paramagnetic material. The amount of heat absorbed by the gas will be denoted by Q_M. The temperature differences between the gas and the paramagnetic material in this part of the cycle will be neglected throughout the analysis. At the end of the magnetization the gas and the paramagnetic material both have the temperature T_{Mu}.

The paramagnetic material thereupon moves into the regenerator. The regenerator consists, as already stated, of helium gas. The temperature of this gas decreases from approximately temperature T_{Mu} at the warm side to approximately temperature T_{Du} at the cold side. In fig. 2.3 the temperature of the gas is indicated by the broken line in the centre of the figure. For the sake of simplicity a linear temperature distribution is shown. On its way through the regenerator the paramagnetic material is cooled by heat transfer to the gas. Due to the great heat capacity of the gas compared to that of the paramagnetic material the resulting temperature increase of the gas is relatively small. In the schematic representation this temperature increase is neglected and a constant temperature distribution is shown. To effect the heat transfer from the paramagnetic material to the gas the temperature of the former must be higher than that of the gas.

At the cold side of the regenerator the paramagnetic material therefore emerges with a temperature T_{Dk} slightly above the gas temperature at that side. It moves from the regenerator into the cold transport gas, which at that moment has the temperature T_{Di}. By heat transfer the temperatures of the paramagnetic material and the gas are equalized, assuming here again a perfect heat transfer. When the magnetic field is thereupon removed, the paramagnetic material and the gas cool down together to the temperature T_{Du}. From the gas an amount of heat Q_D is transferred to the paramagnetic material.

After demagnetization the paramagnetic material moves back through the regenerator into the warm transport gas. On its way through the regenerator the paramagnetic material is reheated. The temperature of the paramagnetic

material is now slightly lower than that of the gas. When it finally enters the warm transport gas its temperature is T_{Mk}. In the mean time the warm transport gas has been cooled to temperature T_{Mi} in the cycle performed by the warm transport gas itself. By heat transfer from the paramagnetic material to the gas the temperatures of the former and the latter are equalized again. The next cycle starts when the magnetic field is "switched on" once more.

In any part of the regenerator the temperature of the paramagnetic material is higher at the moment it moves from the warm side to the cold side than at the moment it moves in the opposite direction. It is obvious that in this way an amount of energy is transported in each complete cycle through the regenerator. In normal regenerators in which a gas is cooled down, an analogous situation is found. The energy transport by the gas in that case is constant along the regenerator. This energy transport is called the regeneration loss. In the regenerator of the magnetic refrigerator the transport of energy is not the same in every cross-section, since magneto-caloric effects can occur in the regenerator. It is thus incorrect to use the name regeneration loss in this case. We shall therefore introduce the name energy flow in the regenerator. This energy flow can thus be different at both sides of the regenerator.

The cycles of the warm and the cold transport gas are very simple. Since both parts of the gas are stationary, however, in the schematic representation of fig. 2.3 their cycle cannot be indicated directly. An indirect method therefore had to be used to represent these. We shall discuss the cycle of the warm transport gas; that of the cold transport gas is completely analogous.

The warm transport gas is represented by the square C. In each revolution in the refrigerator the paramagnetic material and the cooler are in the warm transport gas once, whereas the warm stabilizer passes through this part of the gas twice. We shall first ignore the presence of the stabilizer and discuss the influence of the stabilizer on the cycle of the warm transport gas later. The fact that the paramagnetic material enters the warm transport gas is indicated by extending the cycle of this material into square C. The cooler moves into the warm transport gas from the other side, of course when the paramagnetic material is not present. The path of the cooler is indicated by the line A. Since the cooler has a constant temperature, this is a single line along which the cooler moves to and fro.

The temperature fluctuation of the warm transport gas during a complete revolution of the refrigerator is represented by the curve w. The cycle of the warm transport gas is indicated indirectly by this curve. When the paramagnetic material enters the warm transport gas, the latter is at temperature T_{Mi}. As has already been stated, the paramagnetic material discharges during its stay in the transport gas an amount of heat Q_M and the gas is heated by this to temperature T_{Mu}. Neglecting the influence of the stabilizer, the gas remains at this temperature until the cooler moves in. Since the temperature of the cooler T_{M0}

is lower than that of the gas it can absorb heat from the warm transport gas. The transport gas cools down, which is indicated by the exponential decrease of its temperature in the curve w. Since the transport gas must again discharge the amount of heat Q_M in a stationary situation, its temperature must decrease to T_{Mi}. Therefore T_{M0} must be lower than T_{Mi} too. After the cooler has moved out again the transport gas remains at this temperature till the paramagnetic material moves in once more and the next cycle begins.

By the influence of the stabilizer the cycle of the warm transport gas is practically unchanged. The stabilizer moves through the warm transport gas once from the regenerator side and once from the other side. In the first case it has approximately temperature T_{Mk} and the transport gas then has the temperature T_{Mi}. The stabilizer is cooled down to temperature T_{Mi}. However, the amount of heat discharged by it is very small, since materials with a very low specific heat can be used for the stabilizer. For example, molybdenum or Al_2O_3 may be used, which have a specific heat about 30 times lower than that of helium. Therefore the amount of heat discharged by the stabilizer can practically be neglected. For the same reason the amount of heat absorbed by it during its passage in the other direction is negligible too. The heating and the cooling of the stabilizer is therefore an effect that can be neglected in the description of the cycle of the transport gas.

The cycle of the cold transport gas is completely analogous to that of the warm transport gas. Figure 2.3 is self-explanatory in this respect. The denotation of the temperatures occurring in this cycle as shown in this figure is used in the further analysis of the refrigerator.

The further analysis of the refrigerator will be discussed in sec. 2.7. First we shall discuss in the next section the performance of work in the refrigerator. The theory of the regenerator will then be dealt with in sec. 2.6. This theory, which deviates in many respects from that of the normal regenerators, can be treated more or less independently. However, it is convenient to discuss this theory before proceeding to the further analysis of the refrigerator.

2.5. The work performed in the idealized cycle

The shaft power of the magnetic refrigerator is much lower than that of the precooler, which must necessarily be used in combination with it. Generally we are only interested in the power consumed by the total system and for this reason it is hardly necessary to calculate the shaft power of the magnetic refrigerator very accurately. It can be approximated as the difference between the amount of heat discharged per second to the precooler and the refrigerating capacity. Actually, the shaft power is slightly greater due to the friction of the pistons and the drive mechanism. However, these corrections are very small.

Nevertheless the work performed in the different parts of the cycle will be

analysed to help us to understand the processes in the new refrigerator better. It will be discussed for the idealized cycle described in sec. 2.3. The most important facts about the idealized cycle are recapitulated in brief:

(a) magnetization and demagnetization are performed isothermally,
(b) magnetization of the working substance is constant when it is cooled down in the regenerator,
(c) its magnetization is zero during reheating in the regenerator.

Let it be assumed that the working substance is an ideal paramagnetic material ($\Theta = 0$) and that the paramagnetic material is moved with respect to the magnetic field.

To displace the paramagnetic material in the magnetic field a force must be exerted on it, e.g. by a rod. This external force must act against the force exerted on the paramagnetic material by the magnetic field. We lay the movement of the paramagnetic material along the y-axis of a rectangular coordinate system. In this direction the force exerted by the magnetic field has a component

$$K = M \, \mathrm{d}H/\mathrm{d}y. \tag{2.11}$$

The force exerted by the rod is opposite in sign and when the paramagnetic material is displaced from a point where the magnetic field is H_1 to a point where it is H_2, the rod performs an amount of work

$$W = -\int_{H_1}^{H_2} M \, \mathrm{d}H. \tag{2.12}$$

This amount of work for the different phases of the cycle and the amount of heat discharged by the paramagnetic material at the same time are shown schematically in fig. 2.4. The discharged heat was already determined in sec. 2.2.

To magnetize the paramagnetic material it is brought at constant temperature T_2 from zero field to a point where the field has the strength H. The work performed by the rod is then $W = -\frac{1}{2} CH^2/T_2$, where $C = mc$, c is the Curie constant and m the mass of the paramagnetic material. It is remarkable that at the same time an amount of heat Q_M is discharged by the paramagnetic material, while it performs work on the rod, as follows from the negative sign for W. Moreover, W and Q_M are equal except for the sign, but this is only due to the use of an ideal paramagnetic material. For a non-ideal paramagnetic material W and Q_M are different. When the paramagnetic material is then cooled in the regenerator, it is at the same time gradually pulled out of the magnetic field to a point where the field is $(T_1/T_2)H$. The magnetic moment $(C/T_2)H$ is thus kept constant. The work performed on the refrigerator through the rod is now $(C/T_2)\, H\, [H - (T_1/T_2)\, H]$ where T_1 is the temperature at the cold side of the regenerator. Since the regenerator is thermally insulated, no heat is discharged or absorbed by it.

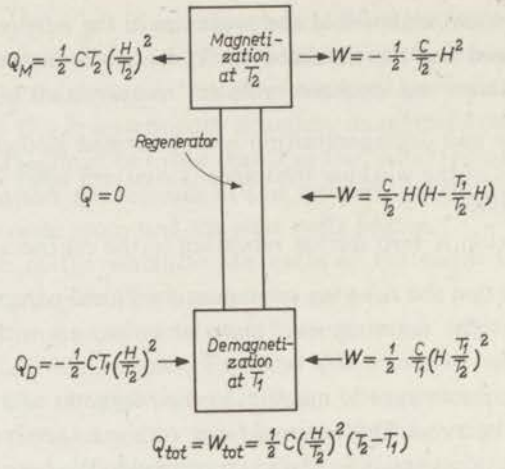

Fig. 2.4. The work performed in the different phases of an idealized refrigerator and the amount of heat that is discharged by it at the same time.

To demagnetize the paramagnetic material it is pulled completely out of the field, its temperature being maintained constant at T_1. Thus the amount of work is $\frac{1}{2}\ (C/T_1)\ [(T_1/T_2)\ H]^2$. At the same time it absorbs the amount of heat $\frac{1}{2}\ C\ T_1 (H/T_2)^2$.

When the paramagnetic material is finally reheated in the regenerator, outside the magnetic field, no work is performed on it and no heat is exchanged with the outside.

For the difference between the heat discharged and absorbed in the cycle, the same figure is found as for the total amount of work performed: $Q_{\text{tot}} = W_{\text{tot}} = \frac{1}{2}\ C\ (H/T_2)^2\ (T_2 - T_1)$.

If this cycle is compared to normal refrigerating cycles, the most remarkable fact is that heat is discharged by it during magnetization at the same time as work is performed by it, and that on demagnetization it absorbs heat while work is performed on it. Furthermore, the largest amount of work is performed on it when the paramagnetic material cools down in the regenerator; this amount is approximately twice as much as the amount of heat Q_M. This apparent abnormal behaviour is caused by the fact that part of this work is converted into the potential energy $-m\sigma H$ of the system consisting of the paramagnetic material and the magnet. During the cooling down of the paramagnetic material in the regenerator the work is even completely converted into potential energy since σ remains constant. However, if σ is not constant during regeneration, as can occur in the actual refrigerator, part of this work is converted into heat. The magneto-caloric effects that thus occur in the regenerator play an important role in the regenerator theory discussed in the next section.

2.6. Theory of the regenerator

2.6.1. *Introduction*

Regenerators are used widely in low-temperature cycles as a method to transfer heat from one gas flow to another gas flow. These regenerators consist normally of a matrix of finely divided material through which flows the gas to be cooled down or reheated. The heat discharged by the gas during its flow from the warm side to the cold side is stored in the regenerator material. After a certain time the gas flow in the regenerator is reversed, so that the gas now flowing from the cold side to the warm side must be reheated. During reheating it consumes the amount of heat discharged in the regenerator in the preceding period.

The regenerator in the magnetic refrigerator performs approximately the same task. However, there are two fundamental differences between this regenerator and "normal" regenerators. These differences are:

(a) the regenerator material is replaced by helium gas and a paramagnetic material is cooled down and reheated in this gas;
(b) contrary to the situation in normal regenerators, heat can be developed in the paramagnetic material during the time it is in the regenerator.

The use of helium gas as a regenerator is possible because its specific heat is much greater than that of the paramagnetic material. This is illustrated by fig. 2.5 where the specific heat of helium per cm^3 at several pressures and that of a paramagnetic material, Dy_2GaSbO_7 (see sec. 4.3.2) are shown as a function of temperature. We have included in this figure the specific heat of a typical constructional material such as stainless steel.

The heating of the paramagnetic material by magneto-caloric effects makes the regenerator theory very difficult. It is obvious that the constant enthalpy transport that exists in normal regenerators has no equivalent in the magnetic case. In the next section we shall therefore discuss the heat balance of the regenerator.

2.6.2. *The heat balance of the regenerator*

Let us first briefly describe the situation in normal regenerators. The gas in these regenerators is always slightly warmer than the regenerator material when it flows to the cold side and slightly colder than this material when it flows to the warm side. These temperature differences are necessary to effect the heat transfer. It is obvious that an amount of energy is transported through the regenerator in this way. Schalkwijk [10]) showed that there is actually a flow of enthalpy through the regenerator and that this flow of enthalpy is constant along the regenerator. The enthalpy transported through the regenerator is the regeneration loss.

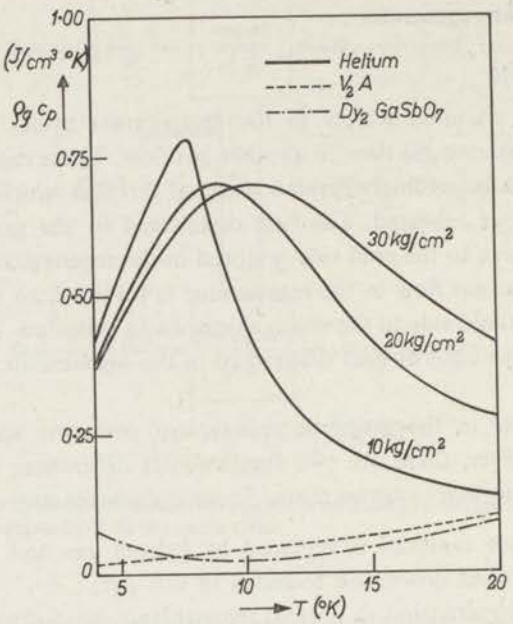

Fig. 2.5. The specific heat per cm³ of helium at several pressures, of a paramagnetic material (Dy_2GaSbO_7) and stainless steel (V2A).

In the regenerator of the magnetic refrigerator the same situation exists if a non-magnetic material is cooled down in it. In this case the enthalpy flow can obviously be better replaced by a flow of internal energy. The enthalpy of an incompressible material is not a useful quantity. It is equal to the internal energy plus a term which is linearly proportional to the pressure. The latter part of the enthalpy is constant in this case since the pressure is constant. The flow of internal energy can be written

$$J = \oint (w\, u_0)\, \mathrm{d}t. \tag{2.13}$$

The integration over a complete cycle is indicated by $\oint$, w is the mass flow of the material in the regenerator and u_0 is the internal energy of this material. Just as in normal regenerators, J is constant along the regenerator.

If a paramagnetic material is used, however, the flow of internal energy is no longer constant along the regenerator. Heat can be developed or absorbed in the paramagnetic material since it can perform work while it is in the regenerator. Since the heat developed or absorbed must be carried off or supplied by the material itself in a stationary situation, the following equation for J is obtained:

$$J_{n+1} - J_n = \Delta R. \tag{2.14}$$

Here J_{n+1} and J_n are the energy flows through cross-sections of the regenerator

at the places $(n + 1)$ and (n), respectively, and ΔR is the heat developed in the section of the regenerator between the two cross-sections.

This equation, of course, follows directly from the principles of thermodynamics. We shall now discuss how ΔR can be found. To do this we shall stylize the regenerator as follows.

The regenerator is taken as filling the part $(1 - f)$ of a fixed volume V_R. This volume has a cylindrical shape and its cross-sectional area perpendicular to the cylinder axis is denoted as B. The paramagnetic material flows through channels in the gas which occupy the part f of V_R. During a time $\frac{1}{2} t_p$, called the warm period, it flows from the warm side to the cold side. Next it flows during an equal time, called the cold period, in the opposite direction. At the beginning and the end of both periods the channels are empty. The system is placed in a magnetic field that does not vary appreciably over the cross-section of the regenerator, but which may vary along the regenerator. This field does not have to be constant in time. Temperature differences inside the paramagnetic material are neglected as this material will be divided into very small particles.

In the regenerator a coordinate x parallel to the axis will be used, that is 0 at the cold side and 1 at the warm side. We shall now consider a small section of the regenerator between x_n and x_{n+1} as shown in fig. 2.6. In this section heat

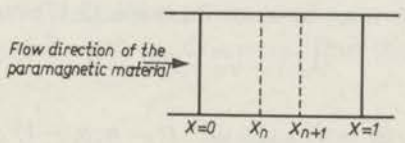

Fig. 2.6. Heat transfer to a flow of paramagnetic material in a section of the regenerator between x_n and x_{n+1}.

is transferred from the gas to the flow of paramagnetic material. In the appendix to this chapter the following equation is derived for this flow of heat:

$$dQ/dt = \int_{x_n}^{x_{n+1}} [f B \varrho_m (\partial u_0/\partial t + T_m \partial s_M/\partial t) + w (\partial u_0/\partial x + T_m \partial s_M/\partial x)] \, dx. \quad (2.15)$$

In this equation B is the cross-sectional area of the regenerator, H the magnetic field, s_M the field-dependent part of the entropy of the paramagnetic material, u_0 its internal energy in zero field, ϱ_m its effective density and w the flow of paramagnetic material. The effective density is the product of the normal density and the filling factor of the channels. This effective density is introduced in order that it may vary in time and along the regenerator. This may happen, for instance, if the paramagnetic material moves out of the regenerator and is replaced by the non-magnetic material of the stabilizers. The regenerator is then empty as far as paramagnetic material is concerned.

The mass flow w will then also change in time and along the regenerator. The relation between w and ϱ_m is the equation of continuity:

$$f B \, \partial \varrho_m / \partial t + \partial w / \partial x = 0. \tag{2.16}$$

In eq. (2.15) the first part of the integrand on the right-hand side presents the heat absorbed by the paramagnetic material in the section, while the second part is the heat carried off by that part of the paramagnetic material which moves through this section.

Using the equation of continuity (2.16) and integrating over a complete cycle, the following equation is obtained:

$$\oint \frac{\mathrm{d}Q}{\mathrm{d}t}\,\mathrm{d}t = fB \int_{x_n}^{x_{n+1}} \mathrm{d}x \oint \frac{\partial (\varrho u_0)}{\partial t}\,\mathrm{d}t + fB \int_{x_n}^{x_{n+1}} \mathrm{d}x \oint T_m \frac{\partial (\varrho_m s_M)}{\partial t}\,\mathrm{d}t +$$

$$+ \oint (w u_0)_{n+1}\mathrm{d}t - \oint (w u_0)_n \mathrm{d}t + \int_{x_n}^{x_{n+1}} \mathrm{d}x \oint T_m \frac{\partial (w s_M)}{\partial x}\,\mathrm{d}t. \tag{2.17}$$

For a stationary situation the integral on the left-hand side and the first integral on the right-hand side must be zero. Equation (2.17) may now be written as

$$J_{n+1} - J_n - \Delta R = 0, \tag{2.18}$$

where

$$J_i = \oint (w\, u_0)_i \,\mathrm{d}t, \quad (i = n, n+1) \tag{2.19}$$

and

$$\Delta R = -\int_{x_n}^{x_{n+1}} \mathrm{d}x \oint [f B T_m \, \partial (\varrho_m s_M)/\partial t + T_m \, \partial (w\, s_M)/\partial x]\,\mathrm{d}t. \tag{2.20}$$

Here J is the energy transport in the regenerator and ΔR is called the magnetic heating.

To calculate J and ΔR the temperature of the paramagnetic material in the regenerator must be known at any moment. These temperatures can, however, only be obtained by solving the differential equations describing the regenerator. These equations will be discussed in the sections below. A solution is only known when $H = 0$ and all material properties are constant in the regenerator. In secs 2.6.6 and 2.6.7 therefore a method will be discussed to calculate approximate values for J and ΔR.

2.6.3. *The differential equations of the regenerator*

The differential equations which describe the regenerator are obtained if eq. (2.15) is combined with equations for the heat transfer and for the temperature variation of the regenerator gas.

For a very small section dx of the regenerator, eq. (2.15) may be written as

$$d\Phi_h = [f B\varrho_m (\partial u_0/\partial t + T_m \partial s_M/\partial t) + w (\partial u_0/\partial x + T_m \partial s_M/\partial x)]\, dx. \quad (2.21)$$

Here $d\Phi_h$ is the heat flow to the paramagnetic material in dx. The heat transfer from the gas to the paramagnetic material in this section is described by

$$d\Phi_h = (a F/l)(T_g - T_m)\, dx. \quad (2.22)$$

Here a is the heat-transfer coefficient, $(F/l)dx$ is the heat-transfer surface available in this section and T_g the temperature of the gas. The length of the regenerator is l and F is the total heat-transfer surface of the stylized regenerator. We shall later on discuss how F may be found.

The temperature decrease of the gas caused by the flow of heat to the paramagnetic material is given by

$$d\Phi_h = -B(1-f)\varrho_g c_p (\partial T_g/\partial t)\, dx. \quad (2.23)$$

It is assumed that the pressure variations are so small that the specific heat of the gas is represented with sufficient accuracy by c_p and its density by ϱ_g. Elimination of $d\Phi_h$ gives two partial differential equations. For a purely paramagnetic material s_M is a function of α according to eq. (2.4). Furthermore u_0 is only a function of T_m and $du_0/dT_m = c_0$. Thus the differential equations can be written as

$$(aF/l)(T_g - T_m) = f B\varrho_m \left(c_0 \frac{\partial T_m}{\partial t} + T_m \frac{\partial s_M}{\partial \alpha} \frac{\partial \alpha}{\partial t}\right) + \\ + w\left(c_0 \frac{\partial T_m}{\partial x} + T_m \frac{\partial s_M}{\partial \alpha} \frac{\partial \alpha}{\partial x}\right) \quad (2.24)$$

and

$$(aF/l)(T_g - T_m) = -B(1-f) c_p \varrho_g \partial T_g/\partial t. \quad (2.25)$$

The mass flow will be written as $w = w_1 \varphi(x, t)$ and the effective density as $\varrho_m = \varrho_1 \psi(x, t)$. The constants w_1 and ϱ_1 are the mean values of w and ϱ during one of the periods; φ and ψ are periodic functions of t. The total amount of paramagnetic material flowing through the regenerator in one period equals the total amount flowing in the opposite direction during the other period. Thus,

$$w_1 \int_0^{\frac{1}{2}t_p} \varphi\, dt = -w_1 \int_{\frac{1}{2}t_p}^{t_p} \varphi\, dt = m_k.$$

The cold period, during which φ is positive, has been chosen from $t = 0$ to $t = \frac{1}{2} t_p$ and the warm period ($\varphi < 0$) from $t = \frac{1}{2} t_p$ to $t = t_p$.

The equations (2.24) and (2.25) can be brought to dimensionless form, by introduction of the dimensionless variables $\xi = (x/l)$ and $\tau = (t/\frac{1}{2}\, t_p)$:

$$\Lambda^+ (T_g - T_m) = \frac{1}{\Delta} \left(\frac{\partial T_m}{\partial \tau} + \frac{T_m}{c_0} \frac{\partial s_M}{\partial \alpha} \frac{\partial \alpha}{\partial \tau} \right) \psi + \left(\frac{\partial T_m}{\partial \xi} + \frac{T_m}{c_0} \frac{\partial s_M}{\partial \alpha} \frac{\partial \alpha}{\partial \xi} \right) \varphi \quad (2.26)$$

and

$$\Lambda^+ (T_g - T_m) = -\Gamma^+ \partial T_g / \partial \tau, \quad (2.27)$$

where *)

$$\Lambda^+ = a\, F / w_1 c_0, \quad (2.28)$$

$$\Gamma^+ = V_R (1 - f)\, \varrho_g c_p / \tfrac{1}{2}\, t_p w_1 c_0 = V_g \varrho_g c_p / m_k c_0 \quad (2.29)$$

and

$$\Delta = \tfrac{1}{2}\, t_p w_1 / f\, \varrho_1 V_R = m_k / f\, \varrho_1 V_R. \quad (2.30)$$

The functions φ and ψ are also transformed to the dimensionless variables. Then the mass flow is $w_0 \varphi\,(\tau, \xi)$ and the effective density is $\varrho_0 \psi\,(\tau, \xi)$. It is easily verified that $w_0 = \frac{1}{2}\, t_p w_1$ and $\varrho_0 = \varrho_1 l$.

Solutions that describe a stationary regenerator must satisfy the condition that the temperatures in the regenerator are the same after a complete cycle. Thus

$$\begin{aligned} T_m\,(\xi, \tau + 2) &= T_m\,(\xi, \tau) \\ \text{and} \qquad T_g\,(\xi, \tau + 2) &= T_g\,(\xi, \tau). \end{aligned} \quad (2.31)$$

During the warm period the paramagnetic material flows into the regenerator at the warm side at a constant temperature T_h and during the cold period it enters the regenerator at the other side at a constant temperature T_l. This yields the boundary conditions

$$\begin{aligned} T_m\,(0, \tau) &= T_l \qquad (0 < \tau < 1), \\ T_m\,(1, \tau) &= T_h \qquad (1 < \tau < 2). \end{aligned} \quad (2.32)$$

In the differential equations Γ^+ and Λ^+ are functions of T_g and T_m and w_0. The magnetic field, appearing in α, can be some more or less arbitrary function of ξ and τ. A solution to these equations is not available. If the magnetic terms are left out, the equations are reduced to the regenerator equations of Hausen, which will be discussed in the next section.

2.6.4. *The regenerator equations of Hausen*

Equations (2.26) and (2.27) are reduced to a much simpler form if

$$\begin{aligned} \alpha &= 0, \\ \Delta &= \infty, \\ \Lambda^+ &= \text{constant}, \\ \Gamma^+ &= \text{constant and} \\ \varphi &= \text{independent of } \xi. \end{aligned}$$

*) The same notation as in the normal regenerator theory is used. To prevent confusion, however, an index + is added in the right upper corner.

Generally Λ^+ and Γ^+ can only be constant if the material properties such as c_0, c_p, etc., are constant. The equations are then essentially the same as those which Hausen [11]) derived for normal regenerators:

$$\Lambda^+ (T_g - T_m) = \varphi \, \partial T_m / \partial \xi \tag{2.33}$$

and

$$\Lambda^+ (T_g - T_m) = -\Gamma^+ \, \partial T_g / \partial \tau. \tag{2.34}$$

If Λ^+ and Γ^+ are, however, not constants, eqs (2.33) and (2.34) can only be solved numerically. Such solutions have been discussed by several authors [12,13]).

We shall briefly discuss the analytical solution to the equations of Hausen and the formula for the regeneration loss in this case. In the following sections this will be used to find an approximation for J and ΔR in eq. (2.18).

From the equations of Hausen a second-order differential equation for T_g and a simple differential equation for T_m can be derived. These equations are

$$-\frac{\Lambda^+}{\Pi^+} \frac{\partial T_g}{\partial \tau} = \varphi \left(\frac{\partial T_g}{\partial \xi} + \frac{1}{\Pi^+} \frac{\partial^2 T_g}{\partial \xi \partial \tau} \right), \tag{2.35}$$

and

$$T_m = T_g + \frac{1}{\Pi^+} \frac{\partial T_g}{\partial \tau}, \tag{2.36}$$

where

$$\Pi^+ = \Lambda^+ / \Gamma^+. \tag{2.37}$$

An infinite number of eigenfunctions can be found that satisfy these equations and the periodicity conditions (2.31). From these eigenfunctions a solution can be obtained that satisfies the boundary conditions (2.32). Hausen has shown that the zeroth eigenfunction (eq. (2.38)) describes the central part of a regenerator if Λ^+ is large. The higher eigenfunctions are only necessary to adjust the solution to the boundary conditions. They decay, however, exponentially from both ends of the regenerator.

The zeroth eigenfunction is

$$T_g = T_0 + g_R \left[\xi - (\Pi^+ / \Lambda^+) \int_0^\tau \varphi \, d\tau \right], \tag{2.38}$$

$$T_m = T_g - (g_R / \Lambda^+) \, \varphi. \tag{2.39}$$

The value of the constants T_0 and g_R is found from the boundary conditions if the complete solution is determined. The equations (2.38) and (2.39) have the required periodicity, for φ is a periodic function and $\int_0^2 \varphi \, d\tau = 0$. The zeroth eigenfunction thus gives a linear temperature distribution that moves up and down periodically in the central part of the regenerator. The complete solution for $T_m(\xi, \tau)$ is shown schematically in fig. 2.7, for $\tau = 0$, 1 and 2.

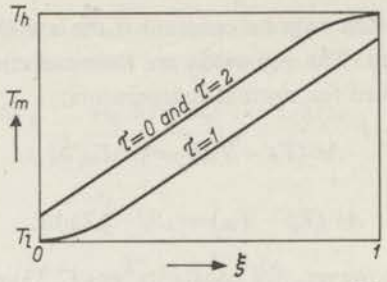

Fig. 2.7. The temperature distribution in a regenerator with constant Λ^+ and Γ^+.

It is easily shown that $\int_0^2 \varphi T_g \, d\tau = 0$. This is very convenient in deriving a relation for the regenerator loss. The regenerator loss is equal to the energy transport J which is constant along the regenerator in this case. Thus J may be determined in the central part of the regenerator from the zeroth eigenfunction. Since $c_0 \, (= \partial u_0/\partial T_m)$ is constant, substitution of (2.39) in (2.19), transformed to dimensionless coordinates, gives

$$J = -(g_R/\Lambda^+) \, w_0 c_0 \int_0^2 \varphi^2 \, d\tau. \tag{2.40}$$

The minus sign in J means that the energy transport goes from the warm side to the cold side, since $g_R \, (= \partial T_g/\partial \xi)$ is positive. This is of course the right direction for the regeneration loss. Equation (2.40) shows that the regeneration loss is proportional to the temperature gradient in the central part of the regenerator.

If $\varphi = 1$ during the cold period and $\varphi = -1$ during the warm period, the temperature gradient for $\Gamma^+ \to \infty$ is easily found to be

$$g_R = [\Lambda^+/(\Lambda^+ + 2)] \, (T_h - T_l). \tag{2.41}$$

The regeneration loss is then

$$J = [2 \, w_0 c_0/(\Lambda^+ + 2)] \, (T_h - T_l). \tag{2.42}$$

Using a simplified theory, based on arguments of symmetry and conformity, Schalkwijk [10]) was able to show that for finite Γ^+ the regeneration loss becomes

$$J = [2 \, w_0 c_0/(\Lambda^+ - \Omega + 2)] \, (T_h - T_l), \tag{2.43}$$

where Ω is a function of Π^+. He found the empirical equation

$$\Omega = \Pi^+ + 2 - 2{\cdot}35 \, (\Pi^+)^{1/2}. \tag{2.44}$$

This equation holds for $\Gamma^+ > 1$, the deviation from numerically calculated values of the regeneration loss being less than 1 %. With these equations the efficiency of regenerators with constant values of Λ^+ and Π^+ can be found, if Λ^+ is large and no magneto-caloric effects occur.

2.6.5. *Stylizations for a numerical regenerator calculation*

The equations of Hausen, with variable values of Λ^+ and Γ^+, can be solved numerically as mentioned before. The same would perhaps be possible with eqs (2.26) and (2.27). Such a solution is, however, very difficult because of the magnetic terms and is beyond the scope of this preliminary investigation of the magnetic refrigerator. A method which gives the energy flow in the regenerator with moderate accuracy is, for the time being, sufficient. For this purpose we shall make the following stylizations.

(a) It is assumed that Γ^+ is so large that the temperature variations of the regenerator can be neglected.
(b) The mass flow of paramagnetic material in the regenerator is stylized as shown in fig. 2.8. It has a positive constant value during part of the cold period, a constant negative value during part of the warm period and it is zero for the rest of the time.
(c) The effective density is stylized in very much the same way, except that it is also positive during the warm period.
(d) Finally, Λ^+ is taken as independent of τ as long as $\varphi \neq 0$, and it is taken as zero when $\varphi = 0$.

The first stylization reduces the regenerator problem to that of a heat exchanger. This stylization is rather rough since Γ^+ is actually not very large. For example, in the refrigerator discussed in sec. 3.10 it has a minimum value of 4 at the warm side (see fig. 3.10). At the cold side Γ^+ is 10 and inside the regenerator it has at some places much higher values. If no magnetic effects were present the temperature fluctuations for such values of Γ^+ would have only a slight effect on the regeneration loss. If, for example, we substitute in eq. (2.44) $\Lambda^+ = 50$ and $\Gamma^+ = 8$, assuming that these values are constant along the regenerator, we see that $\Omega = 3{\cdot}55$. The regeneration loss is then only 7% greater than for the case that $\Gamma^+ = \infty$. However, the temperature fluctuations will have a stronger influence on the magnetic terms, if these are present. The order of magnitude of these temperature fluctuations can be found as follows. The temperature fluctuations are proportional to the amount of heat transferred from the paramagnetic material to the gas. In general this heat load is mainly due to the non-magnetic terms in the differential equations, as discussed in sec. 2.6.7. Thus the temperature fluctuations can be estimated using eq. (2.44) and neglecting the magnetic terms. If, moreover, we use the approximation that $\partial T_m/\partial\tau = \partial T_g/\partial\tau$ and $\partial T_m/\partial\xi = \partial T_g/\partial\xi$, we see that $(\Gamma^+ + 1/\Lambda)\,\partial T_g/\partial\tau = -\varphi\,\partial T_g/\partial\xi$. Using the stylized mass flow, discussed below, integration over the cold period from $\tau = 0$ to $\tau = 1$ yields for the total temperature change in the cold period $\Delta T_g = (\Gamma^+ + 1/\Lambda)^{-1}\,\partial T_g/\partial\xi$. In the example of sec. 3.10 we find that $\Delta T_g = 2{\cdot}0$ °K at the cold side of the regenerator. Fortunately the temperature fluctuations in the rest of the regenerator are smaller, since

Γ^+ is larger or $\partial T_g/\partial\xi$ is smaller there. The temperature fluctuations are thus not very small and the stylization, on the basis of which the fluctuations can be neglected, is rather rough. However, this stylization will be used none the less, since a calculation with finite Γ^+ is too complicated.

The stylized mass flow $w_0\varphi$ is represented in fig. 2.8 by the broken line for

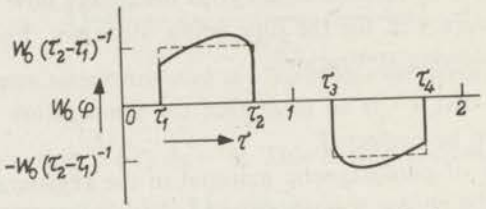

Fig. 2.8. The stylized and the actual mass flow in the regenerator.

one complete period between $\tau = 0$ and $\tau = 2$. The actual mass flow is represented by the fully drawn curve. The last one is zero from $\tau = 0$ to τ_1, from τ_2 to τ_3, and from τ_4 to $\tau = 2$. Between τ_1 and τ_2 and between τ_3 and τ_4 the actual mass flow is part of a function closely resembling a sine function. The exact shape of $w_0\varphi$ in those intervals depends on the drive mechanism of the pistons.

The stylized mass flow is such that φ has a constant value $(\tau_2 - \tau_1)^{-1}$ between τ_1 and τ_2 and a constant value $-(\tau_2 - \tau_1)^{-1}$ between τ_3 and τ_4. Moreover, $(\tau_4 - \tau_3)$ is made equal to $(\tau_2 - \tau_1)$ by shifting one of these points if necessary. The constant w_0 is chosen such that the total mass transported through the regenerator in each period is equal to the total mass of the paramagnetic material. Finally τ_1, τ_2, τ_3 and τ_4 are assumed to be independent of ξ.

The stylization of the mean density is very close to reality. It is indeed constant from the moment the leading edge of the paramagnetic material arrives at a point in the regenerator till the moment the trailing edge passes. During the rest of the time no paramagnetic material is present at that point and thus the regenerator is then empty. For the effective density we may therefore write $\varrho_m = \varrho_0|\varphi|$, where ϱ_0 must be chosen $\varrho_1 l\,(\tau_2 - \tau_1)$.

According to the last stylization, Λ^+ is constant when $\varphi \neq 0$ and $\Lambda^+ = 0$ when $\varphi = 0$. The last part of this stylization is absolutely correct since no paramagnetic material is in the regenerator during that part of the cycle and therefore no heat can be transferred to it. During the rest of the cycle Λ^+ is in reality not constant. It depends on the mass flow in the regenerator and the temperatures of the gas and the paramagnetic material. This situation exists in normal regenerators too and a mean value of the heat-transfer number is always used. Since the results are quite satisfactory there, it seems justified to do the same here.

2.6.6. *Calculation of the energy flow*

To obtain an equation for the energy flow in the regenerator we shall treat the magneto-caloric effects as small perturbations that do not influence the temperature difference between the paramagnetic material and the regenerator gas. It will be shown later that in the major part of the regenerator the magnetic heating is slight compared to the amount of heat already transferred without magnetic effects. In this respect we recall that the mean field on the paramagnetic material is approximately proportional to $(T - \Theta)$ when it moves through the regenerator. Thus the magneto-caloric effects, being proportional to a change of $H^2/(T - \Theta)^2$ can be small indeed. This point is discussed further in the next section.

Since the additional heat that must be transferred in the regenerator due to the magneto-caloric effects is slight, we can obtain a rather good approximation of the energy flow J if the magnetic terms in eq. (2.26) are left out. By the stylization discussed in the preceding section, this equation obtains only when $\varphi \neq 0$. Furthermore in the equation ψ must be replaced by $|\varphi|$. It then becomes

$$\varphi = (\tau_2 - \tau_1)^{-1} \quad \text{(cold period)}$$

$$\Lambda^+ (T_g - T_m) = |\varphi| \, (1/\Lambda) \, \partial T_m/\partial\tau + \varphi \, \partial T_m/\partial\xi \tag{2.45}$$

$$\varphi = -(\tau_2 - \tau_1)^{-1} \text{(warm period)}$$

In this equation T_g is independent of τ according to our stylization. Moreover, the boundary conditions (2.32) are independent of τ also, although they are different in each period. In this case we obtain in the two periods different values of T_m, which are also independent of τ. They are found from the equation

$$T_g - T_m = (\varphi/\Lambda^+) \, \partial T_m/\partial\xi \qquad \varphi = \pm (\tau_2 - \tau_1)_-{}^1. \tag{2.46}$$

This equation indeed yields two different values of T_m for the two periods; furthermore both are independent of time. This equation is developed in a power series of $(\Lambda^+)^{-1}$ for a further approximation as follows. Equation (2.46) is written

$$T_g - T_m = (\varphi/\Lambda^+) \, \partial T_g/\partial\xi - (\varphi/\Lambda^+) \, \partial(T_g - T_m)/\partial\xi. \tag{2.47}$$

The last term of this equation can be obtained by differentiation of (2.46). Repeating this procedure a number of times we obtain

$$T_g - T_m = \frac{\varphi}{\Lambda^+} \frac{\partial T_g}{\partial\xi} - \left(\frac{\varphi}{\Lambda^+}\right)^2 \frac{\partial^2 T_g}{\partial\xi^2} + \left(\frac{\varphi}{\Lambda^+}\right)^3 \frac{\partial^3 T_g}{\partial\xi^3} \ldots (-1)^{n-1} \left(\frac{\varphi}{\Lambda^+}\right)^n \frac{\partial^n T_m}{\partial\xi^n}. \tag{2.48}$$

We shall assume that $\partial^n T_m/\partial\xi^n$ and the derivatives of T_g are of the same

order of magnitude as $\partial T_g/\partial\xi$. The successive terms in eq. (2.48) will then decrease rapidly. To calculate T_m we shall use only the first term, as normally $\Lambda^+ \geqslant 50$ so that the second term is already much smaller. Thus

$$T_{m1} = T_g - [1/\Lambda^+ (\tau_2 - \tau_1)]\, \partial T_g/\partial\xi \quad \text{(cold period)}$$
$$\text{and} \tag{2.49}$$
$$T_{m2} = T_g + [1/\Lambda^+ (\tau_2 - \tau_1)]\, \partial T_g/\partial\xi \quad \text{(warm period)}.$$

A simple relation for J is now obtained by substituting T_m in eq. (2.19). Using the dimensionless coordinate τ in that equation, we find

$$J = w_0 \int_0^2 \varphi u_0 \, d\tau = w_0 \, [u_0 (T_{m1}) - u_0 (T_{m2})]. \tag{2.50}$$

The substitution of T_{m1} and T_{m2} gives

$$J = -(2\, m_k c_0/\Lambda^*)\, \partial T_g/\partial\xi, \tag{2.51}$$

where

$$\Lambda^* = \Lambda^+ (\tau_2 - \tau_1). \tag{2.52}$$

Since $(T_m - T_g)$ is small, we have written

$$u_0(T_m) = u_0(T_g) + c_0 \, [T_m - T_g].$$

Using eq. (2.51) we can determine the energy flow in the regenerator from the temperature gradient of the gas. Furthermore, this equation contains well determined quantities such as m_k and c_0. We shall discuss later on in sec. 2.6.10 how Λ^+ can be obtained.

2.6.7. *The heat load of the regenerator*

In the preceding section we have assumed that the amount of heat transferred in each period from the paramagnetic material to the gas (or the other way round) in a section $\Delta\xi$ is large compared to the magnetic heating in that section. This will be discussed here in more detail.

The assumption that this is at least true in the major part of the regenerator is subsequently confirmed by the result of the calculations in chapter 3. In fig. 3.11 the heat load ΔL and the magnetic heating ΔR of a section $\Delta\xi$ of the regenerator are shown as a function of the place in the regenerator in a typical case. Except for the warm side of the regenerator, the heat load in this regenerator is mainly due to the non-magnetic terms.

We can make this understandable as follows. The heat load of a section $\Delta\xi$ is obviously

$$\Delta L = a\, F\, |T_g - T_m|\, (\tau_2 - \tau_1)\, \tfrac{1}{2}\, t_p\, \Delta\xi. \tag{2.53}$$

If no magneto-caloric effects occur, this equation can be reduced, by substitution of (2.49) and (2.28), to

$$\Delta L = m_k c_0\, |\partial T_g/\partial\xi|\, \Delta\xi = \tfrac{1}{2}\, \Lambda^*\, |J|\, \Delta\xi. \tag{2.54}$$

The temperature distribution must then be such that $\Delta R = 0$. In this case the mean value of a must be approximately the same everywhere in the regenerator. Thus the temperature at each point is approximately $T_g \approx (\Theta + \bar{H}/\bar{a})$ where $\bar{a}$ is the mean value of a and $\bar{H}$ is the mean value of the magnetic field on the paramagnetic material during the warm period. In the regenerator H is made to decrease smoothly from a value $a_0 (T_h - \Theta)$ at the warm side to approximately $a_0 (T_l - \Theta)$ at the cold side. Thus the temperature in the regenerator decreases smoothly too, from the value T_h at the warm side to the value T_l at the cold side.

Let us suppose that such a temperature distribution has been obtained for which $\Delta R = 0$. If we now calculate J with eq. (2.51) and substitute this in eq. (2.18), this last-named equation is not satisfied for $\Delta R = 0$. Thus the temperature distribution must be slightly changed until eq. (2.18) is satisfied. Then ΔR must assume values that are of the order of magnitude of $(\mathrm{d}J/\mathrm{d}\xi)\,\Delta\xi$. Using eq. (2.51) this is found to be of the order of $(2\, m_k c_0/\Delta^*)\, |\partial^2 T_g/\partial\xi^2|\, \Delta\xi$. Now, comparing ΔL from eq. (2.54) with ΔR we find

$$\frac{|\Delta R|}{|\Delta L|} = \frac{2}{\Delta^*} \frac{|\partial^2 T_g/\partial\xi^2|}{|\partial T_g/\partial\xi|}. \tag{2.55}$$

Thus, as long as $|\partial^2 T_g/\partial\xi^2|$ is of the same order as $|\partial T_g/\partial\xi|$, the magnetic heating is less than the normal heat load by a factor of about $\frac{1}{2}\Delta^*$. The temperature distribution for $\Delta R = 0$ decreases smoothly from the warm side to the cold side and it may be expected therefore that the above derivatives are normally of the same order. Since Δ^* is very large this leads to $|\Delta R| \ll |\Delta L|$.

It should be pointed out that this result is no longer correct if the magnetic field on the paramagnetic material at the cold side of the regenerator is not properly adapted. This situation arises, for example, when the refrigerating capacity is calculated at an operating temperature below or above that for which the refrigerator is designed.

2.6.8. *Approximation for the magnetic heating*

The magnetic heating ΔR is given by eq. (2.20). This equation can be transformed to the dimensionless coordinates $\xi = x/l$ and $\tau = t/\frac{1}{2} t_p$ and applied on a section between ξ_n and ξ_{n+1}:

$$\Delta R = -\int_{\xi_n}^{\xi_{n+1}} \mathrm{d}\xi \int_0^2 [f V_R T_m\, \partial(\varrho_m s_M)/\partial\tau + \tfrac{1}{2} t_p T_m\, \partial(w s_M)/\partial\xi]\, \mathrm{d}\tau. \tag{2.56}$$

In sec. 2.6.6 it was found that T_{m1} and T_{m2} are independent of τ (see eq. (2.46)). By substituting also $\varrho_m = \varrho_0\, |\varphi|$, the first integral in eq. (2.56) can be written

$$f V_R \varrho_0 \int_{\xi_n}^{\xi_{n+1}} \mathrm{d}\xi \left[T_{m1} \int_0^1 \frac{\partial(|\varphi| s_M)}{\partial\tau}\, \mathrm{d}\tau + T_{m2} \int_1^2 \frac{\partial(|\varphi| s_M)}{\partial\tau}\, \mathrm{d}\tau \right] = 0. \tag{2.57}$$

Since $|\varphi|$ is zero for $\tau = 0$, $\tau = 1$ and $\tau = 2$ this equation is also equal to zero and eq. (2.56) is then reduced to

$$\Delta R = \tfrac{1}{2}\, t_p \int_{\xi_n}^{\xi_{n+1}} \mathrm{d}\xi \int_0^2 [T_m\, \partial(ws_M)/\partial\xi]\, \mathrm{d}\tau. \tag{2.58}$$

In numerical calculations the sections $\Delta\xi$ are taken very small, so that mean temperatures $\bar{T}_{m1}$ and $\bar{T}_{m2}$ may be used in each period. Then

$$\Delta R = \tfrac{1}{2}\, t_p \bar{T}_{m1} \Big[\int_0^1 (ws_M)_{n+1}\mathrm{d}\tau - \int_0^1 (ws_M)_n \mathrm{d}\tau\Big] + \\ + \bar{T}_{m2} \Big[\int_1^2 (ws_M)_{n+1}\mathrm{d}\tau - \int_1^2 (ws_M)_n \mathrm{d}\tau\Big]. \tag{2.59}$$

Finally the integral $\frac{1}{2}\, t_p \int_0^1 (ws_M)\, \mathrm{d}\tau$ can be written as a sum $\sum \frac{1}{2}\, t_p\, ws_M \Delta\tau = \\ = \sum s_M \Delta m_k$ and the following obtained:

$$\Delta R = \bar{T}_{m1} [(\sum s_M \Delta m_k)_{c,n+1} - (\sum s_M \Delta m_k)_{c,n}] + \\ + \bar{T}_{m2} [(\sum s_M \Delta m_k)_{w,n+1} - (\sum s_M \Delta m_k)_{w,n}]. \tag{2.60}$$

The indices c and w refer to the cold period and the warm period, respectively, while the indices n and $(n+1)$ indicate the beginning and the end of the nth section. The entropy of the paramagnetic material can be calculated for each amount Δm_k from the temperature and the magnetic field the moment it is at ξ_n and ξ_{n+1}, respectively.

2.6.9. *Calculation of the temperature distribution and the energy flow*

The temperature distribution is now calculated easily. The first value for the temperature gradient of the gas at $\xi = 0$ is chosen equal to that of the temperature distribution that makes α constant for the middle of the regenerator. The temperature difference $\Delta T_1 = T_m - T_g$ between the paramagnetic material and the gas at $\xi = 0$ can now easily be calculated from eq. (2.49), provided Λ^+ is known. The determination of Λ^+ will be discussed later. The paramagnetic material has a temperature T_{Du}, when it flows into the regenerator in the cold period. The gas temperature T_1 at $\xi = 0$ and the temperature T_{Dk} of the paramagnetic material emerging from the regenerator (see fig. 2.3) are now $T_{Du} + \\ + \Delta T_1$ and $T_{Du} + 2\,\Delta T_1$. The gas temperature T_2 at the end of the first section is determined by trial and error till eq. (2.18) is satisfied for this section. To calculate J from eq. (2.52) the temperature gradient at $\xi = 1/N$ is approximated as $N(T_2 - T_1)$. When T_2 has been found, the temperature at the end of the second and the following sections is determined successively in the same way. At the end of the last section the gas temperature T_{N+1} and the temperature difference ΔT_{N+1} are obtained. Now $T_{N+1} + \Delta T_{N+1}$ must be equal to the

temperature T_{Mu} of the paramagnetic material when it flows into the regenerator during the warm period. If T_{Mu} differs too much from $T_{N+1} + \Delta T_{N+1}$, a new temperature gradient at the cold side is chosen. When finally a correct temperature distribution has been found, the energy flow through the regenerator for a magnetic refrigerator, running n cycles per minute, may be written as

$$\Delta P_{DR} = (n/30)\, m_k c_0\, \Delta T_1 \qquad \text{(cold side)} \tag{2.61}$$

and

$$\Delta P_{MR} = (n/30)\, m_k c_0\, \Delta T_{N+1} \qquad \text{(warm side).} \tag{2.62}$$

Besides the contribution of the paramagnetic material to the energy flow through the regenerator there is also a contribution from the stabilizers. The heat capacity of the stabilizers is, however, much lower than that of the paramagnetic material, since their filling factor is much lower and the material used has itself a low heat capacity. Moreover, they do not pass completely through the regenerator. For these two reasons their contribution to the energy flow is very small compared to that of the paramagnetic material. In the refrigerator calculations an estimated value of their contribution to the energy flow through the regenerator is based on the following assumptions.

(a) The stabilizers do not change the temperature distribution in the regenerator which is established by the paramagnetic material.
(b) Their contribution to the energy flow through the regenerator can be calculated as though one stabilizer passed completely through the regenerator and the temperature difference between the stabilizer material and the gas were the same as the temperature difference found for the paramagnetic material.

Then the energy flow through the regenerator, including the contributions of the paramagnetic material and the stabilizers, is obtained by replacing $m_k c_0$ in eqs (2.61) and (2.62) by $(m_k c_0 + m_s c_s)$. This gives

$$\Delta P_{DR} = (n/30)\, (m_k c_0 + m_s c_s)\, \Delta T_1 \tag{2.63}$$

and

$$\Delta P_{MR} = (n/30)\, (m_k c_0 + m_s c_s)\, \Delta T_{N+1}. \tag{2.64}$$

Here m_s is the amount of material in *one* stabilizer and c_s the heat capacity of this material.

2.6.10. *Calculation of the heat-transfer numbers Λ^+ and Λ^**

We have not yet discussed how Λ^+ should be calculated. In the derivation of the differential equation Λ^+ was introduced as

$$\Lambda^+ = a\, F/w_1 c_0. \tag{2.28}$$

In this equation F is the total surface available for heat transfer in the stylized

regenerator. We shall now derive an equation between F and the total heat-transfer surface F_m of the paramagnetic material.

A small section $\Delta x = l\Delta\xi$ of the stylized regenerator has the heat-transfer surface $(F/l)\,\Delta x$. This surface is used only during the time the paramagnetic material moves through the section Δx. At any moment during this time interval this surface is equal in area to that of the paramagnetic material in the section Δx. This amount is $f B \varrho_m \Delta x$. Its surface is $(f B \varrho_m F_m/m_k)\,\Delta x$ where m_k is the total mass of the paramagnetic material. From the equality of the two surfaces it follows that

$$F = f V_g \varrho_m F_m/(1-f)\, m_k, \tag{2.65}$$

where $l = V_g/(1-f)\,B$ has been substituted. The volume of the gas that makes up the regenerator is denoted by V_g.

The right-hand side of this equation contains only quantities that are directly available from the general calculation on which the refrigerator is based and which are discussed later on.

The heat-transfer coefficient a is known for many types of regenerator packings, for instance in the form of small balls and gauzes. Often, however, direct empirical equations are derived from the measurements that give a Λ for a normal regenerator. This Λ is defined as

$$\Lambda = a F_0/\dot{m} c_p,$$

where $\dot{m}$ is the mass flow of the gas, c_p its specific heat at constant pressure and F_0 the heat-transfer surface of the regenerator. The empirical equations give Λ as a function of Reynolds' number, Prandtl's number and certain geometrical factors.

It is convenient to derive a direct equation between Λ^+ and Λ. The heat-transfer number Λ can be calculated with the empirical equation if the paramagnetic material is regarded as a normal regenerator. It has the heat-transfer surface F_m. The amount of gas m_g flows through this regenerator in each period during the time $(\tau_2 - \tau_1)\,\frac{1}{2}\,t_p$. It is equal to the total amount of gas $\varrho_g V_g$ that is used as a regenerator in the magnetic refrigerator. If the velocity of the gas with respect to the paramagnetic material is v, the mass flow of the gas is $\dot{m} = (1-f)\,B\varrho_g v$.

Regarding the gas as the regenerator again, we find $f B \varrho_m v$ for the mass flow of the paramagnetic material where v is the same velocity as above. In the definition of Λ^+ we used the mean mass flow w_1. Since the mass flow has the value $f B \varrho_m v$ only during the part $\tau_2 - \tau_1$ of the cycle and is otherwise zero, the mean value is $(\tau_2 - \tau_1) f B \varrho_m v$. Using these values of the mass flow of the gas and the paramagnetic material, the definition of Λ and those of Λ^+ and Λ^* (eqs (2.28) and (2.52)), the following equation is easily found:

$$\Lambda^* = (\tau_2 - \tau_1)\,\Lambda^+ = (\varrho_g c_p V_g/m_k c_0)\Lambda. \tag{2.66}$$

Finally we can substitute Γ^+ from eq. (2.29):

$$\Gamma^+ = \varrho_g c_p V_g / m_k c_0. \tag{2.29}$$

It then follows that

$$\Lambda^* = \Gamma^+ \Lambda. \tag{2.67}$$

We can now easily obtain Λ^* by calculating Λ and Γ^+. Both these quantities are given by equations that contain only parameters which can be calculated directly from the dimensions of the refrigerator.

2.6.11. *Summary of the regenerator calculations*

In the preceding sections a method has been developed to calculate an approximate value of the energy flow on both sides of the regenerator. Several simplifications were necessary to make this possible. The most important ones have been the assumptions that Γ^+ is large enough to justify the neglect of the variations of T_g and that the variation of the magnetic field is chosen such that the magnetic heating is small compared to the normal heat load of the regenerator.

Using a stepwise calculation, a temperature distribution can be determined that satisfies eq. (2.18). The temperature difference between the gas and the paramagnetic material is also obtained in the course of these calculations. Using these temperature differences the energy flow at both sides of the regenerator follows from eqs (2.61) and (2.62).

The heat-transfer number Λ^* which must be used in the calculations is related to the heat-transfer number Λ of normal regenerators by eq. (2.67). This last quantity can easily be calculated from the empirical equations and the dimensions of the refrigerator.

2.7. Numerical calculations of the stylized refrigerator

2.7.1. *Introduction*

In the following sections we shall discuss the performance of the refrigerator stylized as described in sec. 2.4. Our aim is to calculate the amount of heat delivered per second to the cooler and the amount of heat removed per second from the freezer.

The heat delivered to the cooler can be called the magnetization power as it is produced by the magnetization of the paramagnetic material. This magnetization power can be split up into an undisturbed magnetization power which is obtained by neglecting all losses including the energy flow through the regenerator, and the corrections due to these losses. The undisturbed magnetization power can be calculated by some further stylizations from the temperatures of the warm transport gas and the strength of the magnetic field at the moments the paramagnetic material enters the warm transport gas and emerges from this

part of the gas. The energy flow through the regenerator is calculated as described in the preceding section. The determination of the other losses is discussed later on.

In the same way the term demagnetization power can now be introduced for the heat removed in the process from the freezer. It is split up again into an undisturbed demagnetization power and the losses that can be calculated separately.

In calculating these quantities the same coordinate z will be used that was already introduced in sec. 2.2 in the description of the principle of the magnetic refrigerator. This coordinate and some limiting factors in the design of a magnetic refrigerator are discussed in the next section. The actual calculation of the refrigerator follows in secs 2.7.3-2.7.6.

2.7.2. *The coordinate system and some design limitations*

In the further analysis of the refrigerator itself, the same coordinate z will be used that was already introduced in sec. 2.2. It refers to the position of fictitious planes P with respect to the piston P_1, as shown in fig. 2.9. These planes are perpendicular to the gas flow and their coordinate z is defined by

$$z = V/V_t. \tag{2.68}$$

Here V_t is the total gas volume in the refrigerator and V is the volume between a fictitious plane and the piston P_1. We recall that not only the volume but also the mass of gas between any two coordinates z_a and z_b remains constant since temperature and pressure fluctuations are neglected.

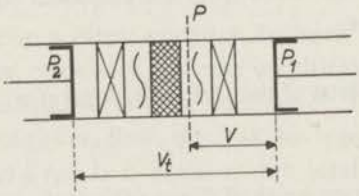

Fig. 2.9. The defintion of the coordinate $z = V/V_t$ that determines the position of a fictitious plane P moving with the gas. The gas volume between P and the piston P_1 is V. The total gas volume between the two pistons is V_t.

It is obvious that this coordinate can be used just as well if the cross-sectional area for the gas flow is not constant in the refrigerator and the direction of the gas flow is not the same in all components. The fictitious planes P, which move with the gas, are chosen everywhere perpendicular to the gas flow, even if the direction of the gas flow changes somewhere. The coordinate z is defined again by eq. (2.68). It is now, of course, a complicated function of the coordinates in some geometrical coordinate system. The amount of gas between two different

coordinates z_a and z_b remains constant again and this is the only thing that matters for the description of the refrigerator.

From the discussion in sec. 2.2 it is obvious that any mixing of the gas in the passive parts and the transport parts of the gas is unimportant. Thus all that is necessary is good stability of the regenerative part of the gas (regenerator). The regenerator moves only from one stabilizer through the paramagnetic material into the other stabilizer and back again. In any design of the refrigerator these components are certainly placed in juxtaposition. Their cross-sectional area will be large and since, moreover, the speed of the refrigerator will be low, the gas velocities in these components are low too. Therefore inertial effects that might cause instabilities are negligible. Furthermore, the direction of the gas flow in the paramagnetic material and both stabilizers is the same. Between z_2 and z_3, z is thus a simple relation of the coordinates of a geometrical coordinate system. We recall that z_2 and z_3 are the coordinates of the beginning and the end of the regenerator. This is convenient when the magnetic field on the paramagnetic material must be calculated during its "passage" through the regenerator.

The total gas volume was divided into five sections (see sec. 2.2):

($0 \ldots z_1$) passive part on the demagnetization side (this part never enters the paramagnetic material),
($z_1 \ldots z_2$) cold transport gas
($z_2 \ldots z_3$) regenerative part or regenerator,
($z_3 \ldots z_4$) warm transport gas,
($z_4 \ldots 1$) passive part on the magnetization side (just as the other passive part it never enters the paramagnetic material).

We shall determine the coordinates of these parts from the dimensions of the various components of the refrigerator. For the volumes available for the gas in these components we shall use the following notation:

V_p volume swept by the pistons at the warm and the cold sides,
V_h gas volume in the freezer,
V_s gas volume in the stabilizer between the freezer and the paramagnetic material,
V_m gas volume between the particles of the paramagnetic material,
V_s gas volume in the other stabilizer,
V_h gas volume in the cooler.

The two stabilizers will have the same construction and therefore the same volumes. The two pistons are also equal in swept volume, as already stated. Finally, it has been assumed for symmetry that the gas volumes in the freezer and the cooler are equal. If this is not so, the necessary corrections can easily

be found. They will not introduce any essential change in the calculations. The volume variations caused by the pistons on the two sides are

$$V_D = \tfrac{1}{2} V_p [1 - f(\beta)] \tag{2.69}$$

and

$$V_M = \tfrac{1}{2} V_p [1 + f(\beta)]. \tag{2.70}$$

Here V_D is the variable volume on the demagnetization side and V_M the variable volume on the magnetization side. Furthermore β is the crank angle and $f(\beta)$ a periodic function of β with an amplitude of unity. For a normal drive $f(\beta)$ can be written approximately as $\cos \beta$. The demagnetization then occurs approximately at $\beta = 0$ and the magnetization when $\beta = \pi$. However nearly any function for $f(\beta)$ can of course be realized if it were favourable to do so.

The total gas volume is

$$V_t = V_p + 2 (V_h + V_s) + V_m. \tag{2.71}$$

Using fig. 2.1 we can now easily derive equations for z_1, z_2, z_3 and z_4 with the following argumentation.

The passive part on the cold side never enters the paramagnetic material. The moment that V_D is zero, z_1 just reaches the transition between the cold stabilizer and the paramagnetic material. This leads directly to the equation given for z_1 below. For the same reason z_4 lies at the transition from the paramagnetic material to the warm stabilizer when V_M is zero. This gives an equation for z_4.

In the same way, the condition that the regenerator never enters the freezer and the cooler, gives equations for z_2 and z_3. Thus the following equations are obtained:

$$\begin{aligned} z_1 &= (V_h + V_s)/V_t, & z_2 &= (V_p + V_h)/V_t, \\ z_3 &= (V_h + 2\,V_s + V_m)/V_t, & z_4 &= (V_p + V_h + V_s + V_m)/V_t. \end{aligned} \tag{2.72}$$

We shall now discuss a number of limitations in the design of a magnetic refrigerator. These limitations originate from:

(1) a minimum size of some parts of the gas volume;
(2) a minimum value of the heat-capacity number Γ^+ of the regenerator.

It is obvious that the volume of the regenerator must be equal to or less than that of the stabilizers. Hence

$$(z_3 - z_2)\, V_t \leqslant V_s. \tag{2.73}$$

By substitution of z_2 and z_3 it is easily shown that this equation is satisfied if

$$V_p = A_d\, (V_s + V_m) \qquad (A_d \geqslant 1). \tag{2.74}$$

Moreover, the gas volume interspersed among the paramagnetic material must be smaller than both transport parts of the helium. If this condition is not satisfied, the paramagnetic material obviously does not come out of the regenerator completely. Fortunately this condition is fulfilled too if eq. (2.74) is satisfied. This is easily verified by the substitution of (2.74) in

$$(z_2 - z_1)\, V_t \geqslant V_m. \tag{2.75}$$

If $A_d = 1$ we have an equality in both equation (2.73) and equation (2.75). In a practical design it is better to have a small safety margin and we shall therefore use $A_d = 1{\cdot}1$ in the calculations in chapter 3.

If a minimum value of Γ^+ is required, another equation between the volumes is found. Using eq. (2.29) and replacing V_g by $(z_3 - z_2)\, V_t$ in it we obtain

$$(z_3 - z_2)\, V_t \varrho_g c_p / m_k c_0 \geqslant \Gamma^+{}_{\min}. \tag{2.76}$$

Since $m_k = V_m \varrho_m f/(1-f)$, this equation can be reduced to

$$V_p = 2\, V_s + (1 - B_d)\, V_m, \tag{2.77}$$

where

$$B_d \geqslant f \varrho_m c_0\, (\Gamma^+)_{\min}/(1-f)\, \varrho_g c_p. \tag{2.78}$$

In this equation the heat capacity and the density of the gas, as well as the heat capacity of the paramagnetic material all depend on the temperature. Therefore B_d should be calculated at the temperature where $\varrho_m c_0/\varrho_g c_p$ is maximal. From (2.74) and (2.77) it now follows that

$$V_p = [A_d\, (B_d + 1)/(2 - A_d)]\, V_m \tag{2.79}$$

and

$$V_s = [(A_d + B_d - 1)/(2 - A_d)]\, V_m, \tag{2.80}$$

where $1 \leqslant A_d < 2$ and B_d is given by (2.78).

The upper limit for A_d is derived directly from these equations themselves, since neither V_p nor V_s can be negative.

In a design of a magnetic refrigerator we can choose the amount of paramagnetic material and its filling factor. Then the gas volume interspersed in the paramagnetic material is determined. If we choose further values for A_d and B_d (or $\Gamma^+{}_{\min}$) all other gas volumes in the refrigerator, except those of the heat exchangers, are determined by eqs (2.79) and (2.80).

The components of the refrigerator, with exception of the pistons, are moving relative to the coordinate z. The position of a plane fixed for one of these components is described by the equation

$$z = \tfrac{1}{2}\, d\, [1 - f(\beta)] + e_i, \tag{2.81}$$

where $d = V_p/V_t$ and $e_i = (\Sigma'_D V)/V_t$. The sum of all volumes (or parts of

these volumes) on the demagnetization side *) of the plane with exception of V_p is denoted by $\Sigma'_D V$. Thus e_i is the z-coordinate of the plane at the moment $f(\beta) = 1$. We shall call e_i the component coordinate. The gas velocity in a component is

$$v = -(V_t/S)\,\mathrm{d}z/\mathrm{d}t = (V_t\,d/2\,S)\,\mathrm{d}f/\mathrm{d}t, \tag{2.82}$$

where S is the cross-sectional area available for the gas flow in the component. We have chosen the sign in eq. (2.82) such that a *positive gas flow corresponds to a gas flow from the freezer to the cooler.*

If $f(\beta) = \cos\beta$,

$$v = -(\pi n\,V_t\,d/60\,S)\sin\beta, \tag{2.83}$$

where $\mathrm{d}\beta/\mathrm{d}t$ has been replaced by $2\pi n/60$. The number of revolutions per minute is denoted by n. The paramagnetic material and both stabilizers will remain some time in the regenerator during each cycle. For each point e_i in these components the moments can be determined at which it enters or leaves the regenerator. These moments will be called the transition moments. We shall use the following notation:

$$z_2 = \tfrac{1}{2}\,d\,[1 - f(\beta)] + e_i \;\rightarrow\; \begin{cases} \beta_{D1} \\ \beta_{D2} \end{cases}$$

and (2.84)

$$z_3 = \tfrac{1}{2}\,d\,[1 - f(\beta)] + e_i \;\rightarrow\; \begin{cases} \beta_{M1} \\ \beta_{M2}. \end{cases}$$

The moment the point leaves the regenerator is denoted by index 1 and the moment it enters the regenerator by index 2. The demagnetization and the magnetization sides of the regenerator are indicated by the indices D and M.

If $f(\beta)$ has its maximum at $\beta = 0$ and its minimum at $\beta = \pi$, then

$$\beta_{D1} \leqslant 0 \leqslant \beta_{D2}$$

and (2.85)

$$\beta_{M1} \leqslant \pi \leqslant \beta_{M2}.$$

These equations apply to any part of the paramagnetic material and some adjacent parts of the stabilizers which have four transition points. Points in the rest of the stabilizers have only two transition points, as they do not pass completely through the regenerator. In that case only one of the above equations applies.

The equations (2.85) can be derived from the fact that the moment that $\beta = 0$ the z-coordinate of any point in these components is the smallest and when $\beta = \pi$ it is the largest.

---

*) The name demagnetization side will be used for that side of the gas volume where the paramagnetic material is at demagnetization, and also for the corresponding side of the refrigerator; normally it is the cold side.

2.7.3. *Magnetization and demagnetization power*

The calculation of the magnetization power and the demagnetization power in the actual process would be very complicated. The stylized process is therefore used in the calculations. We shall give the most important points of this stylization below (see fig. 2.3).

(a) The heat transfer between the transport gas and the paramagnetic material is so high that the resulting temperature differences can be neglected.
(b) The transport gas has a uniform temperature T_{Mi} at the warm side and T_{Di} at the cold side when the paramagnetic material enters.
(c) Every part of the paramagnetic material has the temperature T_{Mk} or T_{Dk} at the moment it enters the transport gas.
(d) The paramagnetic material and the transport gas have the temperature T_{Mu} and T_{Du} when the paramagnetic material leaves the warm and the cold transport gas, respectively.
(e) The transport gas flows completely through the corresponding heat exchanger.

Of these stylizations the first is very close to reality, since the paramagnetic material has a very large heat-transfer number, as discussed in the regenerator theory.

The second stylization is rather good too. When the paramagnetic material enters the transport gas, this gas has just come from the corresponding heat exchanger. There its temperature has been made nearly equal to the temperature of the heat exchanger. During the passage through the stabilizer its temperature hardly changes, as has been stated earlier. Therefore the temperature of the transport gas is practically uniform when the paramagnetic material enters.

Assumptions (c) and (d) deviate somewhat more from reality. The temperature of the paramagnetic material is not completely uniform, due to the temperature fluctuations in the regenerator when Γ^+ is not very large. Thus the last amount of paramagnetic material coming out of the regenerator has a somewhat different temperature from the first amount. Moreover, not every part of the paramagnetic material will have the same temperature on leaving the transport gas, since these parts are not all magnetized equally. However, it will not be easy to find other stylizations that keep the calculations from becoming too complicated.

The last stylization is rather good since the volume of the heat exchangers can be made much smaller than the volume of the transport gas.

We can now calculate in the thus stylized process the heat discharged by the paramagnetic material to the warm transport gas. Each part of the paramagnetic material $\mathrm{d}m_k$ develops an amount of heat $\mathrm{d}m_k \int T\,\mathrm{d}s$. This integral

must be calculated between the moment β_{M1}, at which that part of the paramagnetic material enters the warm transport gas and the moment β_{M2}, at which it leaves this part of the gas. The total amount of heat discharged to the transport gas is found by integrating over the total amount of paramagnetic material lying between the component coordinates e_1 and e_2. If we replace $\mathrm{d}m_k$ by $m_k\,(e_2 - e_1)^{-1}\,\mathrm{d}e$, we may write

$$Q_M = [m_k/(e_2 - e_1)] \int_{e_1}^{e_2} \mathrm{d}e \int_{s_2}^{s_1} T\,\mathrm{d}s, \tag{2.86}$$

where $s_1 = s\,[H(\beta_{M_1}), T_{Mk}]$ and $s_2 = s\,[H(\beta_{M_2}), T_{Mu}]$.

We can now substitute eq. (2.4) for the entropy $s\,(H, T)$ of the paramagnetic material. The first part of this equation gives the entropy in zero field. Since the temperatures T_{Mu} and T_{Mk} are not far apart, we may use a mean value of the specific heat c_0 in this temperature range. Then the integration in eq. (2.86) over this part of the entropy is easily carried out. The second part of eq. (2.4) represents the field-dependent part of the entropy. Integration over this part of the entropy in eq. (2.86) is only possible if the temperature is known at each moment. Since this temperature rises linearly with the amount of heat developed in the paramagnetic material, a rather good approximation is obtained by substituting a mean value $\bar{T}$ for this temperature. We shall discuss later the value which should be used for $\bar{T}$.

In this way we obtain for Q_m the equation

$$Q_m = m_k \left[c_0\,(T_{Mk} - T_{Mu}) + \frac{\frac{1}{2}\,c\bar{T}}{e_2 - e_1} \int_{e_1}^{e_2} \left\{ \frac{H^2\,(\beta_{M2})}{(T_{Mu} - \Theta)^2} - \frac{H^2\,(\beta_{M1})}{(T_{Mk} - \Theta)^2} \right\} \mathrm{d}e \right]. \tag{2.87}$$

In this equation, except for a factor $(n/60)$, we recognize the first part on the right-hand side as the energy flow at the warm side of the regenerator, given in a somewhat different notation in eq. (2.62). The second part of eq. (2.87), after multiplication by $(n/60)$, gives the undisturbed magnetization power P_{M0} found if the energy transport is zero.

It is now possible to calculate Q_M if T_{Mu} and T_{Mk} are known. Before we proceed to discuss how these temperatures can be determined, we must decide on the value of $\bar{T}$ to be used. The best approximation is to use the mean temperature at which the magnetization occurs. Then we should first calculate the temperature of the paramagnetic material just after it has entered the warm transport gas and before the magnetic field has increased appreciably. This temperature must lie between T_{Mk} (the temperature of the paramagnetic material at the moment it enters the warm transport gas) and T_{Mi} (the temperature of this gas itself at that moment). This temperature can be calculated easily when the magnetic field is exactly zero at that moment. However, in practice the field

is often not zero, so that magneto-caloric effects also occur. The calculation of this temperature is then rather cumbersome. Since, however, the specific heat of the paramagnetic material is much less than that of the helium gas and, moreover, the magneto-caloric effects are slight, a rather good approximation is obtained when we assume that the magnetization of the paramagnetic material begins at temperature T_{Mi}. Then we can use $\bar{T} = \frac{1}{2}(T_{Mi} + T_{Mu})$ as mean temperature.

The undisturbed magnetization power obtained from the second part of eq. (2.87) can now be written as

$$P_{M0} = \frac{n}{60} m_k \frac{c\,(T_{Mu} + T_{Mi})}{4\,(e_2 - e_1)} \int_{e_1}^{e_2} \left[\frac{H^2\,(\beta_{M2})}{(T_{Mu} - \Theta)^2} - \frac{H^2\,(\beta_{M1})}{(T_{Mk} - \Theta)^2} \right] de\,. \quad (2.88)$$

Using this equation and eq. (2.87), we can write for the amount of heat transferred per second to the warm transport gas:

$$P_{M1} = P_{M0} - \Delta P_{MR}. \quad (2.89)$$

Here ΔP_{MR} is the energy flow at the warm side of the regenerator. To include the losses caused by the stabilizers, it is calculated from eq. (2.64), instead from eq. (2.62).

The temperatures T_{Mu} and T_{Mi} are found from an analysis of the cycle of the warm transport gas. The heat developed in the paramagnetic material is transferred to the warm transport gas. This gas is thus heated from temperature T_{Mi} to temperature T_{Mu}, giving the equation

$$P_{M1} = (n/60)\,(z_4 - z_3)\,V_t \varrho_g c_p\,(T_{Mu} - T_{Mi}). \quad (2.90)$$

The transport gas will flow into the cooler at temperature T_{Mu}. According to the stylization it flows completely through the cooler and back again. The effect is then the same as is obtained if the gas flows once through a double-length heat exchanger.

The heat-transfer number of the cooler will be denoted as Λ_M. This heat-transfer number is defined, just as in a normal regenerator, as $\Lambda_M = a\,F/w\,c_p$. Here a and F are the heat-transfer coefficient and the heat-transfer surface of the cooler, whereas w is the mass flow of the gas in the cooler and c_p the specific heat of one gramme of gas. When the cooler has a constant wall temperature T_{M0} the following equation can easily be derived:

$$(T_{Mi} - T_{M0}) = (T_{Mu} - T_{M0}) \exp(-2\,\Lambda_M). \quad (2.91)$$

The factor 2 arises from the "double length" mentioned before.

Using this equation the following equations for T_{Mu} and T_{Mi} can be obtained:

$$T_{Mi} - T_{M0} = \Delta T_{tr} [\exp(2\Lambda_M) - 1]^{-1} \tag{2.92}$$

and

$$T_{Mu} - T_{M0} = \Delta T_{tr} \exp(2\Lambda_M) [\exp(2\Lambda_M) - 1]^{-1}, \tag{2.93}$$

where $\Delta T_{tr} = T_{Mu} - T_{Mi}$ is the temperature difference necessary for the transport of the heat.

Substitution of $T_{Mu} - T_{Mi}$ from eq. (2.90) gives

$$T_{Mi} = T_{M0} + \frac{1}{\exp(2\Lambda_M) - 1} \frac{P_{M1}}{(n/60)(z_4 - z_3) V_t \varrho_g c_p}, \tag{2.94}$$

$$T_{Mu} = T_{M0} + \frac{\exp(2\Lambda_M)}{\exp(2\Lambda_M) - 1} \frac{P_{M1}}{(n/60)(z_4 - z_3) V_t \varrho_g c_p} \tag{2.95}$$

and

$$\tfrac{1}{2}(T_{Mu} + T_{Mi}) = T_{M0} + \frac{P_{M1}}{(n/30)(z_4 - z_3) V_t \varrho_g c_p} \coth \Lambda_M. \tag{2.96}$$

To obtain T_{Mu} and T_{Mi} from these equations we must use an iterative calculation as P_{M1} itself depends on these temperatures. Thus we may determine P_{M1} using an estimated value of the two temperatures and we may calculate new values of these temperatures with eqs (2.94) and (2.95). Using these new temperatures, P_{M1} can be calculated again. The calculation can be repeated till practically constant values for T_{Mu} and T_{Mi} are found.

In exactly the same way similar relations can be derived for the cold side:

$$P_{D1} = P_{D0} + \Delta P_{DR}, \tag{2.97}$$

$$P_{D0} = \frac{n}{60} m_k \frac{c(T_{Du} + T_{Di})}{4(e_2 - e_1)} \int_{e_1}^{e_2} \left[\frac{H^2(\beta_{D2})}{(T_{Du} - \Theta)^2} - \frac{H^2(\beta_{D1})}{(T_{Dk} - \Theta)^2} \right] de, \tag{2.98}$$

$$T_{Di} = T_{D0} + \frac{1}{\exp(2\Lambda_D) - 1} \frac{P_{D1}}{(n/60)(z_2 - z_1) V_t \varrho_g c_p}, \tag{2.99}$$

$$T_{Du} = T_{D0} + \frac{\exp(2\Lambda_D)}{\exp(2\Lambda_D) - 1} \frac{P_{D1}}{(n/60)(z_2 - z_1) V_t \varrho_g c_p} \tag{2.100}$$

and

$$\tfrac{1}{2}(T_{Du} + T_{Di}) = T_{D0} + \frac{P_{D1}}{(n/30)(z_2 - z_1) V_t \varrho_g c_p} \coth \Lambda_D. \tag{2.101}$$

In deriving these equations we have again used a mean temperature at which the demagnetization occurs. This mean temperature is however more uncertain than at the warm side. When the paramagnetic material enters the cold transport gas it is colder than this gas (see fig. 2.3) and it is therefore heated as soon as it

enters. In contrast with the situation at the warm side, magnetization is now high, so that magneto-caloric effects are considerable. The difference between the final temperature of the paramagnetic material and the temperature T_{Mi} of the gas at the moment the paramagnetic material enters, will be relatively larger than at the warm side. If $\frac{1}{2}(T_{Du} + T_{Di})$ is used for the mean temperature of the demagnetization, a lower value is obtained than there will be in reality. In any case, too optimistic a value for P_{D0} will not be obtained.

Finally, it must be said that the temperatures T_{Mk} and T_{Dk} of the paramagnetic material, at the moment this material emerges at respectively the warm and the cold sides of the regenerator, follow directly from the regenerator calculations. These temperatures are used in the above calculations and they must therefore be determined anew in each iteration of these calculations. This means that the regenerator calculations are also repeated every time.

The ratio of the mean temperatures at which magnetization and demagnetization of the paramagnetic material occur, is higher than the ratio of the cooler and the freezer temperatures. It is obvious that for this reason the efficiency of the refrigerator is lower than the efficiency of an ideal refrigerator operating between the cooler and the freezer temperatures. Both the magnetization power and the demagnetization power of the actual refrigerator are lower than those of the ideal refrigerator. Their decrease due to this effect can be called the transport loss, since it originates from the necessity to transport heat from the paramagnetic material to the heat exchangers.

We have now obtained formulae to calculate the undisturbed magnetization power, the undisturbed demagnetization power, and the temperatures of the transport gas on both sides. The influence of the energy flow through the regenerator has been directly incorporated. It will be assumed that the other losses to be discussed in the following sections flow directly to the freezer and the heater. They will then not influence the temperature distribution in the gas nor the value of ΔT_{tr}.

The equations obtained in this section and those describing the regenerator are fully adequate for calculating the complete temperature distribution in the refrigerator and the values of the undisturbed magnetization power, the undisturbed demagnetization power, and the energy flow at both the cold side and the warm side of the regenerator.

2.7.4. *Flow losses*

Due to the gas flow in the various components of the refrigerator a pressure difference between the cylinder on the magnetization side and that on the demagnetization side will arise. The pressure in the cylinder on the magnetization side can be written

$$p_M = \bar{p} + \delta p_M. \tag{2.102}$$

Here $\bar{p}$ is the mean pressure in the refrigerator and δp_M is the variation of the pressure in this cylinder. In the same way

$$p_D = \bar{p} + \delta p_D. \tag{2.103}$$

The subscript D refers to the other cylinder. The pressure difference between both cylinders is then

$$\Delta p = \delta p_M - \delta p_D. \tag{2.104}$$

The work performed by the pistons on the magnetization side and the demagnetization side is, respectively,

$$W_M = -\oint p_M \, \mathrm{d}V_M \tag{2.105}$$

and

$$W_D = -\oint p_D \, \mathrm{d}V_D. \tag{2.106}$$

The work performed by both pistons has a finite, positive value, for δp_M and δp_D are positive when the corresponding volume changes are negative, and negative when the volume changes are positive. It will be shown later on that a good approximation is obtained when it is assumed that the heat resulting from W_D ultimately flows to the freezer and that W_M is converted into heat flowing to the cooler.

The pressure drop Δp over any component can be calculated as a function of the gas flow with equations that can be found in the relevant textbooks. We will not go into the details of such a calculation. For the pressure variations in the cylinders one can write

$$\delta p_D = -b \, \Delta p \tag{2.107}$$

and

$$\delta p_M = (1 - b) \, \Delta p. \tag{2.108}$$

Now b can be calculated from the law of conservation of mass. The flow resistance of a component of the refrigerator will be taken as being concentrated in the middle of this component. Let us assume that at a certain moment this point has the gas coordinate z_f. If $\Delta p = 0$, the mass of the gas on the demagnetization side of z_f (that is, between 0 and z_f) is m_D. That on the magnetization side, between z_f and 1, is m_M. If Δp is not zero, the pressures at both sides of z_f must be such that the total mass of the gas in the refrigerator remains constant. Assuming that $\Delta p \ll p$ this gives

$$(\partial m_M/\partial p)\,(1 - b)\,\Delta p - (\partial m_D/\partial p)\, b\, \Delta p = 0. \tag{2.109}$$

From this equation b may be obtained:

$$b = (\partial m_M/\partial p)/(\partial m_t/\partial p), \tag{2.110}$$

where $m_t = m_D + m_M$. It is now possible to write

$$\partial m_M/\partial p = V_t \int_{z_f}^{1} \left(\frac{\partial \varrho_g}{\partial p}\right)_T \mathrm{d}z \tag{2.111}$$

and

$$\partial m_t/\partial p = V_t \int_{0}^{1} \left(\frac{\partial \varrho_g}{\partial p}\right)_T \mathrm{d}z\,. \tag{2.112}$$

Substitution in (2.110) gives

$$b = \int_{z_f}^{1} \left(\frac{\partial \varrho_g}{\partial p}\right)_T \mathrm{d}z \Big/ \int_{0}^{1} \left(\frac{\partial \varrho_g}{\partial p}\right)_T \mathrm{d}z\,. \tag{2.113}$$

The coordinate z_f of the component is not constant. Therefore b varies during the cycle. The pressure drop Δp is also variable due to the changing gas flow and the variation of the temperature of the component.

This makes it necessary to calculate the flow losses numerically with a computer. From eqs (2.105), (2.106), (2.69) and (2.70) the following equations for the flow losses can be derived:

$$\Delta P_{DF} = (n/60) \sum_i \sum_j [(\delta p_D)_{ij} (V_p/2) (\partial f/\partial \beta) \Delta \beta_i] \tag{2.114}$$

and

$$\Delta P_{MF} = -(n/60) \sum_i \sum_j [(\delta p_M)_{ij} (V_p/2) (\partial f/\partial \beta) \Delta \beta_i]. \tag{2.115}$$

The first summation $\sum_i$ is for a number of steps $\Delta \beta_i$ of the crank angle. The second summation $\sum_j$ involves the components whose contribution to the flow losses is calculated. In these equations the factor $(n/60)$ is added to give the flow losses per second.

Using eqs (2.113), (2.114) and (2.115) and empirical equations for Δp as a function of the gas flow, the flow losses can be calcated.

Let us now discuss the assumption that W_D flows to the freezer and W_M to the cooler. First it will be shown that the flow losses do not always result in a heating of the part that causes the pressure drop. When an ideal gas is used, in fact, no heat at all is developed there.

This can easily be shown by an example. In fig. 2.10 a cylinder is drawn in which a piston can move. The gas in the cylinder can be pushed through the outlet valve o in one channel of the heat exchanger v. From the heat exchanger it flows through the apparatus f, that has a large flow resistance, into a very large surge vessel u. Finally, the gas flows through the other channel of the heat exchanger and through the inlet valve i back into the cylinder. The inlet and

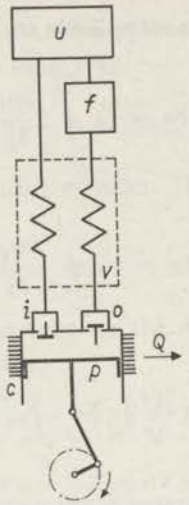

Fig. 2.10. Flow diagram of a system in which heat is developed by a flow resistance; c cylinder, p piston, o outlet valve, i inlet valve, v heat exchanger, f apparatus with large flow resistance and u surge vessel.

outlet valves and the heat exchanger have no flow resistance. Moreover the heat transfer in the heat exchanger is infinite.

The first law of thermodynamics can be used to derive the following equation for the variable volume of the cylinder:

$$-p\,\mathrm{d}V = \mathrm{d}Q + \mathrm{d}U + h\,\mathrm{d}m, \tag{2.116}$$

where $\mathrm{d}Q$ is the heat given out by the cylinder, $\mathrm{d}U$ the change of the internal energy of the gas in the cylinder, $h\,\mathrm{d}m$ the enthalpy of the amount of gas pushed out of the cylinder and $-p\,\mathrm{d}V$ the work done by the piston.

This equation can be integrated over a complete cycle. Then $\oint \mathrm{d}U = 0$, as the internal energy at the beginning and the end of the cycle must be the same in a stationary situation. Hence,

$$-\oint p\,\mathrm{d}V = \oint \mathrm{d}Q + \oint h\mathrm{d}m. \tag{2.117}$$

The enthalpy of an ideal gas does not depend on the pressure. Therefore the pressure drop in the apparatus f will cause no temperature change unless heat or mechanical work is extracted from the gas by this apparatus. This not being the case, there will be no difference between the temperature of the gas when it flows from the heat exchanger to f and its temperature when it returns to the heat exchanger. At the other side of this perfect heat exchanger there can also not be a temperature difference between the in- and outgoing gas flow. The enthalpy of the gas at the inlet and outlet valves of the cylinder must now be equal, for the temperature is the same and the enthalpy does not depend on the pressure. Thus $\oint h\,\mathrm{d}m = 0$. From eq. (2.108) it now follows that the heat

given out by the cylinder must be equal to the work performed by the piston.

When the experiment is repeated with an incompressible liquid, however, the result will be just inverted. The surge vessel u must of course be replaced by some large container partially filled with liquid. The rest of the container can be filled with a gas under pressure.

The enthalpy of an incompressible liquid is

$$h = u + p/\varrho. \tag{2.118}$$

Neither the internal energy nor the density will depend on the pressure p. Hence h is a linear function of p. The expansion in the apparatus f is again isenthalpic, but now an increase in temperature will result. An amount of heat $(p_1 - p_2)/\varrho$ must be removed to cool the liquid to the temperature it had prior to expansion. The pressures p_1 and p_2 are those before and after expansion.

In the heat exchanger the liquid is heated or cooled again to the temperature it had when it came out of the cylinder. This is a direct result of the fact that the specific heat at constant pressure $(\partial h/\partial T)_p$ is independent of the pressure level.

The temperatures of the flow of liquid at the inlet and outlet valves is therefore the same. It follows then that

$$\oint h \, \mathrm{d}m = m\,(p_1 - p_2)/\varrho, \tag{2.119}$$

where m is the total mass that leaves the cylinder at each stroke. The work done by the piston, displacing an incompressible liquid, is

$$-\oint p \, \mathrm{d}V = m\,(p_1 - p_2)/\varrho. \tag{2.120}$$

Both integrals are equal to the amount of heat removed in the apparatus f, when mass m has passed. Hence the work done by the piston is now completely converted into heat at the apparatus causing the flow resistance.

The enthalpy of the helium at the temperatures and pressures that occur in the magnetic refrigerator depends largely on the pressure. It is, however, far from an incompressible liquid. To calculate in this case exactly where the heat is developed is hardly possible. It will therefore be assumed that it is all developed in the adjacent heat exchangers. This will be the best approximation for the following reason.

The helium gas in the cylinder at the magnetization side has a temperature of the order of 15 °K and a pressure of the order of 20 atmospheres. Here the deviation from the behaviour of an ideal gas is slight. Therefore $\oint h \, \mathrm{d}m$ at the boundary between the cooler and the stabilizer will be small. Then most of the flow losses at this side will result in an extra cooler heat load. In the other cylinder the helium gas is at about 4 °K or lower. Here it comes nearer to resembling an incompressible liquid, so that $\oint h \, \mathrm{d}m \neq 0$. A large part of the flow losses at this side will result in heating of the part causing the flow resistance. However, part of this heat will ultimately arrive at a place which has a

lower temperature. The worst situation is when it all flows ultimately to the freezer. Therefore, taking this situation as an approximation, in any case a not too optimistic calculation of the refrigerator will be obtained.

In reality most of the flow losses occur in the paramagnetic material. This will cause a cross-effect with the energy transport in the regenerator.

If the heating by the flow losses could be calculated exactly at any moment, it should be added as an extra term in eq. (2.18). It will then lead to a decrease of ΔR, hence to a change in the entropy at a higher temperature than that of the freezer. To compensate an equal amount of heat, the entropy change can then be smaller than would be necessary at the freezer temperature. Given the condition that a fixed amount of entropy can be absorbed by the paramagnetic material on demagnetization, it is better if the flow losses are absorbed at a temperature above that of the freezer. This cross-effect will therefore have a favourable influence on the refrigerating capacity. However, we will neglect it, as the calculations are too involved.

2.7.5. *Conduction losses*

Conduction losses will occur in those parts that connect a higher temperature to a lower one. For most parts these losses can be determined by the usual methods. Only the heat conduction in the paramagnetic material and the stabilizers is not easily calculated. The temperature difference is bridged where the regenerator is. The regenerator is, however, in movement with respect to the components of the refrigerator. Therefore some mean values must be used.

The distance between the points with the high and the low temperature is

$$l = (z_3 - z_2)\, V_t/(1 - f)\, S. \tag{2.121}$$

This equation follows from the fact that the volume between those points must be equal to the regenerator volume. Now S is the cross-sectional area and f the filling factor in that region. They can, however, be different in the regenerator and in the stabilizer. Still l can be used to calculate the gradient locally. Assuming as an approximation that the temperature distribution in the regenerator is linear, the conduction loss is locally

$$\Delta P_{C1} = (1 - f)\, S^2 \lambda\, (T_{Mu} - T_{Du})/(z_3 - z_2)\, V_t. \tag{2.122}$$

Here λ is the thermal conductivity of a packed bed containing stabilizer material or paramagnetic material. Values of λ can be found in literature [14]) where λ is given as a function of the ratio of the thermal conductivities of the gas and the solid material in packed beds. In eq. (2.122) f, S and λ can be either those of the paramagnetic material or those of the stabilizer. We will use eq. (2.122) to calculate the conduction loss, using that set of values for f, S and λ

which gives the highest value of ΔP_{C1}. In practice these are the values of the paramagnetic material.

To calculate a mean value of the thermal conduction through the wall of the cylinder containing the paramagnetic material and the stabilizers we again use the length given by eq. (2.121) to obtain the temperature gradient. Then the loss caused by thermal conduction through this wall is

$$\Delta P_{C2} = \pi D d \, \lambda_w \, (T_{Mu} - T_{Du}) \, (1 - f) \, S/(z_3 - z_2) \, V_t, \qquad (2.123)$$

where D is the diameter of the cylinder, d the thickness of the wall and λ_w the thermal conductivity of the material of which the wall is made. For f and S we again choose the set that gives the highest value for ΔP_{C2}. In this case they are mostly those of the stabilizers.

2.7.6. *Eddy-current losses*

Eddy currents will be induced in metal parts by the varying magnetic field. To keep the heating as low as possible, the use of metals should be avoided as far as possible in the space where the magnetic field is present. The necessary metal parts should form no closed loops perpendicular to the field. Special constructions to avoid this will be discussed in chapter 3. Thin metal plates parallel to the field will not cause very much harm. The eddy-current heating can then be calculated with normal equations for transformers [15]):

$$\Delta P_E \approx (1/24) \, \varkappa \omega^2 d^2 B_M{}^2 V. \qquad (2.124)$$

Here ΔP_E is the heating caused by the eddy currents in the volume V, $\varkappa$ is the electrical conductivity, ω the angular frequency, B_M the magnetic induction and d the thickness of the plate. For every part where such heating occurs it must be determined where the heat will flow to. If it goes to the cold side it must be subtracted from the refrigerating capacity (ΔP_{DE}) and if it flows to the warm side, it must be added to the magnetization power (ΔP_{ME}).

2.8. Conclusion

In the preceding sections the equations have been derived to calculate the influence of the separate processes that take place in the refrigerator. These processes must now be combined to give a final value of the magnetization power P_M and the demagnetization power P_D.

To calculate the complete refrigerator we proceed as follows.

A preliminary temperature distribution in the helium is chosen such that

$$T_g = T_{D0} \qquad (0 < z < z_2),$$

$$T_g = T_a \qquad (z_2 < z < z_3),$$

$$T_g = T_{M0} \qquad (z_3 < z < 1).$$

Here T_a is the temperature that makes $a = H/(T - \Theta)$ constant during the warm period for the middle section of the paramagnetic material. Starting with the temperature gradient, obtained in this way at the cold side of the regenerator, a new temperature distribution is calculated between z_2 and z_3. The method was outlined at the end of sec. 2.6. For this calculation $T_{Mu} = T_{M0}$ and $T_{Du} = T_{D0}$. Then P_M, T_{Mi}, and a new value of T_{Mu} are calculated with eqs (2.88), (2.90), (2.94), (2.95) and (2.96). Likewise, P_D, T_{Di} and a new value of T_{Du} are determined with eqs (2.97)-(2.101). Using the new values of T_{Du} and T_{Mu}, the temperature distribution in the regenerator ($z_2 < z < z_3$) is determined once more. The process of calculating new temperature distributions and new values of P_M, P_D, T_{Mu}, T_{Mi}, T_{Du} and T_{Di} is repeated till a stationary situation is obtained.

Now the other losses are calculated as described in secs 2.7.4-2.7.6. These losses flow directly to the freezer and the cooler. We will neglect any cross-effect due to the other processes. The final values of the magnetization and the demagnetization power are then

$$P_M = P_{M0} - \Delta P_{MR} + \Delta P_{MF} - \sum_i (\Delta P_{MC})_i + \Delta P_{ME} + \Delta P_{IS} \quad (2.125)$$

and

$$P_D = P_{D0} + \Delta P_{DR} + \Delta P_{DF} + \sum_i (\Delta P_{DC})_i + \Delta P_{DE} + \Delta P_{IS}. \quad (2.126)$$

By ΔP_{IS} the insulation losses are denoted, which can be calculated with relations quoted in the relevant textbooks.

Appendix A

In sec. 2.6.2 the following equation was used for the heat absorbed in a fixed volume by a flow of paramagnetic material:

$$dQ/dt = \int_{x_n}^{x_{n+1}} [f B \varrho_m (\partial u_0/\partial t + T_m \partial s_M/\partial t) + w(\partial u_0/\partial x + T_m \partial s_M/\partial x)]\, dx. \quad (A.1)$$

The quantities ϱ_m, u_0, T_m, w and s_M are functions of the coordinate x and the time t.

This equation can be derived directly from the first law of thermodynamics

$$dq = du' - H'\, d\sigma'. \quad (A.2)$$

Here the quantities u', H' and σ' are taken for a gramme of paramagnetic material. Let us consider the fixed volume V_c shown in fig. A.1, which is part of a cylinder. Through it flows paramagnetic material from left to right. A coordinate x is used along the axis of the cylinder. The volume V_c is between x_1 and x_2. The cross-sectional area of the cylinder is A.

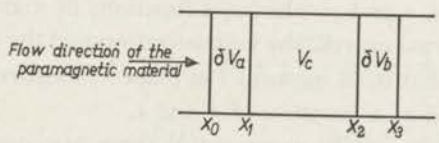

Fig. A.1. The derivation of the first law of thermodynamics for a control volume V_c.

In a short time interval between t_1 and $t_1 + \Delta t$ an amount of paramagnetic material Δm flows from the left-hand side into V_c. This amount of material occupied, at moment t_1, the volume δV_a. During the same time interval another amount of paramagnetic material leaves V_c at the right-hand side. This amount of material, which is not equal to Δm, occupies the volume δV_b at moment $t_1 + \Delta t$.

The volumes δV_a and δV_b are

$$\delta V_a = A v_a \Delta t \quad (A.3)$$

and

$$\delta V_b = A v_b \Delta t. \quad (A.4)$$

Here v_a and v_b are the mean values of the velocity of the paramagnetic material at x_1 and x_2, during the time interval Δt. At moment t volume V_c contains an amount of paramagnetic material m. The total amount of paramagnetic material $m + \Delta m$ that occupied the volume $V_c + \delta V_a$ at moment t_1, is at moment $t_1 + \Delta t$ in volume $V_c + \delta V_b$.

During the time interval Δt the paramagnetic material absorbs an amount of heat ΔQ between x_0 and x_3. With the first law of thermodynamics (A.2)

this amount of heat is found by integration over the total mass $m + \Delta m$ so that

$$\Delta Q = \int_0^{m+\Delta m} [\Delta u' - \tfrac{1}{2}(H_1' + H_2')\,\Delta\sigma']\,\mathrm{d}m, \tag{A.5}$$

where $\Delta u'$ is the change in internal energy of each particle in time interval Δt, $\Delta\sigma'$ the change in its magnetization, H_1' the magnetic field on the particle at moment t_1 and H_2' the field at moment $t_1 + \Delta t$. Thus

$$\Delta u' = u_2' - u_1' \tag{A.6}$$

and

$$\Delta\sigma' = \sigma_2' - \sigma_1', \tag{A.7}$$

where u_1' and σ_1' are the internal energy and the magnetization of the particle on the moment t_1, whereas u_2' and σ_2' are the same quantities of that particle at moment $(t_1 + \Delta t)$. Substitution of (A.6) and (A.7) in (A.5) gives

$$\Delta Q = \int_0^{m+\Delta m} [u_2' - \tfrac{1}{2}(H_2' + H_1')\,\sigma_2']\,\mathrm{d}m - \int_0^{m+\Delta m} [u_1' - \tfrac{1}{2}(H_2' + H_1')\,\sigma_1']\,\mathrm{d}m. \tag{A.8}$$

We now introduce u, σ and ϱ, which are functions of x and t. They represent respectively the internal energy, the magnetization and the density of the paramagnetic material, that is, at moment t at place x. Furthermore, the magnetic field H is introduced as a function of x and t.

Equation (A.8) will now be expressed in these new quantities. In the first integral on the right-hand side of this equation all the quantities are belonging to the paramagnetic material at moment $t_1 + \Delta t$, except H_1'. They can be replaced directly by u, σ and H at moment $t_1 + \Delta t$. However, for a particle that is at moment $t_1 + \Delta t$ at place x, H_1' can be written

$$H_1' = [H - (\partial H/\partial x)\, v\Delta t - (\partial H/\partial t)\,\Delta t]_2. \tag{A.9}$$

All quantities in this equation must be taken as at moment $t_1 + \Delta t$. This is indicated by the index 2 at the foot of the last bracket. The paramagnetic material is at moment $t_1 + \Delta t$ in the volume between x_1 and x_3. If $\mathrm{d}m$ is replaced in the integral by $A\varrho\,\mathrm{d}x$, the integration must be performed from x_1 till x_3. Thus

$$\int_0^{m+\Delta m} [u_2' - \tfrac{1}{2}(H_2' + H_1')\,\sigma_2']\,\mathrm{d}m =$$

$$= \int_{x_1}^{x_3} A\,[u\varrho - \{H - \tfrac{1}{2}(\partial H/\partial x)\, v\Delta t - \tfrac{1}{2}(\partial H/\partial t)\,\Delta t\}\,\varrho\sigma]_2\,\mathrm{d}x. \tag{A.10}$$

The second integral on the right-hand side can be treated in the same way. Now H_2' is written

$$H_2' = [H + (\partial H/\partial x)\, v\Delta t + (\partial H/\partial t)\,\Delta t]_1. \tag{A.11}$$

The index 1 refers to the moment t_1. The mass $m + \Delta m$ is at this moment between x_0 and x_2. Thus, the second integral is

$$\int_0^{m+\Delta m} [u_1' - \tfrac{1}{2}(H_2' + H_1')\,\sigma_1']\,\mathrm{d}m =$$

$$= \int_{x_0}^{x_2} A\,[u\varrho - \{H + \tfrac{1}{2}(\partial H/\partial x)\,v\Delta t + \tfrac{1}{2}(\partial H/\partial t)\,\Delta t\}\varrho\sigma]_1\,\mathrm{d}x. \qquad \text{(A.12)}$$

The integrals on the right-hand side of eqs (A.10) and (A.12) both contain a part between x_1 and x_2. This part is an integration over the fixed volume V_c. The other parts, that between x_0 and x_1 and that between x_2 and x_3, are integrations over the volumes δV_a and δV_b. Since these volumes will become infinitely small, when later on Δt approaches zero, the integrands for these parts can be taken as constant and equal to the mean values. These mean values are indicated by the indices a and b. Substitution of (A.3), (A.4), (A.10) and (A.12) in (A.8) gives

$$\Delta Q = A \int_{x_1}^{x_2} \left\{ \left[\varrho u - \left(H - \tfrac{1}{2}\frac{\partial H}{\partial x} v\Delta t - \tfrac{1}{2}\frac{\partial H}{\partial t}\Delta t\right)\sigma\varrho\right]_2 + \right.$$

$$\left. - \left[\varrho u - \left(H + \tfrac{1}{2}\frac{\partial H}{\partial x} v\Delta t + \tfrac{1}{2}\frac{\partial H}{\partial t}\Delta t\right)\sigma\varrho\right]_1 \right\} \mathrm{d}x +$$

$$+ Av_b\Delta t \left\{ u_b\varrho_b - \left[H_b - \tfrac{1}{2}\left(\frac{\partial H}{\partial x}\right)_b v_b\Delta t - \tfrac{1}{2}\left(\frac{\partial H}{\partial t}\right)_b \Delta t\right]\sigma_b\varrho_b \right\} +$$

$$- Av_a\Delta t \left\{ u_a\varrho_a - \left[H_a + \tfrac{1}{2}\left(\frac{\partial H}{\partial x}\right)_a v_a\Delta t + \tfrac{1}{2}\left(\frac{\partial H}{\partial t}\right)_a \Delta t\right]\sigma_a\varrho_a \right\}. \qquad \text{(A.13)}$$

This equation is now divided by Δt. If then Δt approaches zero one finds

$$\mathrm{d}Q/\mathrm{d}t = A \int_{x_1}^{x_2} \{\partial(\varrho u)/\partial t - \partial(H\varrho\sigma)/\partial t + v\varrho\sigma\,\partial H/\partial x + \varrho\sigma\,\partial H/\partial t\}\,\mathrm{d}x +$$

$$+ Av_b\varrho_b\,(u_b - H_b\sigma_b) - Av_a\varrho_a\,(u_a - H_a\sigma_a). \qquad \text{(A.14)}$$

The heat flow $\mathrm{d}Q/\mathrm{d}t$ is absorbed by the paramagnetic material in the fixed volume V_c since x_0 approaches x_1 and x_3 approaches x_2 when Δt approaches zero. The mass flow $A\varrho v$ is denoted as w. The relation between ϱ and w is the equation of continuity

$$A\,\partial\varrho/\partial t + \partial w/\partial x = 0. \qquad \text{(A.15)}$$

Using this equation, the following can be derived from eq. (A.14):

$$\mathrm{d}Q/\mathrm{d}t = \int_{x_1}^{x_2} [A\varrho\,(\partial u/\partial t - H\,\partial\sigma/\partial t) + w\,(\partial u/\partial x - H\,\partial\sigma/\partial x)]\,\mathrm{d}x. \qquad \text{(A.16)}$$

If this equation is used for a section of the regenerator, the volume $A\,(x_2 - x_1)$ must be replaced by the volume $f\,B\,(x_2 - x_1)$ that is available for the paramagnetic material. Furthermore the density ϱ must be replaced by the effective density ϱ_m. By these substitutions eq. (A.16) can be written

$$\mathrm{d}Q/\mathrm{d}t = \int_{x_1}^{x_2} [f\,B\varrho_m\,(\partial u/\partial t - H\,\partial\sigma/\partial t) + w\,(\partial u/\partial x - H\,\partial\sigma/\partial x)]\,\mathrm{d}x. \qquad \text{(A.17)}$$

Finally, the following thermodynamic equation can easily be derived:

$$\mathrm{d}u - H\,\mathrm{d}\sigma = \mathrm{d}u_0 + T_m\,\mathrm{d}s_M. \qquad \text{(A.18)}$$

Here u_0 is the internal energy of the paramagnetic material without magnetic field, s_M the field-dependent part of its entropy and T_m the temperature of the paramagnetic material.

From eqs (A.17) and (A.18) and by replacing x_2 by x_{n+1} and x_1 by x_n, eq. (A.1) is obtained.

3. A DESIGN FOR A MAGNETIC REFRIGERATOR

3.1. Introduction

On the basis of the theory developed in the preceding chapter we have worked out a design for a refrigerator operating between 15 °K and 4 °K in order to determine the merits of a refrigerator using the new cycle. We would emphasize that this design is given as an example and that a large number of other designs are possible particularly with regard to the mechanical part of this design.

The refrigerator designed is intended to be used in cascade with a Philips gas-refrigerating machine (model A 20) [16]. This precooler can produce a lowest temperature of 12 °K. This is convenient, since the gas refrigerating machine can be used to cool the superconducting magnet coil of the magnetic refrigerator to this temperature. With the superconducting magnet coil a field of about 15 kOe can be obtained easily at this temperature. When the magnetic refrigerator is then started, it can be used to cool the coil to lower temperatures. The operating temperature of the precooler will rise again, since it must then absorb the heat rejected by the magnetic refrigerator. We have chosen an operating temperature of the precooler of 15 °K, where it produces about 45 W.

In the calculations we have tried to obtain the optimum efficiency by varying the magnetic field, the size of several components and the speed of the refrigerator. However, complete optimization was not carried through, since that would have required too much time.

Data on material properties, heat transfer and flow resistance have been obtained from several sources. The last two subjects are treated extensively in relevant textbooks. To do calculations on the Stirling thermal engines readily manageable equations have already been derived from the available data. These equations could be used directly in the calculations of the magnetic refrigerator. Since such equations are not interesting in themselves, they will not be summarized. Data on the thermal properties of helium have been obtained mainly from the measurements of Lounasmaa [17]. They have been extrapolated in some cases to lower temperatures.

In the following sections the subjects given below will first be discussed:

(a) the choice of the paramagnetic material (sec. 3.2),
(b) the pressure of the helium (sec. 3.3),
(c) the generation of the magnetic field (sec. 3.4).

The last-named is of great importance for the mechanical construction that will be dealt with briefly in sec. 3.5. In sec. 3.6 the results of the calculations will be shown.

3.2. The choice of the paramagnetic material

In general a suitable working substance should have the following properties:

(1) a high value of the Curie constant C per unit of volume;
(2) a susceptibility that approximately follows a Curie-Weiss law down to the lowest temperatures that occur in the refrigerator; the value of Θ should be low;
(3) low specific heat, especially at the lowest temperatures;
(4) not too low thermal conductivity;
(5) good chemical stability.

It is obvious that a high value of the Curie constant per unit of volume is desirable. With increasing value of C, the magnetization power and the demagnetization power will rise for the same amount of material. This follows directly from eqs (2.88) and (2.98). Moreover, it will be seen later that a high value of C generally leads to high efficiencies. However, a high value of C is usually allied to a high magnetic ordering temperature. If this temperature approaches the lowest temperature occurring in the refrigerator, excessive deviations of the Curie-Weiss law are to be expected.

A low specific heat is, of course, favourable for a low value of the energy flow through the regenerator. This is particularly important at the cold side of the regenerator. Usually the specific heat at low temperatures is mainly due to the magnetic contribution and this contribution is greater when the ordering temperature is higher.

It is obvious that good chemical stability and a not too low thermal conductivity are desirable. The materials normally used for adiabatic demagnetization are chemically not very stable. Most of them are easily dehydrated. Moreover they are too diluted magnetically.

To obtain suitable working substances for our magnetic refrigerator, the susceptibility and the entropy of a number of materials have been determined as a function of temperature. These measurements are discussed in chapter 4. It was found that the most suitable substances are mixed oxides with the general formula $R_2M_2O_7$. Here R is Dy, Ho or Er and M is Ti, Sn or Ga/Sb. Substances which are more diluted are obtained by replacing R partly by La or Yt. In table 3-I the data are collected of the materials that can be used in magnetic refrigerators. Some substances used for adiabatic demagnetization below 1 °K are also included in this table for comparison. The Curie constants of some of the mixed oxides are more than twenty times higher than those of the other materials. Still, their ordering temperature lies well below 2 °K. At 4 °K the susceptibility deviates slightly from the Curie-Weiss law. The smallest deviation is found for Dy_2GaSbO_7 and Ho_2GaSbO_7. For those oxides where M = Ti, the deviation is about 10% and if M = Sn the deviation is 30%. The latter type of material is therefore less suitable for the magnetic refrigerator.

TABLE 3-I

Properties of working substances for a magnetic refrigerator

chemical formula	density	Curie constant		asymptotic	ordering temp.	specific heat *)	
		per gramme	per cc	Curie temp.	T_C or T_N	a_s	b_s
	(g/cm^3)	($°K\ cm^3/g$)	($°K$)	($°K$)	($°K$)	($J/°K^4\ g$)	($J/°K/g$)
Dy_2GaSbO_7	7·87	0·042	0·33	0·15	< 2	$1{\cdot}0.10^{-6}$	0·095
Ho_2GaSbO_7	8·12	0·042[5]	0·34[5]	−0·3	< 2	—	—
$Dy_2Ti_2O_7$	6·95	0·047	0·32	0·1	< 2	$2{\cdot}2.10^{-6}$	0·078
$Ho_2Ti_2O_7$	6·98	0·048	0·33[5]	0·6	< 2	$2{\cdot}2.10^{-6}$	0·19
$Dy_2Sn_2O_7$	8·10	0·035	0·28	1·8	< 2	—	—
$Ho_2Sn_2O_7$	8·21	0·038	0·31	0·6	< 2	—	—
$FeNH_4(SO_4)_2.12\ H_2O$	1·71	0·009	0·015	0·061	$\approx 0{\cdot}06$	$7{\cdot}3.10^{-6}$ **)	$2{\cdot}3.10^{-4}$ **)
$K\ Cr(SO_4)_2.12\ H_2O$	1·83	0·0037	0·0068	0·095	$\approx 0{\cdot}06$	$8{\cdot}3.10^{-6}$ **)	$2{\cdot}7.10^{-4}$ **)

*) The specific heat of these substances can be written $c = a_s T^3 + b_s T^{-2}$.

**) Data obtained from D.G. Kapadnis, Thesis, Leiden, 1956.

There is no simple way to determine which combination of the Curie constant and the specific heat is most favourable. An answer to this question can only be obtained by a complete optimization of a refrigerator for different working substances. Moreover, the answer might depend largely on the desired operating temperature of the refrigerator. Thus the choice of the working substance remains somewhat arbitrary after all.

The compound $Dy_2Ti_2O_7$ has been chosen as the working substance for the design of the refrigerator for the following reasons:

(a) the Curie constant of this material is among the highest in table 3-I;
(b) the magnetic contribution to the specific heat is one of the lowest.

3.3. The pressure of the helium gas

The pressure level of the helium gas in the magnetic refrigerator must be chosen such that

(a) no phase transitions occur in the refrigerator,
(b) the specific heat is as high as possible.

The first condition sets a lower and a higher limit for the pressure level. If the pressure lies below the critical pressure of 2·26 atmospheres, the helium will be liquified as soon as the temperature drops below 5·19 °K. It may be expected that the refrigerator will then not operate properly.

At the high side the pressure is limited by the melting line. As may be seen from fig. 3.1 the pressure should be below 25 atmospheres. In this figure the

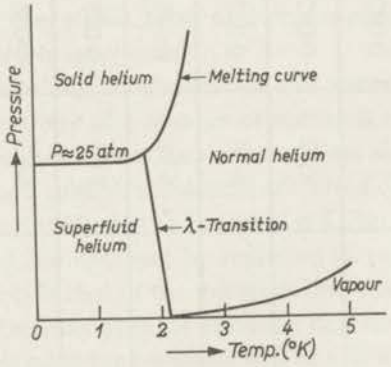

Fig. 3.1. Schematic pressure-temperature diagram for helium.

transition line from the normal state to the superfluid state is shown too. The temperature at which this transition occurs depends only slightly on the pressure. A high pressure is, however, somewhat more favourable than a low one.

Fortunately the second condition demands a high pressure too. Figure 2.5

shows that the specific heat of helium per unit of volume increases above 10 °K with the pressure. Below 10 °K it varies only slightly with the pressure, unless much lower pressures are considered.

The above considerations have led to the choice of a pressure level of 20 atmospheres for the helium in the refrigerator. Thus there is a safe margin below the melting line if the operating temperature drops below ≈2 °K.

3.4. The magnetic field

3.4.1. *Variation of the magnetic field*

It is obvious that the magnetic field should be obtained with a magnet or coil wound with superconducting wires. Otherwise the magnet will consume at least 500 times more energy than the refrigerator itself. There are several alternatives in making the field on the place of the paramagnetic material variable. The main methods are:

(1) variation of the field by electronic control of the current through the coil;
(2) displacement of the magnet with respect to the paramagnetic material;
(3) displacement of the paramagnetic material with respect to the magnet.

Of these methods the first one is less favourable, as hitherto superconductors have not been very suitable for rapidly changing magnetic fields due to the degradation effect. Moreover, an approximately constant value of $H/(T-\Theta)$ is needed in the regenerator. This is not easily realized by varying the current of a magnet in view of the shortness of the space occupied by the paramagnetic material.

Of the two remaining possibilities we have chosen the last one. It has the important advantage that only the paramagnetic material and the stabilizers have to be moved in the magnetic field. These components and their housings can largely be made of non-metallic materials; any metal part can be constructed such that eddy currents are small. The heat exchangers (freezer and cooler) must remain stationary and a movable connection between these and the stabilizers must be used. The design of this connection will be discussed later.

A schematic drawing of the arrangement of the paramagnetic material and the coils generating the field is shown in fig. 3.2. The paramagnetic material p is placed in a cylindrical container c together with the two stabilizers s_1 and s_2. The container can be moved by a rod up and down in a tube t. Around this tube three coils are placed. The first one e produces the main magnetic field and the two other coils f and g generate a smaller field of opposite sign. With these three coils a resulting field is obtained that decreases rapidly in the direction of the smaller coils. The last coil g can be replaced by a solid superconducting cylinder. This cylinder is cooled below the superconducting transition temperature before

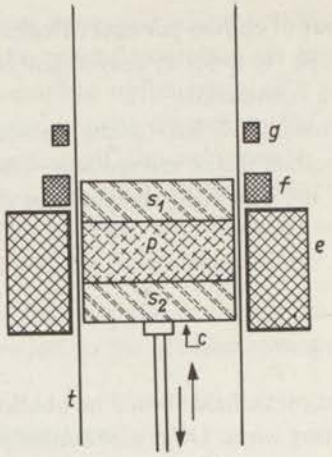

Fig. 3.2. Schematic drawing of the arrangement of the paramagnetic material and the magnet coils;
(c) unit with the paramagnetic material and both stabilizers; (e), (f) and (g) magnet coils; (p) paramagnetic material; (s_1) and (s_2) stabilizers; (t) tube.

the current through the other coils is switched on. In this cylinder the magnetic field thus remains zero.

The paramagnetic material will be moved by means of a rod connected to a drive mechanism. It will therefore move roughly harmonically. At first sight it may perhaps seem surprising that a harmonic movement can be used. However, this will become clear in sec. 3.9, where the phase of this movement with respect to the displacement of the paramagnetic material through the regenerator is discussed.

3.4.2. *Shape of the magnetic field*

The paramagnetic material is displaced from a region where the magnetic field is high to a region where this field is very low. Thus a magnetic field that decreases rapidly in one direction is needed. However, it is desirable that the field strength should be approximately the same for points lying in a plane perpendicular to this direction. In that case the problem can be treated one-dimensionally.

If the paramagnetic material is isotropic the direction of the magnetic field is arbitrary. Small sintered balls of paramagnetic material will be used canceling any anisotropy of the material itself, satisfying the above condition.

There is a magnetic field with the required properties that satisfies the Maxwell equations. This field, which seems to be the only solution of the problem, is represented by the equations

$$\begin{aligned} H_x &= H_0 \exp(-ky) \sin(kx), \\ H_y &= H_0 \exp(-ky) \cos(kx), \\ H_z &= 0. \end{aligned} \tag{3.1}$$

Here H_x, H_y and H_z are the components of the field in the x-, y- and z-directions of a rectangular coordinate system and k is an arbitrary constant. Such a field is generated, for instance, by an infinite flat pole, of which the magnetization is

$$I = (H_0/2\,\pi)\cos(kx). \tag{3.2}$$

The origin of the coordinate system is chosen on the surface of the pole and the positive y-direction is perpendicular to this surface, pointing away from the pole.

It is obvious that this solution is not a very useful one in practice, as a set of cylindrical coils will be used for preference. In this case the magnetic field is rotationally symmetric and an exponentially decreasing field has not the required property. Nevertheless the deviations can be expected to be small.

If the magnetic field along the axis of the coil system is known, the field off the axis may be calculated as follows. By integration we can calculate the magnetic potential on the axis. Using a cylindrical coordinate system ϱ, φ, y the magnetic potential Φ off the axis can be developed as a power series of ϱ^2:

$$\Phi = \Phi_0 + \varrho^2\Phi_1 + \varrho^4\Phi_2 + \varrho^6\Phi_3 + \ldots, \tag{3.3}$$

where Φ_1, Φ_2, Φ_3, etc. do not depend on ϱ. Since the field must be rotationally symmetric, φ does not enter these quantities either.

In the region where the current density is zero, Φ must satisfy the Laplace equation

$$\Delta\Phi = 0. \tag{3.4}$$

Substitution of eq. (3.3) gives an expression containing successive powers of ϱ^2. Since this expression must be zero for any value of ϱ the coefficients in this expression must vanish. This yields the following equations for Φ_1, Φ_2, Φ_3, etc.:

$$\Phi_1 = -\frac{1}{4}\frac{\partial^2\Phi_0}{\partial y^2},$$

$$\Phi_2 = -\frac{1}{64}\frac{\partial^4\Phi_0}{\partial y^4}, \tag{3.5}$$

$$\Phi_3 = \frac{1}{2304}\frac{\partial^6\Phi_0}{\partial y^6}.$$

The magnetic field itself is the gradient of Φ. Thus the following equations for H_ϱ and H_y are obtained:

$$H_\varrho = -\frac{\varrho}{2}\frac{\partial H_{y0}}{\partial y} + \frac{\varrho^3}{16}\frac{\partial^3 H_{y0}}{\partial y^3} - \frac{\varrho^5}{384}\frac{\partial^5 H_{y0}}{\partial y^5} + \ldots$$

and (3.6)

$$H_y = H_{y0} - \frac{\varrho^2}{4}\frac{\partial^2 H_{y0}}{\partial y^2} + \frac{\varrho^4}{64}\frac{\partial^4 H_{y0}}{\partial y^4} + \ldots,$$

where $H_{y0} = \partial\Phi_0/\partial y$.

Using these equations the magnetic-field strength at points of the axis can be determined. For an exponentially decreasing field $H_{y0} = H_0 \exp(-ky)$ eqs (3.6) are reduced to

$$H = H_{y0} [(\varrho/2) k - (\varrho^3/16) k^3 + (\varrho^5/384) k^5 - \ldots]$$

and (3.7)

$$H_y = H_{y0} [1 - (\varrho^2/4) k^2 + (\varrho^4/64) k^4 + \ldots].$$

These equations show that for an exponentially decreasing field the ratio of the field strength on the axis and at a point off the axis is independent of y. It is obvious that then the ratio of the field strength at points with different y-co-ordinates and the same ϱ-coordinate is independent of this value of ϱ.

An exactly exponentially decreasing magnetic field can not be easily realized with coils, however. In the design of the magnetic refrigerator we have tried to obtain a field that decreases roughly exponentially at least for the region where the field is already low.

Up till now only the external field has been discussed. The magnetization of the paramagnetic material causes a demagnetization field which reduces the field experienced by individual spheres. At the warm side of the regenerator this effect is practically negligible; at the cold side it must be accounted for in a more accurate calculation. Since the magnetization of the paramagnetic material in a first approximation is constant during the passage of this material through the regenerator in the warm period, the demagnetizing field is constant too during this passage. Thus the external field is reduced by a constant amount in this period. During the cold period the magnetization of the paramagnetic material is nearly zero and no correction is necessary. The magnetizing power and the demagnetization power are calculated using the value of the magnetic field at the moment the paramagnetic material leaves the regenerator. At those moments the same approximation can be used to determine the magnetic field on the individual particles. During the magnetization in the warm transport gas and the demagnetization in the cold transport gas the fluctuation of the magnetic field is not easily calculated. This, however, is not important since the exact shape of this field variation does not enter into the calculations.

The strength of the demagnetizing field depends also on the shape of the space occupied by the paramagnetic material. In the refrigerator discussed here this space is a flat disk 7 cm in diameter and 2 cm in thickness. The demagnetizing field decreases somewhat at the edge of this disk. This is advantageous since the external field decreases in this direction too, so that finally the remaining field experienced by the individual spheres decreases less than the external field.

The shape of the magnetic field used in our calculations is shown in fig. 3.3. It represents a mean value of the field experienced by the spheres in the same cross-section of the disk.

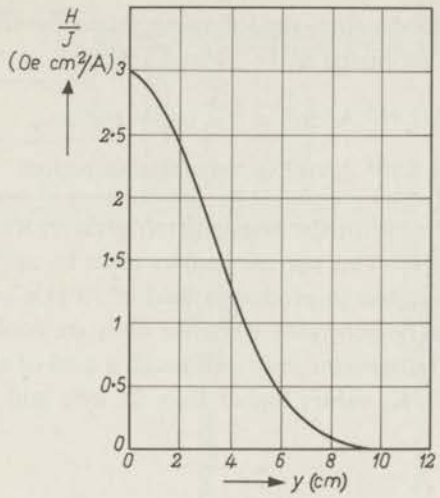

Fig. 3.3. Shape of the magnetic field used in the calculations of the performance of the magnetic refrigerator. The ratio of the magnetic field and the current density in the whole coil is shown as a function of the distance from the centre of the main coil in the direction of the smaller coils.

3.4.3. *Design of the magnet coils*

The most suitable material for the coils is Nb_3Sn. The transition temperature of this material is 18 °K. The coils can be connected thermally to the freezer of the magnetic refrigerator. The whole system is then first cooled by the precooler to 12 °K, which is the lowest temperature attainable with the precooler. At this temperature the superconducting wires of the coils can already carry sufficient current to generate a magnetic field of about 15 kOe with a coil of moderate size. After the current through the coils has been switched on, the magnetic refrigerator is started. The coils are cooled gradually by the refrigerator itself so that the current through the coils can be increased.

Data on the characteristics of Nb_3Sn at higher temperatures are scarce. The first measurements by Kunzler [18]) on niobium-clad Nb_3Sn wire give a critical current larger than 10 A per wire at 12 °K and 15 kOe. The external diameter of this wire was 0·038 cm. With this wire about 300 turns per cm² of the cross-section of the winding space can be obtained in a coil. The current density in a ready coil is then 3.10^3 A/cm². For the ribbon-type wire of R.C.A. only data at lower temperatures are available. At 4·2 °K and 15 kOe the critical current is 120 A per wire in the stable region. At higher currents the wire becomes unstable and only after "training" can currents of 300 A per wire be obtained. Using recent measurements by Hancox [19]) on the current density in sintered-Nb_3Sn cylinders, it may be estimated that the current density at 12 °K is lower by about a factor 5 than at 4·2 °K. As 300 turns per cm² in a coil can be

obtained with the ribbon wire, the following values for the current density in a ready coil can be estimated at 12 °K and 15 kOe:

$$J_c \geqslant 7{\cdot}2.10^3 \text{ A/cm}^2 \text{ in the stable region,}$$

$$J_c \geqslant 1{\cdot}8.10^4 \text{ A/cm}^2 \text{ in the unstable region.}$$

In calculating the coils for the magnetic refrigerator, we have used a current density of 5.10^3 A/cm^2. This current density must be easily attainable.

If the coils are designed to produce a field of 15 kOe at 12 °K, a considerably higher field can be generated when the coils are cooled down to a lower temperature by the refrigerator itself. Although a field of about 75 kOe should be attainable at 4·2 °K, values higher than 25 kOe will not be used in our calculations.

3.5. Mechanical design

A drawing of a possible design of a magnetic refrigerator is shown in fig. 3.4. As stated earlier, the paramagnetic material and both stabilizers are mounted in a movable unit c. This unit moves up and down in the tube t, from the centre of the coil e in the direction of the smaller coils f and g. Two end pieces h and i are attached to the movable unit. These end pieces are somewhat smaller than the tube t, so that annular spacings a_1 and a_2 are obtained. The helium that flows through the paramagnetic material and the stabilizers is led through these spacings to the freezer k and the cooler l.

The cooler and the freezer must have a high heat-transfer number. For this purpose the helium must flow through narrow channels having a large heat-transfer surface. Both components can be made, for instance, of copper ribbon wound into a flat coil with interspersed spacers. In our design the ribbon is 1·5 cm wide and 0·3 mm thick and the spacers are 0·15 mm thick. The coil can be soldered on one side to a piece of copper in which slots have been machined. The helium flowing through the coil can be conducted away through these slots.

The heat discharged to the copper ribbon is conducted to the copper piece. Due to the high thermal conductivity of copper the temperature difference over the ribbon is negligible.

The cooler is connected by a heavy slab of copper to the header (b) of the gas refrigerating machine to ensure good thermal contact. The distance between the cooler and the header of the gas refrigerating machine must be kept as short as possible to reduce the temperature difference over the copper connection, unless some other method is used to transport the heat from the cooler to the gas refrigerating machine.

The pistons drawn in fig. 2.1 have been replaced by one displacer (n). This has several advantages. The only pressure difference across the displacer is

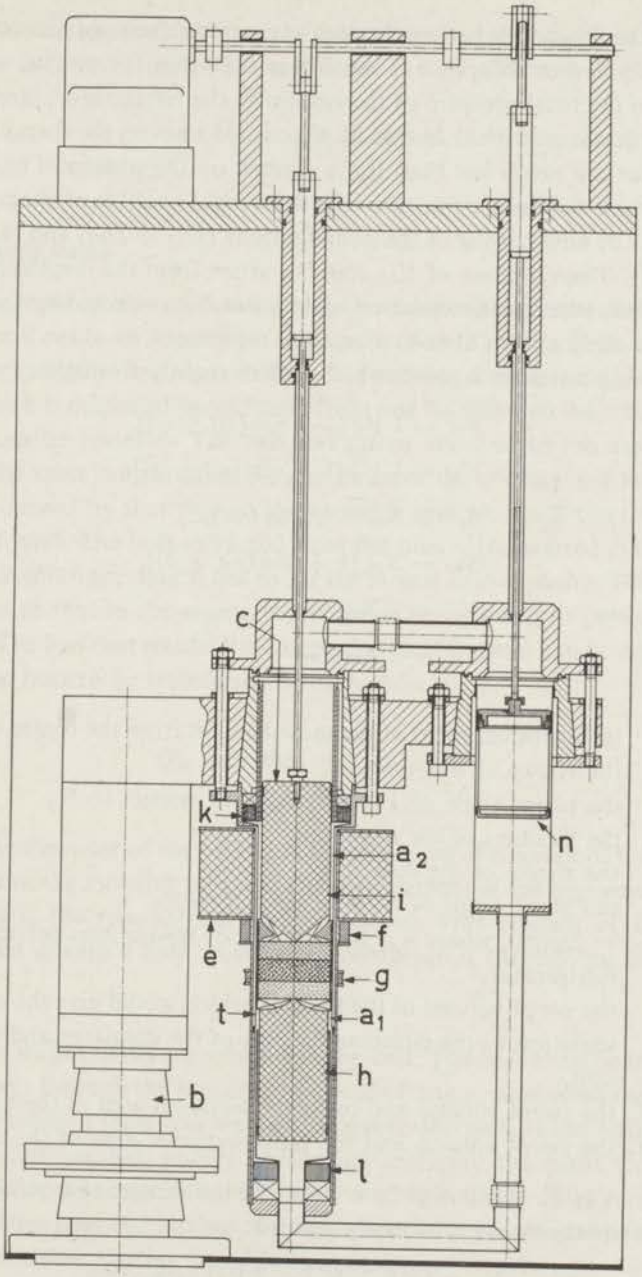

Fig. 3.4. Drawing of the magnetic refrigerator;
(a_1) and (a_2) annular spacings; (b) header of the gas refrigerating machine; (c) movable unit with the paramagnetic material and both stabilizers; (e) main magnet coil; (f) and (g) additional magnet coils; (h) and (i) end pieces of the movable unit; (k) cooler; (l) freezer; (n) displacer; (t) tube.

caused by the flow of the helium through the various components of the refrigerator. This pressure difference is much less than that for pistons which must stand up to the total pressure of the helium in the refrigerator. Hence the displacer seal is not as critical as that of pistons. Moreover, the forces exerted on the displacer are much less than those exerted on the pistons.

The variable volumes, denoted in the theoretical analysis of chapter 2, as V_p (see sec. 2.7.2) now consist of the combinations $(U_{11} + U_{12})$ and $(U_{21} + U_{22})$, respectively. The variation of U_{11} and U_{21} arises from the displacement of the movable unit, whereas the variation of U_{12} and U_{22} is caused by the displacer. Both parts carry out an almost sinusoidal movement.
The following notation is used, which differs slightly from that in sec. 2.7.2:

$$V_D = \tfrac{1}{2} V_p [1 - \cos(\omega t + \gamma)], \tag{3.8}$$

$$V_M = \tfrac{1}{2} V_p [1 + \cos(\omega t + \gamma)], \tag{3.9}$$

$$S_c = S_{c0} [1 + \cos(\omega t)], \tag{3.10}$$

$$S_v = S_{v0} [1 + \cos(\omega t + \delta)], \tag{3.11}$$

$$V_c = 2 S_{c0} O_c, \tag{3.12}$$

$$V_v = 2 S_{v0} O_v. \tag{3.13}$$

Here

S_c	is the displacement of the movable unit from the centre of the coil e,
$2 S_{c0}$	the stroke of this unit,
γ	the phase angle of V_D and V_M with respect to S_c,
S_v	the position of the displacer,
$2 S_{v0}$	the stroke of the displacer,
δ	the phase angle of S_v with respect to S_c,
ω	$= 2\pi n/60$, where n is the number of revolutions per minute of the refrigerator,
V_p	the swept volume of the pistons, which would give the same volume variation as the combined action of the displacer and the movable unit,
V_c and O_c	the swept volume and the cross-sectional area of the movable unit,
V_v and O_v	the swept volume and the cross-sectional area of the displacer.

Generally, V_p, V_c and γ will be chosen for the design of a refrigerator. The following equations are now easily verified:

$$V_v = (V_c^2 + V_p^2 - 2 V_p V_c \sin\gamma)^{1/2}, \tag{3.14}$$

$$\sin\delta = [V_p \sin(\gamma) - V_c]/V_v, \tag{3.15}$$

$$\cos\delta = (V_p/V_v)\cos\gamma, \tag{3.16}$$

$$V_s = (V_c + V_v - V_p)/2. \tag{3.17}$$

Here V_s is a dead space that must be added to the volumes V_h in eqs (2.72). Normally γ is in the order of 25° and since $V_c > V_p$, δ must lie between 90° and 180°.

By substitution of $\omega t + \gamma = \beta$ in eqs (3.8) and (3.9), they are transformed to those used in chapter 2.

3.6. Additional losses

The movement of the unit containing the paramagnetic material and both stabilizers will cause an extra loss, since part of the tube t will be cooled and reheated periodically. In this unit there is a moving temperature gradient (see fig. 2.1), which is displaced periodically from one stabilizer to the other through the paramagnetic material. The two end pieces attached to the movable unit remain at the same temperature. At any moment the cooling and reheating of the tube is caused by that part of the movable unit at which the temperature gradient is found. The heat extracted from the tube is transferred mainly to the helium gas in this unit, since it has by far the largest heat capacity. The situation is analogous to that in the regenerators. If the heat transfer is perfect, no loss will occur. The loss that results from imperfect heat transfer can be estimated as follows. The heat to be transferred in each cycle is

$$Q_w = \pi D l_1 d_1 \int_{T_{Du}}^{T_{Mu}} (\varrho c)_w \, \mathrm{d}T. \tag{3.18}$$

Here D is the diameter of the tube t, d_1 the thickness of the wall of t, l_1 the sum of the stroke of the movable unit and the displacement of the regenerator in this unit, and $(\varrho c)_w$ the specific heat of the material. This amount of heat must be transferred during a half cycle of the refrigerator, through an area

$$O = \pi D l_2. \tag{3.19}$$

Here l_2 is the length of the regenerator in the unit. The heat must be transferred from the tube t through the helium to the wall of unit c, conducted through this wall and transferred from this wall to the gas in the unit. If the wall of unit c is made of non-metallic, poorly conducting material, the main temperature difference will occur across this wall. It is therefore better to make it of a metal which has better heat conduction. However, special precautions must be taken to prevent excessive heating by eddy currents.

The heat transfer at the inner side of the wall of the unit e is equal to that in the paramagnetic material. The transfer of heat from the tube t to the wall can be estimated from the velocity of the unit with respect to the wall. Since this velocity is much larger than that of the gas in the unit, we may safely assume that the heat transfer here is at least as big as at the inner side.

Thus an overall heat-transfer coefficient a_t may be used, that is

$$a_t = \tfrac{1}{2}\, a_i, \tag{3.20}$$

where a_i is the heat-transfer coefficient in the paramagnetic material.

Since the amount of heat Q_w must be transferred in the time interval $(30/n)$ from the tube t to the helium in unit c, the temperature difference is

$$\Delta T_s = (n/30)\, Q_w/a_t O. \tag{3.21}$$

The extra loss resulting from this imperfect heat transfer is approximately

$$\Delta P_s \approx (n/60)\, \pi\, D l_1 d_1 (\overline{\varrho}\, \bar{c})_w\, \Delta T_s = 2\,(n/60)^2\, Q_w^2/a_t O\, (T_{Mu} - T_{Du}), \tag{3.22}$$

where $(\overline{\varrho}\, \bar{c})_w = (T_{Mu} - T_{Du})^{-1} \int_{T_{Du}}^{T_{Mu}} (\varrho c)_w \, \mathrm{d}T$.

This equation has been used to estimate this extra loss in sec. 3.7. Due to the periodic movement of the displacer something of the same kind happens. However, if a relatively wide gap between the displacer and the wall is used, the helium in the gap moves up and down with the displacer. It will then function as a regenerator for the cylinder wall. Since the heat transfer here is much bigger than in the former case, the resulting loss is negligible here.

3.7. Design data

In table 3-II the most important dimensions of the refrigerator are given. The size of this refrigerator was determined by the following conditions.

(a) The size of the refrigerator must be matched to the capacity of the precooler at 15 °K. Allowing for some insulation losses this capacity is about 40 W.
(b) The magnetic field to be used should not exceed 25 kOe. The refrigerator should however be able to cool with a lower field strength (e.g. 15 kOe).
(c) The refrigerator should make about 160 revolutions per minute.

The maximum value of the field is somewhat arbitrary. A value of 25 kOe was chosen, as a field of this magnitude will be easily obtainable with a superconducting coil, if this coil is cooled by the refrigerator itself.

The speed of the refrigerator must be low, since the calculations have shown that the flow losses increase rapidly if a higher speed is chosen. We performed no optimization with regard to the speed, however.

The above conditions and the chosen paramagnetic material determine the total amount of material to be used. Moreover, it was decided to use small spheres of this material. In practice this yields a filling factor of 63 %. Furthermore a minimum value of 8 was chosen for Γ^+ at the cold side and the stabilizers were designed 10 % larger than the regenerator ($A_d = 1{\cdot}1$).

These conditions determine the main dimensions of the refrigerator, as discussed in sec. 2.7.2, with the exception of the diameter of the paramagnetic-

material container. This diameter is chosen as small as is compatible with not too high a value of the flow losses. The total displacement of the paramagnetic material required is determined by the form of the magnetic field.

To obtain a high efficiency we varied the diameter of the spheres, the phase angle γ and the stroke of the unit with paramagnetic material. All other dimensions listed in table 3-II were determined by the design itself.

TABLE 3-II

Data of the refrigerator design

paramagnetic material	$Dy_2Ti_2O_7$
shape	sintered spheres of 15.10^{-3} cm diam.
sintered density	6·25 g/cm³
diameter of the container	7 cm
length of the section filled with paramagnetic material	2 cm
filling factor	63 %
stabilizers	
shape of the stabilizer material	stainless-steel gauzes
wire diameter	0·01 cm
diameter of the container	7 cm
length of the section filled with stabilizer material	1·66 cm
filling factor	30 %
movable unit	
stroke	10·5 cm
freezer	
heat-transfer surface	coiled strip of copper
spacing in the coil	0·015 cm
width of the strip	1·47 cm
length of the strip	698 cm
thickness of the strip	0·03 cm
cooler	same dimensions as the freezer
annular channel on both sides of the movable unit	
length	13 cm
width	0·1 cm
displacer	
stroke	10·5 cm
diameter	7·0 cm
phase with respect to the movable unit	175°
secondary data	
gas volume of the regenerator	37·7 cm³
volume of the warm transport gas	35·5 cm³
volume of the cold transport gas	35·5 cm³
amount of paramagnetic material	303 g
phase of the movable unit with respect to V_M	25°

3.8. The calculated capacity of the refrigerator

The refrigerating capacity P_D of this refrigerator was calculated for several operating temperatures and for several values of the magnetic field. The results

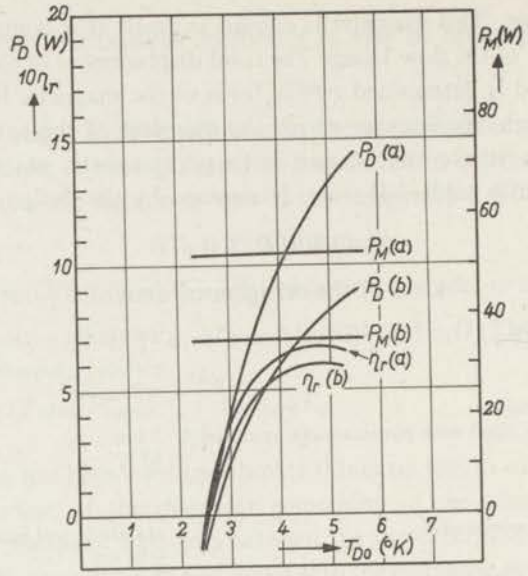

Fig. 3.5. The calculated values of the refrigerating capacity P_D, the magnetization power P_M and the relative efficiency η_r of the refrigerator, the dimensions of which are listed in table 3-II, as a function of the freezer temperature. The cooler temperature is 15 °K, the speed 160 r.p.m. and the phase angle $\gamma = 25°$. The curves (a) are for a magnetic field of 25 kOe and the curves (b) for a magnetic field of 20 kOe.

of these calculations are shown in fig. 3.5, where, in addition to P_D the magnetization power P_M and the efficiency η_r are also shown. Here η_r is the efficiency relative to a Carnot cycle operating between the same temperatures. To calculate η_r we have neglected all mechanical losses. Thus η_r is equal to $Q_D/\eta_c(Q_M - Q_D)$, where η_c is the efficiency of the Carnot cycle. We have done this as η_r is used to calculate Q_M/Q_D when the efficiency of a series system of two refrigerators is to be determined. If mechanical losses were included in η_r a wrong value of Q_M/Q_D would be obtained.

It will be noted that the efficiency of the cycle for fields of 20 kOe and 25 kOe is very high compared to the efficiency of refrigerators used normally at higher temperatures. The cause of this high efficiency will be discussed in sec. 3.10.

The lowest temperature that can be obtained with this refrigerator is 2·5 °K. This figure is, however, not very reliable, since the working substance $Dy_2Ti_2O_7$ then deviates considerably from the Curie-Weiss law. This deviation is not included in the calculations.

The refrigerating capacity as a function of the cooler temperature T_{M0} is shown in fig. 3.6 for a freezer temperature of 4·2 °K. If the magnetic field is kept constant, the refrigerating capacity decreases rapidly with increasing T_{M0}. This was to be expected as the magnetization of the paramagnetic material is lower as T_{M0} increases. If the field strength is increased proportionally with

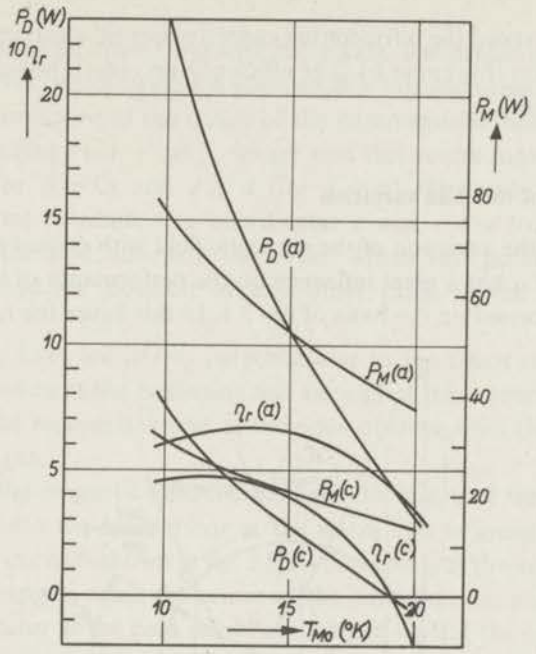

Fig. 3.6. The refrigerating capacity and the efficiency as a function of the cooler temperature T_{M0}. The freezer temperature is 4·2 °K, the speed 160 r.p.m. and the phase angle $\gamma = 25°$. The curves (a) are for a field of 25 kOe and the curves (c) for a field of 15 kOe.

T_{M0}, the refrigerating capacity and the efficiency decrease much more slowly. However, Γ^+ at the warm side decreases rapidly with T_{M0}. The results of the calculations are therefore less reliable as in the regenerator theory it was assumed that $\Gamma^+ = \infty$.

The influence of the speed on the refrigerating capacity is shown in fig. 3.7.

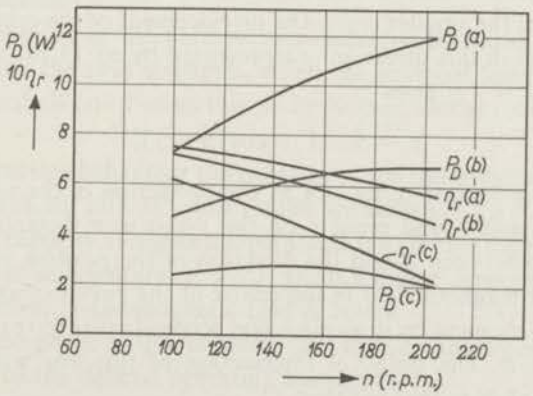

Fig. 3.7. Refrigerating capacity and efficiency as a function of speed. The cooler temperature is 15 °K, the freezer temperature 4·2 °K and the phase angle $\gamma = 25°$. Curves (a) are for a field of 25 kOe, curves (b) for a field of 20 kOe and curves (c) for a field of 15 kOe.

With increasing speed the refrigerating capacity rises till a maximum is reached, (e.g. at 180 r.p.m. for curve b). The efficiency decreases, however, as the flow losses grow rapidly.

3.9. The phase of the field variation

The phase of the variation of the magnetic field with respect to the variation of the volume V_M has a great influence on the performance of the refrigerator. This will be discussed on the basis of fig. 3.8. In this figure the magnetic field H

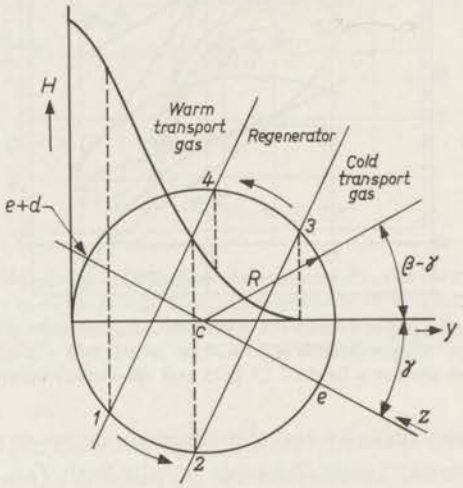

Fig. 3.8. Graphical evaluation of the strength of the magnetic field on the paramagnetic material at any moment of the cycle.

is shown as a function of the distance y from the centre of the main magnet coil in the direction of the smaller coils. The displacement of the centre of the paramagnetic material in this direction is represented by eq. (3.10). Substitution of $S_e = y$ and $\omega t = \beta - \gamma$ gives

$$y = S_{e0} [1 + \cos (\beta - \gamma)]. \tag{3.23}$$

Thus y can be represented in fig. 3.8 as the projection of the end point of the vector R that rotates round point c on the y-axis at a distance S_{e0} from the origin. The angle between R and the direction of the positive y-axis is $(\beta - \gamma)$. The value of the magnetic field in the centre of the paramagnetic material can be found at any moment by drawing a line perpendicular to the y-axis through the end point of R. The point of intersection of this line with the H-curve yields the value of H at that moment.

The position of the centre of the paramagnetic material *with respect to the gas* (z-coordinate) can also be obtained using R. In that case R must be projected

on a line that forms an angle $(-\gamma)$ with the y-axis. The projection of R on this line is $R \cos \beta$. We can determine a scale on this line such that this projection represents the movement of the centre of the paramagnetic material. Applying eq. (2.81) and taking $f(\beta) = \cos \beta$, we see that this centre moves between the coordinates e (for $\beta = 0$) and $e + d$ (for $\beta = \pi$). Obviously the right scale is obtained if we attribute the coordinates e and $e + d$ to the points of intersection of the said line with the circle. These two points being determined, we can find the position of any other place in the helium by its coordinate.

In fig. 3.8 two lines are drawn perpendicular to the z-axis representing the coordinates z_2 and z_3 at the beginning and the end of the regenerator. Between these lines lies the regenerator and at the sides of these lines the cold and the warm transport gas.

The value of the magnetic field the moment the centre of the paramagnetic material moves into the regenerator at the warm side is found by projecting point 1 on the H-curve as shown in fig. 3.8. In the same way projection of point 2 gives the field strength, when the centre of the paramagnetic material emerges from the regenerator at the cold side. Points 3 and 4 yield the field strength at the equivalent moments in the cold period.

Figure 3.8 shows directly that the variation of the volume V_D leads in phase by an angle γ with respect to the displacement of the paramagnetic material *from the farthest point in the low-field region.*

The effect of a variation of the phase angle is now easily determined. We see directly that the field strength at moment 1 and at moment 2 decreases if γ is made smaller. Moreover, the field strength increases at moment 4. The consequence is that the magnetization power decreases. Since the field strength at moment 2 decreases more rapidly, however, the refrigerator is better adapted for lower temperatures.

For any other point in the paramagnetic material the same method can be used to determine the field strengths, when the material leaves or enters the regenerator. We shall not discuss this point further, as the result is practically the same.

To demonstrate this behaviour the capacity of the refrigerator was calculated for phase angles of 20° and 25°. The results are shown in fig. 3.9. As expected, the refrigerating capacity at higher temperatures is lower for the lesser value of γ. However, at lower temperatures $\gamma = 20°$ yields a higher capacity than $\gamma = 25°$, since the adaptation of the magnetic field is better.

Variation of the phase of the magnetic field thus makes it possibles to adapt the refrigerator to the desired operating temperature.

We wish to point out here that a better adaptation to the desired operating temperature can also be obtained by changing the current through the two smaller coils f and g shown in fig. 3.4.

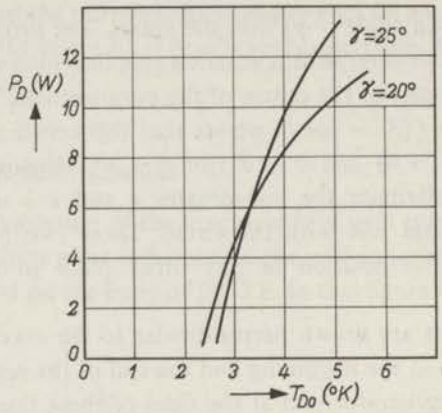

Fig. 3.9. The refrigerating capacity for two different phase angles of the variation of the magnetic field. The magnetic field is 25 kOe, the cooler temperature 15 °K and the speed 160 r.p.m.

3.10. Detailed results for one operating temperature

3.10.1. *Magnetization power, demagnetization power and losses*

In this section the results of the calculations for one operating temperature of the refrigerator will be discussed in more detail. We have chosen for this purpose an operating temperature at which the strength of the magnetic field at the cold side of the regenerator is correctly adapted. The main results are given in table 3-III.

The undisturbed demagnetization power of the refrigerator at this temperature is 10·45 W. Only 20% of this amount is consumed by the various losses. Still, the efficiency of this refrigerator is not 80%, but 72% of that of a Carnot cycle operating between the same temperatures. The reduction of the efficiency arises from the fact that the magnetization and the demagnetization occur at mean temperatures deviating from the cooler and the freezer temperatures. These mean temperatures are respectively $T_M = \frac{1}{2}(T_{Mu} + T_{Mi}) = 15{\cdot}71$ °K and $T_D = \frac{1}{2}(T_{Du} + T_{Di}) = 4{\cdot}03$ °K. The refrigerator thus operates effectively between T_M and T_D. Even a Carnot cycle operating between T_M and T_D would have an efficiency of only 91·5% of the efficiency of one operating cycle between the cooler and freezer temperatures. As said before, this effect has the character of an extra loss, the transport loss.

At the cold side the flow loss is the largest loss. The speed of the refrigerator is restricted by the size of this loss which is proportional to n^3. The third power is caused by an increase in the flow losses per cycle, that is approximately proportional to the second power of the gas velocity and thus proportional to n^2. As the flow losses are calculated per second, the loss per cycle is multiplied by n, so that a proportionality with n^3 results.

TABLE 3-III

Detailed results of the calculations for one operating temperature

freezer temperature T_{D0}			4·2 °K
cooler temperature T_{M0}			15·0 °K
speed n			120 r.p.m.
magnetic-field strength H			25 kOe
phase of the displacement of the movable unit (γ)			25°
temperatures of the cold transport gas	T_{Du}		3·85 °K
	T_{Di}		4·19 °K
temperatures of the warm transport gas	T_{Mu}		16·39 °K
	T_{Mi}		15·02 °K
undisturbed demagnetization power P_{D0}			10·45 W
energy flow through the regenerator ΔP_{DR}			−0·60 W
demagnetization power before other losses P_{D1}			9·85 W
other losses:			
flow losses	ΔP_{DF}	−0·96 W	
conduction losses	ΔP_{DC}	−0·39 W	
eddy-current losses	ΔP_{DE}	−0·10 W	
additional loss (sec. 3.6)	ΔP_{DS}	−0·10 W	
insulation loss *)	ΔP_{DI}	≪0·10 W	
sum of other losses	ΔP_D		−1·55 W
demagnetization power after losses P_D			8·3 W
undisturbed magnetization power P_{M0}			39·11 W
energy flow through the regenerator ΔP_{MR}			0·17 W
magnetization power before other losses P_{M1}			38·93 W
other losses:			
flow losses	ΔP_{MF}	0·35 W	
conduction losses	ΔP_{MC}	−0·39 W	
eddy-current losses	ΔP_{ME}	0·10 W	
additional loss (sec. 3.6)	ΔP_{MS}	−0·10 W	
insulation loss *)	ΔP_{MI}	≪0·10 W	
sum of other losses	ΔP_M		−0·04 W
magnetization power after losses P_M			38·89 W
efficiency $\eta = P_D/(P_M - P_D)$			0·28
relative efficiency $\eta_r = \eta/\eta_c$			0·72

*) The insulation losses have been calculated assuming high vacuum and a radiation shield at 60 °K, mounted on the intermediate freezer of the precooler.

If the speed of the refrigerator is doubled, the flow losses at the cold side increase from 1 W to 8 W. Since the demagnetization power increases by 10 W, the refrigerating capacity at the double speed is only 38 % higher. The magnetization power is twice as large, however, and the efficiency is much lower.

It will be noted that the flow loss at the cold side is nearly 3 times higher than at the warm side. The reason is that the compressibility of the helium is much lower at the cold side than at the warm side. Equation (2.113) shows that b is high so that the largest part of the flow losses finally goes to the cold side. It may, however, be that the cross-effect with the magneto-caloric effect mentioned in sec. 2.7.4 in practice reduces the flow losses at the cold side considerably.

The sum of the losses at the warm side is negligible. The magnetization

power is therefore practically equal to the undisturbed magnetization power. It may seem surprising that the energy flow at the warm side of the regenerator is very small. This is, however, due to the temperature distribution in the regenerator which is nearly flat at the warm side due to the slightness of the gradient of the magnetic field at that side.

3.10.2. *Temperature distribution, regenerator load, Λ^* and Γ^+*

The temperature distribution and Γ^+ along the regenerator of this refrigerator are shown in fig. 3.10. In the middle of the regenerator Γ^+ is really very large,

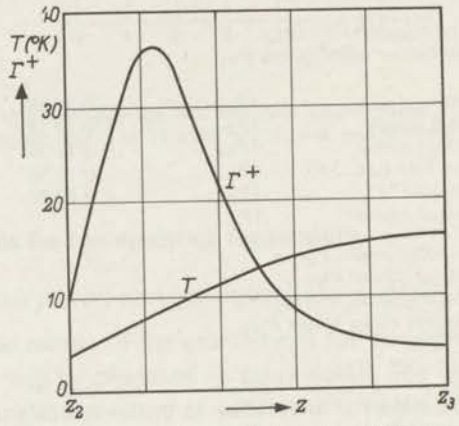

Fig. 3.10. The temperature distribution and the value of Γ^+ along the regenerator.

so that the approximation based on $\Gamma^+ = \infty$ is rather good. At the warm side Γ^+ decreases to a value of about 5. Fortunately the slight gradient in the temperature distribution at the warm side makes the heat load rather small there. The temperature fluctuations are therefore still slight.

At the cold side, the temperature fluctuation for the calculated temperature distribution is 2·0 °K, so that the temperature will vary from 3·2 °K to 5·2 °K. Since this temperature fluctuation is rather large, the theory deviates considerably from reality here. However, Γ^+ rises steeply at this side so that the deviation is restricted to a small part of the regenerator. Therefore the calculated value of the energy transport at the cold side of the regenerator is expected to be rather good after all.

Finally, the heat load ΔL, the magnetic heating ΔR (see secs 2.6.7 and 2.6.8) (both taken for sections of 1/20 of the regenerator length) and the heat-transfer number Λ^* are shown along the regenerator in fig. 3.11. The assumption made in the regenerator theory, that $\Delta L \gg \Delta R$, appears to be true, except at the warm side, where ΔL is small. Since the temperature differences between the paramagnetic material and the regenerator are small here too, the fact that $\Delta L \approx \Delta R$ here will hardly influence the behaviour of the regenerator.

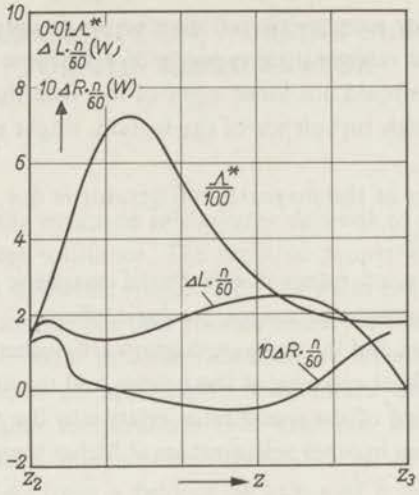

Fig. 3.11. The heat load ΔL, the magnetic heating ΔR (both for sections of 1/20 of the regenerator and multiplied by $(n/60)$) and the heat-transfer number Λ^* along the regenerator.

3.10.3. *Influence of the value of the Curie constant on the efficiency*

We shall now discuss the desirability of a high Curie constant per unit of volume. Let us suppose that in the designed refrigerator the Curie constant were much smaller. Then the undisturbed demagnetization power and the undisturbed magnetization power would decrease proportionally with this quantity. Except for the transport loss, the losses will not decrease, however, since they do not depend on the Curie constant. This is particularly true for the flow losses and the conduction losses both of which are relatively high. The efficiency of the refrigerator will therefore decrease when the Curie constant is smaller. Of course this can be compensated by using a higher magnetic field. The possibility of generating a higher field is limited, however, by the maximum current through the superconducting wires, particularly at the higher temperatures. On the other hand, it is obvious that a still higher value of the Curie constant will lead to a higher output and greater efficiency, till ultimately the transport loss becomes too high.

3.10.4. *Forces on the drive mechanism*

The force exerted by the magnetic field on the paramagnetic material is 120 kg maximum for the refrigerator discussed in this chapter. Via the connecting rod this force is transmitted to the drive mechanism. The design of a drive mechanism for such forces presents no problems.

3.11. Conclusions

From the results of the calculations discussed in this chapter, we can conclude

that the prospects for a magnetic refrigerator are promising. It appears that the efficiency and the refrigerating capacity of a machine of moderate size are high. However, we should not loose sight of the fact that secondary effects, for instance a very high turbulence of the helium, might undo these auspicious results.

The high efficiency of the magnetic refrigerator is due, in general terms, to the following effects.

(1) The combination of rather concentrated magnetic materials and high magnetic fields gives large magneto-caloric effects.
(2) The magnetization and the demagnetization are isothermal to a high degree, due to the great heat capacity of the helium and the excellent heat contact.
(3) The total heat load of the regenerator relative to the refrigerating capacity is much lower than in other refrigerators at higher temperature (e.g. Stirling refrigerators).

With higher magnetic fields, higher values of the refrigerating capacity and the efficiency can be obtained. We have estimated that the refrigerator discussed in this chapter will have a capacity of 35 watts at 4·2 °K if a magnetic field of 40 kOe is used. The losses are then relatively slight, with exception of the transport loss.

The magnetic refrigerator must be operated in cascade with a precooler. Using the model A20 gas refrigerating machine as precooler, the overall efficiency of this system is comparable to that of the best system using the Joule-Thomson refrigerating cycle. If the efficiency of the precooler could be increased, the system using the new magnetic refrigerator will surpass any other refrigerating system for temperatures below ≈ 10 °K.

The design of the new refrigerator resembles that of Stirling refrigerators in many respects. The belief is therefore justified that the new refrigerator will be the equal of the Stirling refrigerator in reliability and ease of operation, and surpass the Joule-Thomson cycle in these respects. A disadvantage is the use of moving parts at the lowest temperature, just as in the Stirling refrigerator.

The temperature range of the new cycle is greater than that of the Joule-Thomson cycle; this range is restricted by the low vapour pressure of helium at low temperatures in the last-named cycle.

The general conclusion from our analysis of the magnetic refrigerator is that further experimental investigation of this type of refrigerator is highly interesting.

4. MEASUREMENTS ON WORKING SUBSTANCES FOR THE REFRIGERATOR

4.1. Introduction

The feasibility of the magnetic refrigerator depends to a high degree on the quality of the working substance. The required properties of such a working substance have been discussed in sec. 3.2. The main requirement was a high value of the Curie constant per unit volume and none the less a low magnetic-ordering temperature. With the materials that are normally used below 1 °K it is possible to obtain an appreciable temperature drop by adiabatic demagnetization at higher temperatures. For example, Casimir, De Haas and De Klerk [6]) obtained a temperature of about 1 °K by demagnetization of $FeNH_4(SO_4)_2 \cdot 12\,H_2O$ from a field of 24 kOe and a temperature of 10 °K. Nevertheless, these substances are too diluted to be used in the magnetic refrigerator discussed in this thesis. Moreover, they are chemically not very stable. A number of more concentrated and chemically stable materials have therefore been investigated.

The susceptibility of such materials was determined down to the temperature of liquid helium using the inductive method. The measurements between 12 °K and 80 °K have been carried out in a special cryostat mounted on top of a gas refrigerating machine. For lower temperatures a normal metal dewar filled with liquid helium was used. These measurements are discussed in sec. 4.2.

Some of the materials investigated follow a Curie-Weiss law down to 2 °K with only small deviations. They therefore appeared suitable as working substance for the magnetic refrigerator. To verify this point further they have been used for adiabatic demagnetization from temperatures above 12 °K. The entropy and the specific heat of these materials could be derived from these experiments. The results of these experiments are discussed in sec. 4.3.

No general rules can be given for the selection of suitable materials. The behaviour of magnetic materials is determined mainly by the strength of the interactions of the magnetic ions with the crystalline field and with each other. As several mechanisms are responsible for these interactions and no systematic information as to their magnitude is available, it is hardly possible to predict the ordering temperature of a substance. However, it is well known that the interactions are less for the ions of the rare-earth metals than for those of the transition metals. Attention has therefore been concentrated on substances containing rare-earth metals.

If the interactions of the ions with each other and with the crystalline field are slight, the Curie constant is given by the relation

$$C = (N_c/3)\, J\,(J+1)\, g^2 \mu_B{}^2/k. \qquad (4.1)$$

In this equation k is the Boltzmann constant, J the inner quantum number, g the spectroscopic splitting factor and μ_B the Bohr magneton. If N_c is the number of magnetic ions per cm^3, then C is the Curie constant for 1 cm^3 of material. Ions with a high value of $p = g\,[J\,(J+1)]^{1/2}$ will give a high value of the Curie constant. For that reason Gd^{3+}, Dy^{3+}, Ho^{3+} and Er^{3+} have been selected for our investigations.

Alloys of the rare-earth metals were considered in the first place. The use of the alloys containing rare-earth ions in concentrations of a few per cent, has been reported by Little and Parks [20]) for application below 1 °K. The behaviour of some more concentrated alloys that were investigated by us was, however, not very favourable. The idea of using alloys in the magnetic refrigerator was therefore abandoned. The measurements of the susceptibility of those alloys will not be discussed in this thesis.

Following a suggestion of Dr P. F. Bongers we have investigated a number of mixed oxides with the general formula $R_2M_2O_7$. In this formula R is Gd, Dy, Ho or Er and M is Ti, Sn or Ga/Sb. Some of these materials proved to be very successful for our purpose. The measurements carried out on these materials will be discussed in this chapter.

4.2. Susceptibility measurements

4.2.1. *The mutual-inductance bridge*

A very simple type of ballistic mutual inductance bridge was used for the susceptibility measurements. This bridge, which is a modified Hartshorn bridge, has been described by Nicol [21]). The schematic diagram is shown in fig. 4.1. The bridge consists of a standard mutual inductance M_s, a coil system M_x (measuring coil), two variable resistors R_1 and R_2, a galvanometer G, a battery B and

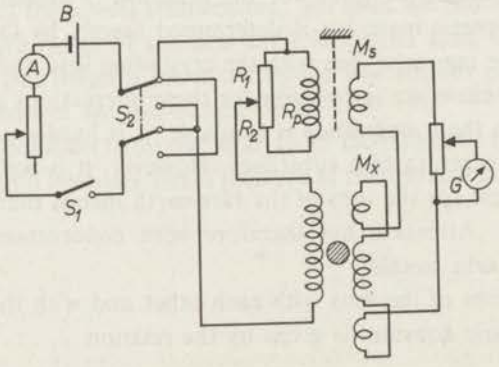

Fig. 4.1. Modified ballistic Hartshorn bridge.

some switches. The galvanometer (Kipp, type Zernike C) has a period of 7 seconds. When the direction of the current through primary coils is reversed, no deflection of the galvanometer will result if

$$M_x = R_1 M_s (R_1 + R_2 + R_p)^{-1}. \tag{4.2}$$

In this equation R_p is the resistance of the primary coil of M_s. The variable resistors are mounted on one axis and connected such that $(R_1 + R_2)$ is constant. The mutual inductance M_x is then directly proportional to R_1.

Two mutual inductances made by ourselves have been used for M_s. They were calibrated against a standard mutual inductance. The measured values of their mutual inductance is 6·63 mH and 2·06 mH.

The sample of paramagnetic material is placed in the centre of the coil system M_x. The change of the mutual inductance of M_x, caused by the presence of the sample, is proportional to its susceptibility.

4.2.2. *The measuring coil*

Some of the measurements were carried out in a cryostat mounted on the header of the gas refrigerating machine. Since this cryostat is partly made of copper, special precautions had to be taken to prevent the induction of eddy currents in the copper parts when the current in the coil system M_x is reversed. Such eddy currents will cause double deflections of the galvanometer.

The measuring coil M_x therefore has two concentric primary coils, through which the current flows in opposite directions. It is well known that the magnetic field outside such a coil system falls off rapidly if the magnetic fluxes produced by the two coils are equally large. The diameter of the inner coil is about 0·8 times that of the outer coil. The field produced by the inner coil must then be larger than the field of the outer coil. Since the current through the coils flows in opposite direction, the resulting field on the axis of the coil system is equal to the difference of the fields of the coils. To improve the homogeneity of this magnetic field extra turns were laid on the ends of both coils.

The magnetic field hardly penetrates in the copper parts of the cyrostat, so that only small eddy currents are induced in them. At 80 °K no double deflections were caused by such eddy currents. At about 15 °K, small double deflections were still found, obviously owing to the much lower electrical resistivity of the copper parts at those temperatures. In the measurements in the metal dewar such double deflections were not observed *).

The secondary coil consists, as usual, of a central coil and two additional

*) Double deflections were caused in some measurements by the paramagnetic material itself. The following, well-known method was used to determine the correct value of R_1 when too large double deflections occurred. Two values of R_1 were determined such that the deflections of the galvanometer are roughly equal in opposite directions. The value of R_1 leading to a zero deflection of the galvanometer if no double deflections occurred, is found by linear interpolations between the two said values of R_1.

coils on both sides of the central coil. Each additional coil has exactly half the number of turns of the central coil and is wound in the opposite direction. The mutual inductance between the primary coil system and the secondary coil should therefore be exactly zero. Due to small inhomogeneities a small mutual inductance is found in practice.

Between the measurements in different temperature ranges the measuring coil M_x was sometimes reheated to room temperature. It was therefore necessary that the residual mutual inductance of this coil system should remain constant. This required a rigid mechanical construction. The coil forms were therefore made of leaded bronze and after the coils had been wound they were joined together by a screw. The construction of the coil system is shown in fig. 4.2.

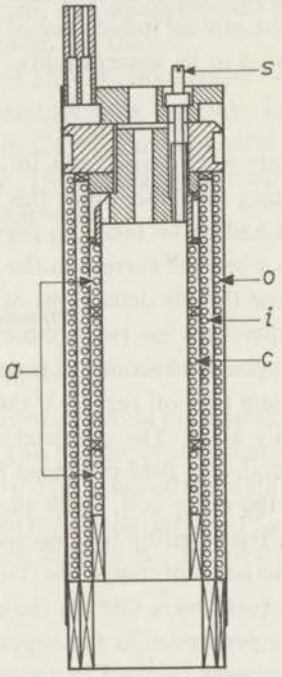

Fig. 4.2. Construction of the measuring coil;
(o) outer primary coil; (i) inner primary coil; (c) central part of the secondary coil; (a) additional parts of the secondary coil; (s) screw to join the coil forms.

To reduce eddy currents in the coil forms leaded bronze was used, since it is non-magnetic and has a rather high electrical resistivity. Moreover axial slots were cut in the coil forms over nearly the whole length. This construction proved to be very successful. Only very small double deflections of the galvanometer were found with this coil system. These double deflections cause an uncertainty of 10^{-3} mH in the determination of the mutual inductance.

The residual mutual inductance of the empty coil system, used in most of the experiments, was $M_0 = 7{\cdot}2.10^{-2}$ mH. This value changed by less than 3% in the course of the experiments. A change in M_0 between 80 °K and 4·2 °K was not observable. When a sample of 8·3 gramme $Dy_2Ti_2O_7$ was inserted in the measuring coil, its mutual inductance at 20 °K increased to $48{\cdot}8.10^{-2}$ mH. Due to the variation of M_0 the accuracy of the susceptibility measurement is thus about $5^0/_{00}$. At 80 °K the accuracy is then about 2% and at 4·2 °K $1^0/_{00}$. When diluted samples are used the accuracy decreases of course. For our purpose the accuracy attained is, however, more than sufficient.

The dimensions of the coil system used in most measurements are given in table 4-I.

TABLE 4-I

Dimensions of the measuring coil

primary coil P_1	
diameter of the coil form	28·0 mm
length of the coil	80·0 mm
number of turns	2515
correcting coils at both ends	142 turns each
primary coil P_2	
diameter of the coil form	22·5 mm
length of the coil	80·0 mm
number of turns	3805
correcting coils at both ends	140 turns each
central part of the secondary coil S_c	
diameter of the coil form	18·0 mm
length of the coil	25·0 mm
number of turns	2844
additional parts of the secondary coil	
diameter of the coil form	18·0 mm
length of each part	12·5 mm
number of turns of each part	1422
mutual inductance M_0 of the empty coil system	
(measured at 80 °K)	$7{\cdot}2.10^{-2}$ mH
constant E_1 *)	$2{\cdot}07.10^3$ cm^{-1}
constant E_2 *)	$10{\cdot}1.10^3$ cm^{-1}

*) These constants are discussed in sec. 4.2.3 and the appendix.

4.2.3. *Calculation of the susceptibility and the Curie constant from the measurements*

It is easily shown that the susceptibility of the sample is proportional to $(R_1 - R_0)$, where R_1 is the value of the variable resistor R_1 to compensate the mutual-inductance bridge when the sample is in the measuring coil, and R_0 the value of this resistor when the measuring coil is empty. If the susceptibility of the sample obeys a Curie-Weiss law, $R_1 - R_0$ is proportional to $(T - \Theta)^{-1}$. From a graph of $(R_1 - R_0)^{-1}$ as a function of T can be concluded whether the Curie-Weiss law is valid for this material.

From the measurements of M_x, the shape of the sample and the geometrical configuration of the measuring coil it is possible to calculate the magnitude of the susceptibility. In general such calculations are much easier if the sample is spherical. For this reason only spherical samples have been used. The relation between χ and M_x can, however, be determined more directly by measuring the mutual inductance M_{cp} between a small test coil in the centre of the measuring coil and the primary coils, and the mutual inductance M_{cs} between this coil and the secondary coil. If the cross-sectional area of the coil multiplied by the number of turns is O, the following constants can be obtained:

$$E_1 = M_{cp}/O \tag{4.3}$$

and

$$E_2 = M_{cs}/O. \tag{4.4}$$

If the test coil is small enough these constants are independent of the dimensions of the test coil. They give directly the magnetic field produced by a current through the primary coils and the secondary coil, respectively, in the centre of the coil system. Therefore E_1 and E_2 are characteristics of the coil system.

For χ the following equation will be derived in the appendix to this chapter:

$$\chi = (M_x - M_0)/E_1 E_2 G. \tag{4.5}$$

Here χ is the susceptibility of one gramme of material and G the weight of the sample.

To determine E_1 and E_2 we have used a test coil of approximately 4 mm diameter and 4 mm length. It had 178 turns of 0·07 mm copper wire distributed over 4 layers. The total effective cross-sectional area, calculated from the inner and outer diameter of the coil was 25·6 cm^2. The measured values of the mutual inductances at 80 °K were: $M_{cp} = 53{\cdot}3.10^{-3}$ mH and $M_{cs} = 260.10^{-3}$ mH. The values of E_1 and E_2 are mentioned in table 4-I. Due to the thermal contraction of the coils these values of E_1 and E_2 vary from 80 °K to 4 °K less than $1^0/_{00}$. This is far below the accuracy with which E_1 and E_2 are determined (see the appendix).

We can make now a graph of χ^{-1} as function of T. This graph will be a straight line if the material obeys a Curie-Weiss law. The slope of this line is the Curie constant and the interaction of this line with the T-axis yields Θ.

The errors introduced by deviations from the correct position of the sample and by a not quite spherical shape are much smaller than the uncertainty in the value of $(E_1 \times E_2)$.

4.2.4. *Preparation of the samples*

The samples were prepared by Dr Bongers by heating the oxides of the components to temperatures between 1400 °C and 1500 °C for several hours. In the preparation of R_2GaSbO_7 gallium oxide and antimony oxide were first heated together at a much lower temperature to obtain $GaSbO_4$. The material thus obtained was ground to a powder with a particle size of approximately 1 micron. From this powder half-spheres were obtained by compressing it in a mould. They were sintered for a few hours at high temperatures to obtain rigid bodies. Their density was approximately 85% of the crystalline density. Finally a spherical sample was obtained by glueing two half-spheres together with a very thin sheet of copper (25 micron) between them. The volume of the sample is about 1·5 cm^3. A small carbon resistor was glued to the copper (1/10-watt Allan-Bradley resistor). This resistor was used to measure the temperature of the sample between 4·2 °K and 14 °K in the susceptibility measurements and over the whole temperature range in the adiabatic-demagnetization experiments.

In the derivation of eq. (4.5) it is assumed that the sample is homogeneously magnetized. As the sample is spherical this is true if the sample is of crystalline density. For a sample of compressed powder the situation is somewhat uncertain. Since, however, the powder particles are very small compared to the size of the sample, it can be assumed that the mean magnetization is homogeneous over volumes that are large compared with the particle size.

The magnetic fields inside a powdered sample have been discussed extensively by De Klerk [22]). If the powder particles are spherical themselves, the magnetic field on the particles and the field on the paramagnetic ions is equal to the external field. If the particles have an arbitrary shape these fields cannot be calculated exactly. Since, however, the relative density of the sample is high and the particles are small, the measured susceptibility in our case will not deviate appreciably from that measured on a sample of spherical shape and crystalline density.

4.2.5. *Temperature measurement*

The temperature of the sample during the measurements in liquid helium, liquid hydrogen and liquid nitrogen can be obtained directly from the vapour pressure of these liquids. Some measurements were, however, performed

between 4·2 °K and 14 °K. The sample was suspended in that case in the vapour above boiling liquid helium. The susceptibility was measured while the sample was heating slowly. Of course, the results are less reliable since the uniformity of the temperature distribution in the sample is not certain. Still, these measurements are useful in giving an approximate value of the susceptibility in this temperature range.

The temperature curve of the resistor was calculated with the empirical equation of Clement and Quinnel [23]):

$$\log R + K/\log R = A + B/T. \tag{4.6}$$

The constants in this equation were obtained from calibration points in the liquid helium and the liquid hydrogen. The accuracy of the temperature determination according to the data available from literature is approximately 0·05 °K.

4.2.6. *The cryostat on the gas refrigerating machine*

A drawing of the cryostat mounted on the gas refrigerating machine is shown in fig. 4.3. It is used both for the susceptibility measurements between 12 °K

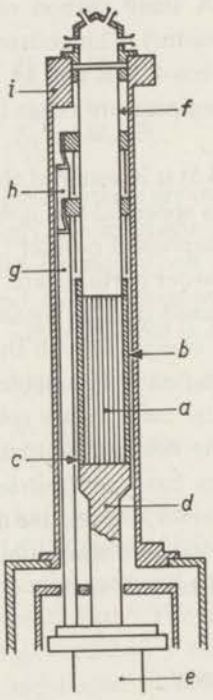

Fig. 4.3. Schematic drawing of the cryostat mounted on the gas refrigerating machine; (a) the cryostat proper; (b) and (c) copper and brass wall of (a); (d) copper rod connecting (a) to the gas refrigerating machine; (e) header of the gas refrigerating machine; (f) stainless-steel tube; (g) and (h) copper rods; (i) outer wall.

and 80 °K and for the adiabatic-demagnetization experiments discussed in sec. 4.3. The actual cryostat is the cylinder a. The wall of this cylinder consists of 2 mm thick copper (b), in which a large number of axial slots have been cut to reduce eddy currents originating from the measuring coil. The copper wall is surrounded by a thin brass wall c to make it pressure-tight. The cryostat is connected by a 30 mm thick copper rod d to the header e of the gas refrigerating machine. At the upper side the cryostat is connected to a stainless-steel tube f, through which objects can be inserted into the cryostat. Since the upper part of this tube is warm, heat will flow through the wall of this tube into the cryostat. To reduce the heat influx into the cryostat the tube f is cooled at $\frac{1}{3}$ and $\frac{2}{3}$ of its height to 15 °K and 60 °K, respectively, by means of copper rods g and h connecting these points to the header and the intermediate freezer of the gas refrigerating machine. The cryostat and the copper rods are gold-plated to reduce the heating by radiation from the outer wall i.

The copper wall b is necessary to obtain a uniform temperature of the cryostat when no liquid is condensed in it. However, it causes some double deflection of the galvanometer in the susceptibility measurements, notwithstanding the axial slots and the special construction of the measuring coil.

4.2.7. *Susceptibility of* R_2GaSbO_7

The susceptibility of mixed oxides with the general formula R_2GaSbO_7 for R = Gd, Ho, Dy and Er was measured. In fig. 4.4 the reciprocal value of the susceptibility per gramme, χ^{-1}, is shown as a function of temperature. All four materials remain paramagnetic down to 2 °K, the lowest temperature of the

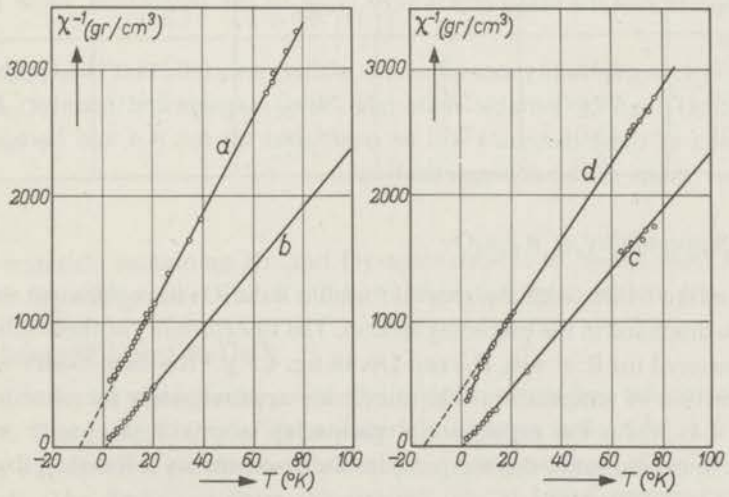

Fig. 4.4. The reciprocal value of the susceptibility as a function of temperature for four different materials with the formula R_2GaSbO_7.
Curve a: Gd_2GaSbO_7, curve b: Dy_2GaSbO_7, curve c: Ho_2GaSbO_7, curve d: Er_2GaSbO_7.

measurements. Above 8 °K the experimental points lay well on the straight lines. At lower temperatures they lay above the straight line for the Gd, Ho and Dy compounds and below this line for the Er compound. It is remarkable that the asymptotic Curie points for Gd_2GaSbO_7 and Er_2GaSbO_7 have high negative values, whereas those of Ho_2GaSbO_7 and Dy_2GaSbO_7 are low.

The value of Θ, the Curie constant and the effective moments p of these materials are listed in table 4-II. For comparison, the theoretical value of p for the free ions is included in this table.

TABLE 4-II

Magnetic data for R_2GaSbO_7

compound	Θ (°K)	c (°Kcm³/g)	$p_{exp.}$	$p_{theor.} = g[J(J+1)]^{1/2}$	lattice parameter (Å)
Gd_2GaSbO_7	−10·0	0·027	8·2	7·94	10.24
Ho_2GaSbO_7	− 0·3	0·042[5]	10·4	10·60	10·12
Dy_2GaSbO_7	0·15	0·042	10·5	10·63	10·20
Er_2GaSbO_7	−15·2	0·033[5]	9·2	9·59	10·12

It appears that the value of p is very close to the theoretical value for the free ion.

From the susceptibility measurements we may conclude that Ho_2GaSbO_7 and Dy_2GaSbO_7 can be suitable materials for a magnetic refrigerator. Further discussion of these materials will be postponed till sec. 4.4 and be combined with the results of the demagnetizations.

4.2.8. *Susceptibility of* $R_2Sn_2O_7$

The mixed oxides with the general formula $R_2Sn_2O_7$ have the same structure as those discussed in the preceding section. The susceptibility of these substances was measured for R = Gd, Ho and Dy. In fig. 4.5 χ^{-1} for these oxides is shown as a function of temperature. The curves are approximately the same as those in fig. 4.4. Again the experimental points lay above 8 °K pretty well on straight lines, and below this temperature the susceptibility is less than that given by the Curie-Weiss law.

The Curie constant, the asymptotic Curie point and the effective moments derived from the measurements are listed in table 4-III.

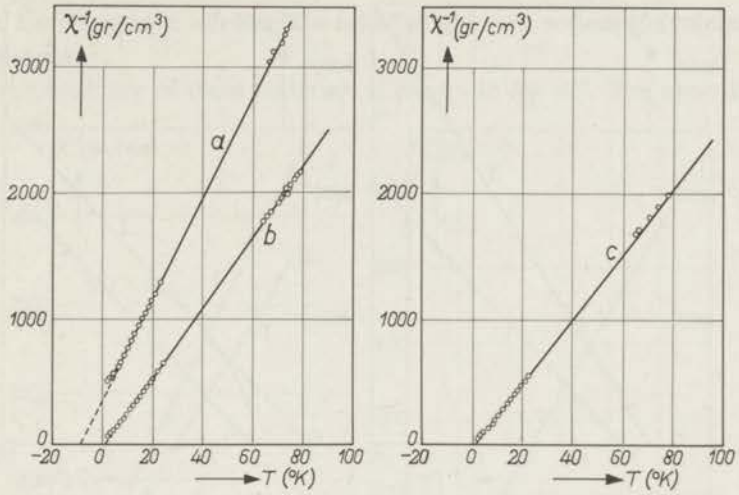

Fig. 4.5. The reciprocal value of the susceptibility as a function of temperature for three different materials with the general formula $R_2Sn_2O_7$.
Curve a: $Gd_2Sn_2O_7$, curve b: $Dy_2Sn_2O_7$, curve c: $Ho_2Sn_2O_7$.

TABLE 4-III

Magnetic data for $R_2Sn_2O_7$

compound	Θ (°K)	c (°Kcm³/g)	$p_{exp.}$	$p_{theor.} = g[J(J+1)]^{1/2}$	lattice parameter (Å)
$Gd_2Sn_2O_7$	−9·0	0·025	8·1	7·94	10.39
$Ho_2Sn_2O_7$	0·6	0·038	10·2	10·60	10·32
$Dy_2Sn_2O_7$	1·8	0·035	9·7	10·63	10·34

The materials containing Ho and Dy again appear to be the most suitable ones for the refrigerator. There will be further discussion in sec. 4.4.

4.2.9. *Susceptibility of* $R_2Ti_2O_7$

Another set of mixed oxides with the same structure has the composition $R_2Ti_2O_7$. The susceptibility of these materials is shown in fig. 4.6 for R = Gd, Ho, Dy and Er. The curves are practically the same as those of the preceding materials. The deviations from the straight line at lower temperatures are, however, somewhat less for Ho and Dy. Further magnetic data are listed in table 4-IV.

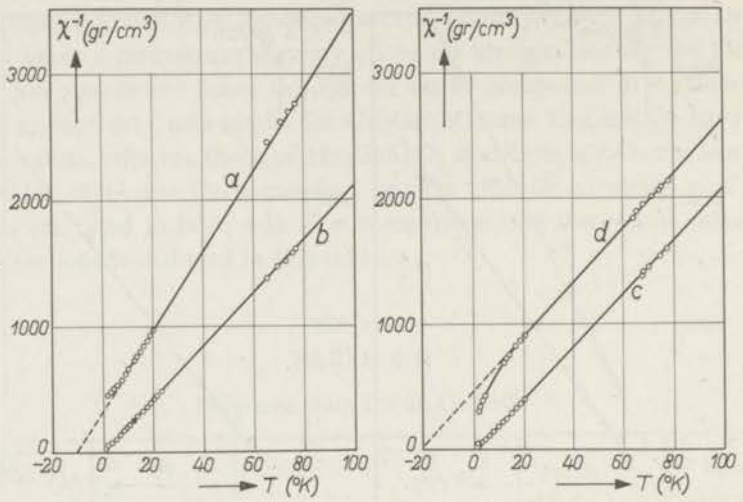

Fig. 4.6. The reciprocal value of the susceptibility for four different materials with general formula $R_2Ti_2O_7$.
Curve a: $Gd_2Ti_2O_7$, curve b: $Dy_2Ti_2O_7$, curve c: $Ho_2Ti_2O_7$, curve d: $Er_2Ti_2O_7$.

TABLE 4-IV

Magnetic data for $R_2Ti_2O_7$

compound	Θ (°K)	c (°Kcm³/g)	$p_{exp.}$	$p_{theor.} = g[J(J+1)]^{1/2}$	lattice parameter (Å)
$Gd_2Ti_2O_7$	−10·4	0·032	8·1	7·94	10.21
$Ho_2Ti_2O_7$	0·6	0·048	10·2	10·06	10·08
$Dy_2Ti_2O_7$	0·1	0·047	10·0	10·63	10·08
$Er_2Ti_2O_7$	−22·0	0·046	10·1	9·59	10·04

The materials containing Ho and Dy are in this case too the most suitable ones for the refrigerator. In sec. 4.4 these results are discussed in more detail.

4.2.10. *Susceptibility of diluted materials*

From the demagnetization experiments discussed later on it appears that $Dy_2Ti_2O_7$ is the most favourable working substance for the magnetic refrigerator among the materials discussed in the preceding sections. To obtain some more information on this material and to obtain a working substance suitable for lower temperatures, the susceptibility of the more diluted compounds $Dy_{0.8}Y_{1.2}Ti_2O_7$, $Dy_{0.2}Y_{1.8}Ti_2O_7$ and Gd Y Ti_2O_7 was measured. Since the yttrium ion has no magnetic moment there are less magnetic ions per unit

volume. Each magnetic ion has thus fewer neighbours, so that the interactions must be weaker.

The susceptibility of these materials is shown in fig. 4.7. The experimental

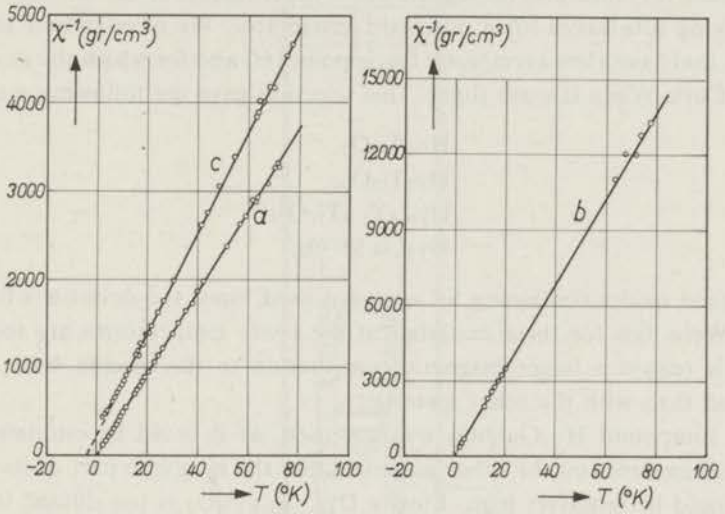

Fig. 4.7. Reciprocal value of the susceptibility of $Dy_{0.8}Y_{1.2}Ti_2O_7$ (curve a), $Dy_{0.2}Y_{1.8}Ti_2O_7$ (curve b) and $GdYTi_2O_7$ (curve c).

points now lay on straight lines down to the lowest temperature. We may conclude from this that the deviations for $Dy_2Ti_2O_7$ and $Gd_2Ti_2O_7$ at the lowest temperatures are caused mainly by interactions among the magnetic ions and not by the crystalline field.

In the measurements of these dilute materials we observed rather large double deflections of the galvanometer. This is rather surprising and we can offer no explanation for the fact that such double deflections were found for these diluted materials, whereas only small double deflections were found for the undiluted materials.

The asymptotic Curie point Θ, the Curie constant and the effective moments of these materials are listed in table 4-V.

TABLE 4-V

Magnetic data for $R_xY_{2-x}Ti_2O_7$

compound	Θ (°K)	c (°K cm³/g)	$p_{exp.}$	$p_{theor.} = g[J(J+1)]^{1/2}$	lattice parameter (Å)
Gd Y Ti_2O_7	—4·4	0·017	7·9	7·94	10·08
$Dy_{0.8}Y_{1.2}Ti_2O_7$	0·0	0·022	9·9	10·63	10·08
$Dy_{0.2}Y_{1.8}Ti_2O_7$	0·0	0·0059	9·7	10·63	10·08

4.3. Adiabatic-demagnetization experiments

From the mixed oxides discussed in the preceding section we selected those substances for adiabatic-demagnetization experiments which seemed suitable as working substances for a magnetic refrigerator. We have chosen the substances that have a low asymptotic Curie point (Θ) and for which the deviations of the Curie-Weiss law are slight. This selection gave the following materials:

$Ho_2Ti_2O_7$,
$Dy_2Ti_2O_7$,
$Dy_{0.8}Y_{1.2}Ti_2O_7$,
$Dy_2Ga\,Sb\,O_7$.

The mixed oxides containing Sn were not used, since the deviations from the Curie-Weiss law for these materials at the lower temperatures are too large. For this reason a larger magnetic contribution to the specific heat can be expected than with the other materials.

The compound Ho_2GaSbO_7 was not used, as it could be estimated from the measurements on the other materials that the magnetic part of its specific heat would be relatively high. Finally $Dy_{0.2}Y_{1.8}Ti_2O_7$ is too diluted for adiabatic demagnetization at higher temperatures. All other materials discussed in the preceding sections have a high negative value of Θ.

The lowest starting temperature for the demagnetizations was about 12 °K, as these experiments were done on a gas refrigerating machine and this is the lowest temperature obtainable in this way. Using a field of 15 kOe, temperatures of about 4 °K were obtained after demagnetization. By these experiments it was verified in the first place that the selected materials did cool down sufficiently. Secondly, data were obtained on their entropy and specific heat.

4.3.1. *The experimental arrangement*

The experiments were carried out in the cryostat, described in sec. 4.2.6, which is mounted on the gas refrigerating machine. This cryostat is placed between the poles of an iron-core magnet. To demagnetize the sample the magnet is rolled away on a pair of short rails, mounted above the gas-refrigerating machine. The magnet, which has a weight of approximately 400 kg, was designed by Dr D. J. Kroon. A magnetic field of 15 kOe in a gap of 6 cm can be obtained with it.

In the cryostat a tube t of 3·3 cm O.D. was inserted from above (fig. 4.8). It was closed at the lower side by a bottom plate (b) that was screwed to the tube. An indium packing was mounted between the tube and the bottom plate to make the system vacuum-tight. At the warm side the tube is connected through some valves to a high-vacuum pump.

The sample p of paramagnetic material is mounted in this tube. Heat contact

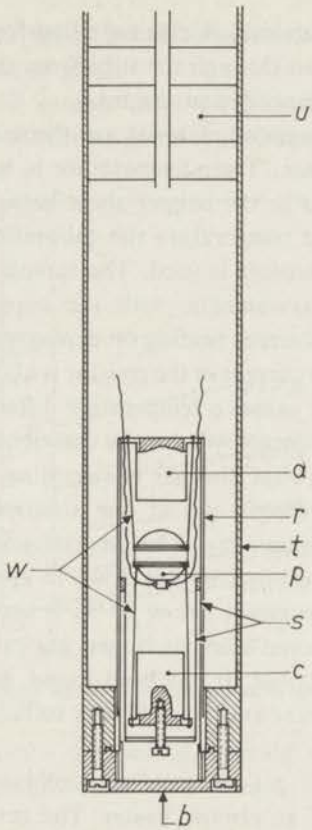

Fig. 4.8. Apparatus used for adiabatic-demagnetization experiments;
(b) bottom plate; (w) stainless-steel wires; (e) and (d) containers with Dy_2O_3; (s) stainless-steel supports; (t) tube; (p) paramagnetic sample; (r) gold-plated cylinder; (u) radiation shields.

between the tube and the cryostat is obtained by condensing a small amount of hydrogen in the cryostat. Below 14 °K the hydrogen solidifies, but the heat conduction is still sufficient to keep the tube at practically the same temperature as the cryostat.

The paramagnetic sample was suspended by 4 stainless-steel wires (w), 0·15 mm in diameter, as shown in fig. 4.8. To reduce the heat influx, the wires were connected at the other side to two containers c and d filled with Dy_2O_3. This material is paramagnetic too, so that it will cool down at the same time as the sample when the magnet is removed. Since its specific heat is much higher, it will not cool down as far as the sample. The heat that can be absorbed by it is, however, considerable, so that it will stay cold relatively long. The temperature difference over the stainless-steel wires is now low, so that there is little heat influx from this source. The containers c and d are mounted with thin stainless-steel supports s on the bottom plate. A gold-plated cylinder r,

attached to the upper container, shields radiation from the sample. To reduce the radiation coming down through the tube from the warm side, a system of radiation shields (u) is suspended in the tube.

The samples of paramagnetic material are the same as those used for the susceptibility measurements. Their temperature is measured with the carbon resistor that was attached to the copper sheet between the two halves of the sample. To determine the temperature the calibration curve obtained during the susceptibility measurements is used. The sample is mounted here, just as in the susceptibility measurements, with the copper sheet parallel to the magnetic field. The eddy-current heating on demagnetization is then negligible. The heat developed by the current in the resistor is about 10^{-6} watt. The transfer of this heat to the sample causes a temperature difference lower than 10^{-3} °K.

The course of the experiments will now be described briefly. After the magnet is placed around the cryostat the gas refrigerating machine is started. The cryostat is filled with hydrogen gas at one atmosphere, whereas the tube t contains low-pressure helium gas. The gas refrigerating machine cools the cryostat and the tube t with its contents down in approximately one hour. As soon as a temperature somewhat below 20 °K is reached the hydrogen gas in the cryostat condenses. Some more hydrogen gas can then be supplied to the cryostat to obtain more liquid. It has been found, however, that the amount of gas present in the cryostat and the tubing is sufficient to obtain an excellent heat contact.

The temperature of the gas refrigerating machine is now stabilized at the desired level by means of an electric heater. The current through the magnet is then switched on. The temperature of the sample is raised by the magnetization. After some minutes the temperature of the sample is equalized again to that of the tube t by heat transfer through the helium gas. When the temperature of the sample is stable, the valve between the tube and the high-vacuum pump is opened. Shortly afterwards the gas refrigerating machine is stopped. This is necessary since it has been found that the vibrations of this machine cause excessive heating of the sample after demagnetization. During the first few minutes after stopping the refrigerator, the temperature of the cryostat does not change appreciably. This time is sufficient to obtain a rather good vacuum.

It is convenient to have the same starting temperature for demagnetizations from different fields. Therefore the temperature of the gas refrigerating machine is stabilized slightly below this temperature. When the helium gas is removed from the tube t, the sample starts to heat slowly (e.g. at a rate of approximately 0·1 °K per minute). As soon as the desired starting temperature for the demagnetization is indicated by the carbon thermometer, the magnet is rolled away. The temperature differences that can occur in the sample have been estimated for the observed heating before demagnetization and it has been

found that they are lower than 10^{-2} °K, even if the heat conduction of the sample was as low as that of glass.

The temperature of the sample after demagnetization is measured as a function of time. Figure 4.9 shows some typical temperature curves obtained

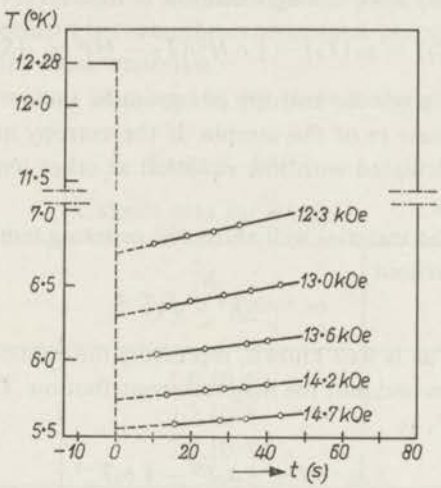

Fig. 4.9. Typical temperature curves after demagnetization.

after demagnetization from a number of differing magnetic fields. The temperature before demagnetization for each series is represented by the line at 12·28 °K.

Figure 4.9 shows that the temperature rises at a rate of approximately 0·1 °K per minute. By extrapolating to the moment of demagnetization the temperature of the sample at that moment is determined. The temperature of a sample has been followed in some instances for a much longer time. The rate of heating remains practically constant, indicating that the temperature equilibrium between the sample and the thermometer is already established before the first temperature determination after demagnetization is obtained.

4.3.2. *Experimental results*

The entropy of the investigated materials as a function of temperature can now be calculated from the experimental results. Since these materials follow very accurately a Curie-Weiss law above 12 °K, the entropy difference between the magnetized and the non-magnetized state at the pre-demagnetization temperature T is obtained from this law and eq. (2.2). This gives

$$s_0 - s_H = \tfrac{1}{2}\, c\, H^2/(T-\Theta)^2, \tag{4.7}$$

where s_0 and s_H are the entropy per gramme at zero field and in a field H at that temperature, and c is the Curie constant per gramme. The entropy of the

material after demagnetization is however not exactly equal to s_H, since the carbon resistor, the copper sheet and a few other parts attached to the sample are cooled down by it. The necessary correction ΔS_a can be calculated from the specific heat of these materials. The entropy of the paramagnetic material at the temperature T_f after demagnetization is then

$$s_0(T_f) = s_0(T_b) - \tfrac{1}{2} c H^2/(T_b - \Theta)^2 + \Delta S_a/m. \tag{4.8}$$

Since this equation gives the entropy per gramme the correction ΔS_a had to be divided by the mass m of the sample. If the entropy at one value of T_b is known it can be calculated with this equation at other temperatures from the experimental results.

For a paramagnetic material well above the ordering temperature the specific heat can often be written

$$c_0 = a_s T^3 + b_s T^{-2}. \tag{4.9}$$

The first part of c_0, as is well known, represents the contribution of the lattice vibrations and the second part the magnetic contribution. The entropy obtained by integrating $c_0 T^{-1}$, is

$$s_0 = l + \tfrac{1}{3} a_s T^3 - \tfrac{1}{2} b_s T^{-2}. \tag{4.10}$$

Here l is equal to the maximum magnetic entropy which for a free magnetic ion is $(R/M) \ln (2J + 1)$, disregarding a contribution of the nucleus to the entropy.

It appeared that the entropy of the investigated materials with exception of $Dy_{0.8}Y_{1.2}Ti_2O_7$ can be represented fairly well by eq. (4.10). The result for Dy_2GaSbO_7 is shown in fig. 4.10, where the solid line represents the entropy

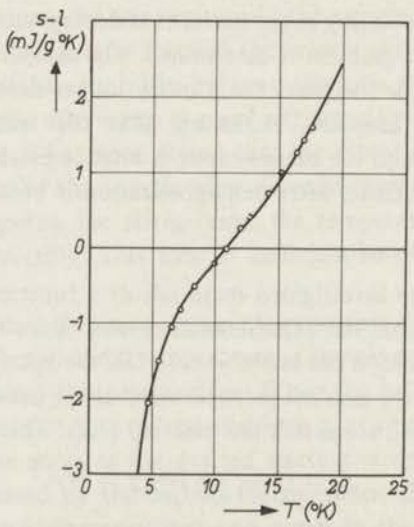

Fig. 4.10. The entropy of Dy_2GaSbO_7 as a function of temperature. The solid curve is obtained from eq. (4.10) with $a_s = 1{\cdot}0.10^{-6}$ (J/°K⁴g) and $b_s = 0{\cdot}095$ (J°K/g).

according to eq. (4.10) with $a_s = 1{\cdot}0.10^{-6}$ (J/°K⁴g) and $b_s = 0{\cdot}095$ (J °K/g). The experimental points were obtained by reading $s_0(T_b)$ from this curve and calculating the entropy at T_f with eq. (4.8). The agreement between the experimental points and the theoretical curve is quite satisfactory.

The results for $Dy_2Ti_2O_7$ and $Ho_2Ti_2O_7$ are represented in the same way in fig. 4.11. The agreement between the experimental points and the theoretical curve is also good for these materials.

In table 4-VI the values of a_s and b_s for these materials are listed.

TABLE 4-VI

Caloric data for $R_2M_2O_7$

compound	a_s (J g^{-1} °K^{-4})	b_s (J g^{-1} °K)
Dy_2GaSbO_7	$1{\cdot}0.10^{-6}$	0·095
$Dy_2Ti_2O_7$	$2{\cdot}2.10^{-6}$	0·078
$Ho_2Ti_2O_7$	$2{\cdot}2.10^{-6}$	0·19

The entropy of $Dy_{0.8}Y_{1.2}Ti_2O_7$ could not be represented by eq. (4.10). This is rather surprising and we can offer no explanation for this fact. Figure 4.12 shows the measured entropy as a function of temperature.

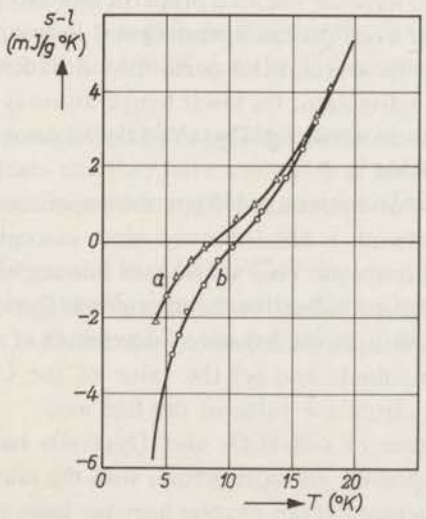

Fig. 4.11. The entropy of $Dy_2Ti_2O_7$ and $Ho_2Ti_2O_7$ as a function of temperature. The solid curves as obtained from eq. (4.10), where $a_s = 2{\cdot}2.10^{-6}$ (J/°K⁴g) and $b_s = 0{\cdot}078$ (J °K/g) for the first material and $a_s = 2{\cdot}2.10^{-6}$ (J/°K⁴g) and $b_s = 0{\cdot}19$ (J °K/g) for the second material.

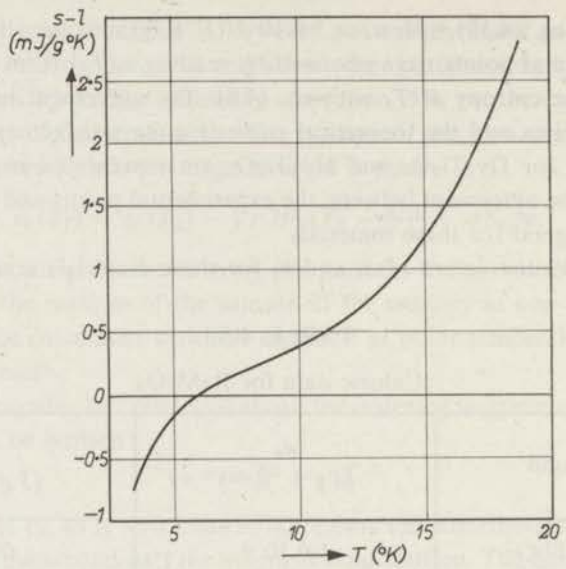

Fig. 4.12. The measured entropy of $Dy_{0.8}Y_{1.2}Ti_2O_7$ as a function of temperature.

4.4. Discussion

The experiments were done primarily to obtain information as to the suitability of the investigated materials as a working substance for a magnetic refrigerator. From the results the conclusion can be drawn that the substances containing Dy and Ho have the required properties for this purpose. Particularly $Dy_2Ti_2O_7$ is suited for a refrigerator operating at a lowest temperature of 4 °K. This is confirmed by the calculations performed on such a refrigerator (see chapter 3). When a refrigerator for lower temperatures is designed, it is better to use a more diluted material, e.g. $Dy_{0.8}Y_{1.2}Ti_2O_7$, since this material follows a Curie-Weiss law down to 2 °K.

The information that is obtained from the experiments on the magnetic structure of these materials is rather limited, since susceptibility measurements on powdered materials are not very valuable in this respect. The most remarkable results are (a) the low value for the asymptotic Curie temperatures Θ for Ho and Dy compounds, (b) the negative value for Θ of more than 10 °K for the Gd and Er compounds and (c) the value of the Curie constant which deviates only slightly from the value of the free ions.

The crystal structure of $Gd_2Ti_2O_7$ and $Dy_2Ti_2O_7$ has been discussed by Roth [24]). These compounds are isostructural with the mineral pyrochlore. The other compounds discussed in this chapter have the same structure [25]). The unit cell contains 8 rare-earth ions. Each ion lies in the centre of a distorted cube of 8 O^{2-} ions. Two of the O^{2-} ions on diametrically opposed corners of the cube lie at a shorter distance then the other six.

No direct information on the splitting of the energy levels of the rare-earth ions in the crystalline field of these compounds are available. Measurements of the fluorescence spectrum of Eu^{3+} in $Gd_2Ti_2O_7$ [26]) yield a splitting of approximately 250 cm^{-1} of the $^7F_1$ level of this ion, indicating that the crystalline field is not very weak.

The raising of the degeneracy of the free-ion ground level of the rare-earth ions in a cubic field has been discussed by Lea, Leask and Wolf [27]). However, it must be expected that the remaining degeneracy of the energy levels in the cubic field is removed further by an axial field due to the two oxygen ions at the shorter distance.

The saturation magnetization of some of the investigated materials at 2 °K was determined by Bongers [25]). He found a value of the saturation magnetization, which is approximately half that of the free ions. Combining this information with our measurements we can conclude for the Dy and the Ho compounds, that

(a) the ground level of the free ions is split such that a few low-lying levels with a high magnetic moment are obtained,
(b) the deviation from the Curie-Weiss law between 2 °K and 8 °K for the undiluted materials is due to the interactions between the magnetic ions.

The first conclusion is necessary to explain the fact that these materials, especially the diluted materials, follow a Curie-Weiss law between 2 °K and 80 °K. In the case of Dy the lowest level will be a Kramers doublet, since the number of electrons is odd.

The second conclusion is based on the fact that the deviations from the Curie-Weiss law between 2 °K and 8 °K for the Dy compounds are reduced by dilution with Y.

The erbium compounds exhibit large deviations of the Curie-Weiss law at the lowest temperatures and they have a negative Θ value of more than 20 °K. However, no conclusions concerning these compounds can be obtained from these measurements.

The splitting of the ground level of the Gd^{3+} ion must be much smaller since it is a S state. The negative Θ value must be due to interactions between the magnetic ions. This is confirmed by the reduction of Θ on diluting with Y.

Appendix B

In sec. 4.2.3 the following equation was used to obtain χ from the measured mutual inductance of the measuring coil

$$\chi = (M_x - M_0)/E_1E_2G. \tag{B.1}$$

This equation can be derived as follows.

The paramagnetic sample is magnetized homogeneously by the magnetic field of the primary coil system. The total magnetic moment of the sample is

$$G\sigma = G\chi H_p = G\chi E_1 i_p. \tag{B.2}$$

Here G is the weight of the sample, σ the magnetic moment per gramme, χ the susceptibility, H_p the magnetic field of the primary-coil system, and E_1 the ratio of H_p to the current i_p in the primary coil system.

When the current i_p is reversed, the magnetization of the sample is reversed too. This causes a voltage e_a in the secondary coil in addition to the voltage induced in that coil when there is no sample in the measuring coil. The voltage e_a is

$$e_a = (M_x - M_0)\,\mathrm{d}i_p/\mathrm{d}t. \tag{B.3}$$

However, this voltage can also be calculated from the magnetic field due to the sample at the secondary coil. Since the sample is spherical and magnetized homogeneously, it has a purely dipole field outside the sample. The same voltage e_a is therefore induced in the secondary coil if the current in a very small test coil at the centre of the sample is reversed. The magnetic moment of the coil must, of course, be the same as that of the sample. If the winding surface of the test coil is F, the current through it must be

$$i_c = G\sigma/F. \tag{B.4}$$

The voltage e_a can be written as

$$e_a = M_{cs}\,\mathrm{d}i_c/\mathrm{d}t, \tag{B.5}$$

where M_{cs} is the mutual inductance between the test coil and the secondary coil; M_{cs} can easily be calculated since it is equal to the mutual inductance M_{sc} between the secondary coil and the test coil. For M_{cs} then easily can be derived

$$M_{cs} = M_{sc} = FE_2, \tag{B.6}$$

where E_2 is the ratio of the magnetic field H_s at the test coil due to the current i_s in the secondary coil to i_s.

Substitution of eqs (B.4) and (B.6) in (B.5) gives

$$e_a = E_2G\,\mathrm{d}\sigma/\mathrm{d}t. \tag{B.7}$$

From eqs (B.7) and (B.2) it then follows that

$$e_a = \chi E_1 E_2 G \, \mathrm{d}i_p/\mathrm{d}t. \tag{B.8}$$

From this equation and (B.3) we obtain finally eq. (B.1).

The constants E_1 and E_2 can now be derived directly using the normal equations to calculate the magnetic field of coils, or they can be determined with a test coil. We have used the latter method, as it is after all more direct. The constant E_2 follows directly from eq. (B.6) if F is known and M_{cs} is measured. In the same way E_1 can be found from the mutual inductance M_{pc} between the same test coil and the primary-coil system, using the equation

$$M_{pc} = FE_1. \tag{B.9}$$

The test coil must be so small that the magnetic field does not vary appreciably over the volume of the coil. This causes no difficulty in the determination of E_1 since the field of the primary coil is very homogeneous in the centre of the coil system. The magnetic field, due to a current through the secondary coil, is not homogeneous. Even over the volume of the test coil we have used (diameter 4 mm, length 4 mm) this field varies by about 1·7%. The use of a still smaller test coil will not give better results, as the accuracy in the determination of M_{cs} and M_{cp} will decrease. Moreover, the value of the effective surface of the coil F becomes more uncertain, since the diameter of the wires is no longer negligible compared to the coil diameter. The best method to obtain accurate values of E_1 and E_2 is to use a large coil and to calculate the necessary correction. For our purpose such a high degree of accuracy in the magnitude of the susceptibility and the Curie constant is however unnecessary. The accuracy of our determination ($E_1 \times E_2$) is estimated as 3%. The real value of ($E_1 \times E_2$) is probably higher than our results. This is in accordance with the slightly too high value of p found for all compounds containing gadolinium.

LIST OF FREQUENTLY USED SYMBOLS

a	heat-transfer coefficient
a_s	coefficient in the relation for the specific heat
b	dividing factor for the flow losses
b_s	coefficient in the relation for the specific heat
c	Curie constant per gramme
c_0	specific heat of the paramagnetic material per gramme in zero field
c_p	specific heat of helium per gramme at constant pressure
d	ratio of the swept volume of the pistons to the total gas volume in the refrigerator
e	coordinate of a component
f	filling factor
$f(\beta)$	function of the crank angle β
g	Landé factor
g_R	slope of the temperature distribution in the regenerator
h	enthalpy of a gas or a liquid per gramme
k	Boltzmann constant
l	length of the stylized regenerator
m_k	mass of the paramagnetic material
n	number of revolutions per minute of the refrigerator
p	pressure of the helium
	effective magnetic moment
q	heat
s	entropy of the paramagnetic material per gramme
s_0	entropy of the paramagnetic material per gramme in zero field
s_M	field-dependent part of the entropy of the paramagnetic material per gramme
t	time
$\frac{1}{2} t_p$	length of both the warm and the cold period of the regenerator
u	internal energy of the paramagnetic material per gramme
u_0	internal energy of the paramagnetic material per gramme in zero field
w	"flow" of paramagnetic material in the regenerator
w_1	mean value of w in both the warm and the cold period
w_0	mean value of w, when the dimensionless time coordinate τ is used
x	coordinate in the stylized regenerator
y	coordinate along the axis of the magnet coils
z	coordinate in the gas volume of the refrigerator
A_d	factor used in a design of the refrigerator
B_d	factor used in a design of the refrigerator
B_M	magnetic induction
B	cross-sectional area of the stylized refrigerator
D	diameter of the tube, in which the paramagnetic material moves

F	heat-transfer surface
F_m	total heat-transfer surface of the paramagnetic material
G	weight of the samples of paramagnetic material in chapter 4
J	inner quantum number
J	energy flow in the regenerator
J_c	critical current through 1 cm² of the cross-sectional area of the winding space of the superconducting coils
ΔL	heat load of a section $\Delta\xi$ of the regenerator
M_x	mutual inductance to be measured
M_s	standard mutual inductance
N	number of sections of the regenerator for numerical calculations
N_c	number of magnetic ions per cm³
P_D	demagnetization power
P_{D0}	undisturbed demagnetization power
P_{D1}	sum of the undisturbed demagnetization power and the energy flow through the regenerator at the cold side
ΔP_{DR}	energy flow through the regenerator at the cold side
ΔP_{DF}	flow loss at the cold side
ΔP_{DC}	conduction loss at the cold side
ΔP_{DE}	eddy-current loss at the cold side
ΔP_{DI}	insulation loss at the cold side
P_M	magnetization power
P_{M0}	undisturbed magnetization power
P_{M1}	sum of the undisturbed magnetization power and the energy flow through the regenerator at the warm side
ΔP_{MR}	energy flow through the regenerator at the warm side
ΔP_{MF}	flow loss at the warm side
ΔP_{MC}	conduction loss at the warm side
ΔP_{ME}	eddy-current loss at the warm side
ΔP_{MI}	insulation loss at the warm side
Q	heat
ΔR	magnetic heating in a section $\Delta\xi$ of the regenerator
T	temperature
T_g	temperature of the gas
T_m	temperature of the paramagnetic material
T_D	mean temperature of the cold transport gas
T_M	mean temperature of the warm transport gas
T_{D0}, T_{Di}, T_{Dk}, T_{Du}	temperatures used in the description of the stylized process (see fig. 2.3, p. 11)
T_{M0}, T_{Mi}, T_{Mk}, T_{Mu}	
V_g	volume of the gas used as regenerator
V_m	volume of the paramagnetic material
V_t	total gas volume of the refrigerator

W	work
α	ratio of the magnetic field to the temperature $T-\Theta$
β	crank angle of the refrigerator drive
γ	phase difference between the displacement of the movable unit and the variation of the gas volume at the warm side of the refrigerator
δ	phase difference between the displacement of the movable unit and the displacer
η	efficiency
$\varkappa$	electrical conductivity
λ	thermal conductivity
μ_B	Bohr magneton
ξ	x/l
ϱ_g	density of the helium
ϱ_m	effective density of the paramagnetic material in the regenerator
σ	magnetization of the paramagnetic material per gramme
τ	$= t/\frac{1}{2}\, t_p$
φ	flow function of the paramagnetic material in the regenerator
χ	susceptibility per gramme
ψ	density function of the paramagnetic material in the regenerator
ω	$2\,\pi\,(n/60)$
Γ^+	heat-capacity number in the regenerator
Θ	asymptotic Curie temperature
Λ^+	heat-transfer number in the regenerator
Λ^*	$= \Lambda^+\,(\tau_2 - \tau_1)$
Λ	heat-transfer number of normal regenerators
Δ	ratio of the mass of the total amount of paramagnetic material and the mass of the amount being in the regenerator
Π^+	$= \Lambda^+/\Gamma^+$
Ω	function of Π^+, used in calculating the regenerator loss
Φ	magnetic potential
Φ_h	heat flow to paramagnetic material in the regenerator

REFERENCES

1) P. Debeye, Ann. Phys. **81**, 1154, 1926.
2) W. F. Giauque, J. Amer. chem. Soc. **49**, 1864 and 1870, 1927.
3) W. J. de Haas, E. C. Wiersma and H. A. Kramers, Physica **1**, 1, 1933/34.
4) W. F. Giauque and D. P. McDougall, Phys. Rev. **43**, 768, 1933.
5) N. Kurti and F. Simon, Nature (London) **133**, 907, 1934.
6) H. B. G. Casimir, W. J. de Haas and D. de Klerk, Physica **6**, 241, 1939.
7) N. Kurti, P. Laîné and F. Simon, C.R. Acad. Sci. Paris **208**, 173, 1939.
8) C. V. Heer, C. B. Barnes and G. J. Daunt, Rev. sci. Instr. **25**, 1088, 1954.
9) See for example, D. de Klerk in S. Flügge (ed.), Encyclopedia of physics, Springer-Verlag, Berlin, 1956, Vol. 15, p. 38.
10) W. F. Schalkwijk, Trans. ASME, Series A, J. Eng. Power **81**, 142, 1959.
11) H. Hausen, Wärmeübertragung in Gegenstrom, Gleichstrom und Kreuzstrom, Springer-Verlag, Berlin, 1950.
12) H. Hausen, Int. J. Heat Mass Transfer **7**, 112, 1964.
13) A. J. Willmot, Int. J. Heat Mass Transfer **7**, 1291, 1964.
14) See for example, McAdams, Heat transmission, McGraw-Hill, 1954, 3rd ed., p. 290.
15) See for example, K. Küpfmüller, Einführung in die theoretische Elektrotechnik, Springer-Verlag, Berlin, p. 271.
16) G. Prast, Philips tech. Rev. **26**, 1, 1965.
17) O. V. Lounasmaa, Thesis, Oxford, 1958.
18) J. E. Kunzler, Rev. mod. Phys. **33**, 501, 1961.
19) R. Hancox, Appl. Phys. Letters **7**, 138, 1965.
20) W. A. Little and R. D. Parks, Phys. Rev. Letters **6**, 539, 1961.
21) J. Nicol, Rev. sci. Instr. **31**, 212, 1961.
22) D. de Klerk, Thesis, Leiden, 1948; see also ref. 9.
23) J. R. Clement and E. H. Quinnell, Rev. sci. Instr. **23**, 213, 1952.
24) R. S. Roth, J. Res. Nat. Bur. Standards **56**, 17, 1956.
25) P. F. Bongers, Philips Research Lab. (private communication).
26) G. Blasse, Philips Research Lab. (private communication).
27) K. R. Lea, M. J. M. Leask and W. P. Wolf, J. Phys. Chem. Solids **23**, 1381, 1962.

Samenvatting

In dit proefschrift wordt de mogelijkheid onderzocht magneto-calorische effecten te gebruiken voor een koelmachine waarmede koude kan worden opgewekt bij een temperatuur van ongeveer 4 °K. Deze effecten treden op bij paramagnetische stoffen. Het adiabetisch demagnetiseren van dergelijke stoffen wordt reeds lang benut als methode om temperaturen ver beneden 1 °K te bereiken. Voor de toepassing bij hogere temperaturen is echter een nieuwe kringloop nodig, die bij voorkeur geschikt moet zijn voor gebruik in een snellopende koelmachine.

De kringloop die voor dit doel gevonden is lijkt in vele opzichten op de Stirling-kringloop, die in koudgaskoelmachines en heetgasmotoren wordt toegepast. In de nieuwe kringloop wordt helium gebruikt voor het overbrengen van warmte van de paramagnetische stof naar een warmtewisselaar en omgekeerd. Bovendien wordt ook helium gebruikt als regenerator. Ten einde fasenovergangen te voorkomen wordt de druk van het helium hoger gekozen dan de kritische druk.

Het nut van de nieuwe koelmachine ter vervanging van het bekende Joule-Thomson-proces wordt in de inleiding besproken.

Het tweede hoofdstuk is gewijd aan een theoretische analyse van de koelmachine die gebaseerd is op de nieuwe kringloop. Nadat het principe van deze kringloop nader is uiteengezet, wordt een vereenvoudigd model ingevoerd voor de tamelijk ingewikkelde processen, die in de nieuwe koelmachine plaatsvinden. Met behulp van dit model is een berekeningsschema uitgewerkt. Bij de analyse wordt veel aandacht besteed aan de regenerator. Het gedrag van deze regenerator wijkt af van het gedrag van normale regeneratoren, omdat arbeid verricht kan worden op de paramagnetische stof tijdens de verplaatsing door de regenerator.

Hoofdstuk 3 bevat het ontwerp van een magnetische koelmachine werkend tussen 15 °K en 4 °K. Het berekende rendement van deze machine blijkt zeer hoog te zijn (60-70% van het rendement van een Carnot-kringloop). Aan het eind van dit hoofdstuk worden de eigenschappen van de nieuwe koelmachine vergeleken met die van een koelmachine werkend volgens het Joule-Thomson-proces.

In hoofdstuk 4 worden de metingen besproken die verricht zijn ten einde geschikte paramagnetische stoffen te vinden voor de nieuwe koelmachine. Een dergelijk onderzoek was nodig, daar de stoffen die normaal voor adiabatische demagnetisatie gebruikt worden, voor ons doel niet geschikt zijn. De onderzochte stoffen zijn een aantal gemengde oxiden van zeldzame aard metalen en andere metalen; de magnetische susceptibiliteit en de entropie van deze stoffen werden gemeten. Hierbij zijn enige stoffen gevonden die zeer geschikt zijn als werkstof voor de nieuwe magnetische koelmachine.

Summary

The possibility of using magneto-caloric effects for a refrigerating machine in which cold can be generated at a temperature of about 4 °K has been investigated in this thesis. These effects are obtained with paramagnetic materials. The adiabatic demagnetization of such materials has long served as a method for attaining temperatures well below 1 °K. A new cycle, however, is needed for application at higher temperatures. It should preferably be suitable for a fast-running refrigerator.

The cycle evolved for this purpose resembles in many respects the Stirling cycle used in gas-refrigerating machines and hot-gas engines. In the new cycle, helium is used to transfer heat from the paramagnetic material to a heat exchanger and vice versa. The helium is also used, moreover, as a regenerator. In order to prevent phase transitions, the helium pressure chosen is above the critical pressure.

The value of the new refrigerator as a replacement for the familiar Joule-Thomson process has been discussed in the introduction.

The second chapter is devoted to a theoretical analysis of the refrigerator based on the new cycle. After a detailed exposition of the principle underlying this cycle, a simplified model for the fairly complicated processes taking place in the new refrigerator is introduced. A calculation scheme is worked out with the aid of this model. In the analysis a great deal of attention is devoted to the regenerator. The behaviour of this regenerator deviates from that of normal regenerators, in that work can be carried out on the paramagnetic material during its passage through the regenerator.

Chapter 3 covers the design of a magnetic refrigerator working between 15 °K and 4 °K. The calculated performance of this machine compared with a Carnot cycle is found to be very high (60-70 %). At the end of the chapter the properties of the new refrigerating machine are compared with those of one working on the Joule-Thomson principle.

In chapter 4 the measurements carried out in order to obtain paramagnetic materials suitable for the new refrigerator are discussed. Such an investigation was necessary, as the materials normally used for adiabatic demagnetization are unsuitable for our purpose. The materials investigated were a number of mixed oxides of rare-earth and other metals. The magnetic susceptibility and the entropy of these materials were measured, a number of them being found to be eminently suitable for the new magnetic refrigerator.

STELLINGEN

I

De magnetische kringloop beschreven in dit proefschrift kan gebruikt worden om, uitgaande van een temperatuur van ongeveer 1 °K, koude bij lagere temperaturen op te wekken. Het verdient aanbeveling hierbij magnetische velden van tenminste 40 kOe te gebruiken.

II

Het verlies aan koude-produktie, dat kan ontstaan bij de magnetische koelmachine indien er gas lekt langs de afdichting van de verdringer, kan worden verminderd door het aanbrengen van een pakket gazen tussen de verdringer en de vriezer.

III

In de koudetechniek worden een aantal kringlopen toegepast, die bij drie verschillende temperaturen in warmtekontakt staan met de omgeving. Bij de laagste temperatuur kan evenveel warmte worden opgenomen als bij de tussen-temperatuur wordt afgestaan, zodat deze hoeveelheid warmte als het ware van het ene temperatuursniveau naar het andere getransporteerd wordt. Het is zinvol voor praktische processen van deze aard relatieve kwaliteitsgetallen op te geven ten opzichte van een geïdealiseerd transport-proces. Dit proces bestaat uit twee kringlopen volgens Carnot, waarbij de één als motor werkt en de ander als koelmachine.

IV

Een koudgaskoelmachine met meerdere variabele ruimten kan zodanig worden uitgevoerd dat een transport-proces wordt verkregen.

V

Tegen het opstellen van grafieken voor het Joule-Kelvin proces, waarbij het temperatuursverschil aan de warme zijde van de laatste warmtewisselaar als parameter wordt gebruikt, zijn ernstige bezwaren in te brengen.

J. W. Dean and D. B. Mann, NBS Technical Note 227.

VI

Voor het opwekken van koude bij temperaturen, die slechts weinig lager zijn dan de kritische temperatuur van helium, komt een koudgaskoelmachine in aanmerking. Deze machine dient in dat geval heliumgas als werkmedium te bevatten, waarbij de minimum druk van dit gas boven de kritische druk gehouden moet worden.

VII

De zuurstof, die voor beademingsdoeleinden bestemd is, wordt onnodig in prijs verhoogd door de eis, dat de zuiverheid hiervan tenminste 99% moet zijn (zie o.a. Ned. Pharmacopee).

VIII

Vloeibare stikstof wordt sinds enige jaren gebruikt voor de koeling van transport-voertuigen, die ingericht zijn voor het vervoer van levensmiddelen. Het gebruik van vloeibare lucht voor dit doel wordt ontraden. De argumenten, die hiervoor worden aangevoerd, zijn aanvechtbaar.

E. A. Rietzschell, Maandblad Ned. Ver. Koeltechn. **59**, 5 (1966).

IX

Bij de berekeningen over het vervuilen van regeneratoren tengevolge van het uitvriezen van verontreinigingen uit de gasstroom, wordt ten onrechte geen rekening gehouden met de periodieke temperatuursveranderingen van het regeneratormateriaal.

H. Hausen in Handbuch der Kältetechnik VIII (Uitg. R. Planck).

X

Uit de experimenten van W. J. O'Sullivan, W. A. Robinson en W. W. Simmons kan alleen worden afgeleid, dat in $CuCl_2 . 2 H_2O$ de tijd tussen twee opeenvolgende verwisselingen van de oriëntaties van de deelroosters langer is dan de relaxatie tijd van het H^+-ion.

W. J. O'Sullivan, W. A. Robinson and W. W. Simmons, Phys. Rev. **124**, 1317 (1961).

XI

N. E. Phillips heeft uit metingen van de soortelijke warmte van bismuth beneden 1 °K voor de effektieve massa van de gaten in de elektronenband een waarde afgeleid, die ongeveer zes maal groter is dan de waarden, die op andere wijze bepaald zijn. Het is echter te betwijfelen of de bijdrage van de elektronen en van de gaten in de elektronenband tot de soortelijke warmte met voldoende zekerheid kan worden vastgesteld om hieruit de effektieve massa van de gaten te bepalen. In het bijzonder kan het feit, dat de bijdrage van het rooster tot de soortelijke warmte niet exakt evenredig hoeft te zijn met de derde macht van de temperatuur, van grote invloed zijn.

N. E. Phillips, Phys. Rev. **118**, 644 (1960).

XII

Het lijkt mogelijk elektron-phonon koppeling in halfgeleiders te bestuderen door metingen van het infrarood emissie-spektrum van een stroomvoerende halfgeleider.

XIII

Naar analogie van de situatie bij kathode-verstuiving, onderstellen Harrison en Magnuson, dat er bij sublimatie van atomen van een niet te heet metaal oppervlak voorkeurrichtingen zullen bestaan, in welke de atomen zullen uittreden. Dit is echter zeer onwaarschijnlijk.

D. E. Harrison and G. D. Magnuson, Phys. Rev. **122**, 1421 (1961).

XIV

Hall, Hayes en Williams hebben uit metingen van de paramagnetische resonantie van tweewaardig mangaan in diverse kristallen, de splittingsparameter a afgeleid. Bij de vergelijking van de door hen gevonden waarden met de waarden, die door Powell, Gabriel en Johnston is berekend, worden de resultaten van die berekening in het geval van 4- en 8-voudige omringing niet geheel juist toegepast.

T. P. P. Hall, W. Hayes and F. I. B. Williams, Proc. Roy. Soc. **78**, 883 (1961).
M. J. D. Powell, J. R. Gabriel and D. F. Johnston, Phys. Rev. Letters **5**, 145 (1960).

XV

Als vervoersmiddel voor algemeen gebruik in de grote steden zou een driewieler nuttiger zijn dan een witte fiets (de z.g. provo-fiets).